NATIONAL ENERGY TECHNOLOGY LABORATORY

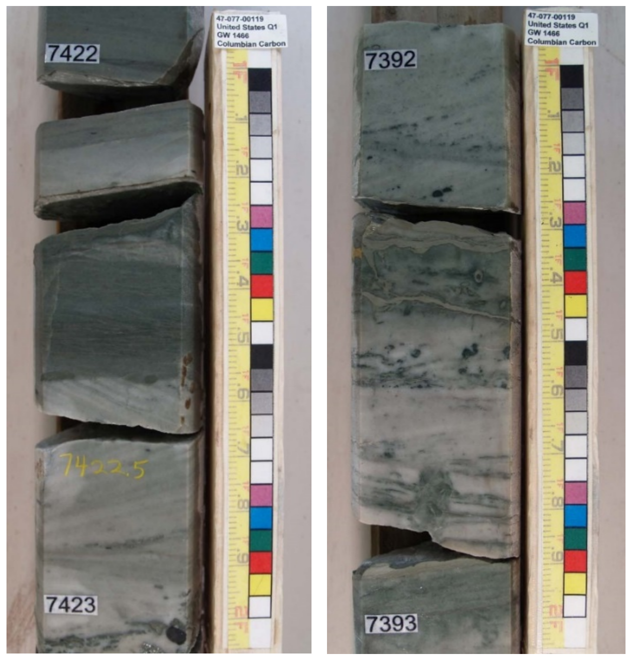

Computed Tomography of the Tuscarora Sandstone from the Preston 119 Well

17 April 2018

U.S. DEPARTMENT OF ENERGY | NATIONAL ENERGY TECHNOLOGY LABORATORY

Office of Fossil Energy

NETL-TRS-9-2018

Disclaimer

Cover Illustration: Example core photo of the Tuscarora Sandstone.

Suggested Citation: Moore, J.; Brown, S.; Crandall, D.; Workman, S.; Dinterman, P.; Moore, J. *Computed Tomography of the Tuscarora Sandstone from the Preston 119 Well;* NETL-TRS-9-2018; NETL Technical Report Series; U.S. Department of Energy, National Energy Technology Laboratory: Morgantown, WV, 2018; p 92. DOI: 10.18141/1433314.

An electronic version of this report can be found at:

http://netl.doe.gov/research/on-site-research/publications/featured-technical-reports

https://edx.netl.doe.gov/ucr

The data in this report can be accessed from NETL's Energy Data eXchange (EDX) online system (https://edx.netl.doe.gov) using the following link: https://edx.netl.doe.gov/dataset/preston-119-well

Computed Tomography of the Tuscarora Sandstone from the Preston 119 Well

Johnathan Moore[1,2], Sarah Brown[1,2] Dustin Crandall[1], Scott Workman[1,3], Philip Dinterman[4], Jessica Moore[4]

[1]U.S. Department of Energy, National Energy Technology Laboratory, 3610 Collins Ferry Road, Morgantown, WV 26507

[2]U.S. Department of Energy, National Energy Technology Laboratory, AECOM, 3610 Collins Ferry Road, Morgantown, WV 26507

[3]U.S. Department of Energy, National Energy Technology Laboratory, USSE2, 3610 Collins Ferry Road, Morgantown, WV 26507

[4]West Virginia Geological and Economic Survey, 1 Mont Chateau Road, Morgantown, WV 26508

NETL-TRS-9-2018

17 April 2018

NETL Contacts:

Dustin Crandall, Principal Investigator

Alexandra Hakala, Technical Portfolio Lead

Bryan Morreale, Acting Executive Director, Research & Innovation Center

This page intentionally left blank.

Table of Contents

This page intentionally left blank.

List of Figures

List of Figures (cont.)

List of Figures (cont.)

List of Tables

This page intentionally left blank.

Acronyms, Abbreviations, and Symbols

Term	Description
2D	Two-dimensional
3D	Three-dimensional
CT	Computed tomography
CTN	Computed tomography number
EDX	NETL's Energy Data eXchange
HU	Hounsfield unit
NETL	National Energy Technology Laboratory
WVGES	West Virginia Geological and Economic Survey

Acknowledgments

This work was completed at the National Energy Technology Laboratory (NETL) with support from U.S. Department of Energy's (DOE) Office of Fossil Energy Oil & Gas Program. The authors wish to acknowledge Alexandra Hakala (NETL Research & Innovation Center), Jared Ciferno (NETL Technology Development and Integration Center) and Elena Melchert (DOE Office of Fossil Energy) for programmatic guidance, direction, and support.

The authors would like to thank Bryan Tennant and Karl Jarvis for data collection and technical support. Thank you to the WVGES for allowing us to work with this core. Thank you to Dustin McIntyre and Mark McKoy for laboratory support. This research was supported in part by appointments from the NETL Research Participation Program, sponsored by the U.S. DOE and administered by the Oak Ridge Institute for Science and Education.

ABSTRACT

The computed tomography (CT) facilities at the National Energy Technology Laboratory (NETL) Morgantown, West Virginia site were used to characterize core of the Tuscarora Sandstone from a vertical well in Preston County WV, the Preston-119 from a depth of 7,165 to 7,438 ft.

The primary impetus of this work is a collaboration between West Virginia Geological and Economic Survey (WVGES) and NETL to characterize core from multiple wells to better understand the geologic framework of key stratigraphic units in West Virginia. As part of this effort, bulk scans of core were obtained from the Pres-119 well, provided by the WVGES. This report, and the associated scans generated, provide detailed datasets not typically available for researchers to analyze. The resultant datasets are presented in this report, and can be accessed from NETL's Energy Data eXchange (EDX) online system using the following link: https://edx.netl.doe.gov/dataset/preston-119-well.

All equipment and techniques used were non-destructive, enabling future examinations to be performed on these cores with the background information gathered through these tests. None of the equipment used was suitable for direct visualization of the pore space, though fractures and discontinuities were detectable with the methods tested. Low resolution CT imagery with the NETL medical CT scanner was performed on the entire core. Qualitative analysis of the medical CT images, give the ability to quickly identify key areas for more detailed study with higher resolution and will save time and resources in future studies. These methods provided a multi-scale analysis of this core that is relevant for many subsurface energy related examinations that have traditionally been performed at NETL.

1. INTRODUCTION

This is a collaboration between West Virginia Geological and Economic Survey (WVGES) and National Energy Technology Laboratory (NETL) to characterize core from multiple wells to better understand the geologic framework of various formations in, West Virginia. As part of this effort, we have obtained bulk scans of core archived by the WVGES; including Pres-119 in Preston County, West Virginia.

The primary objective of this report is to provide core characterization with methods not available to most researchers after obtaining baseline information on sample condition and characteristics using fast computed tomography (CT) scanning techniques on large batches of samples. The data is presented in several formats here and online that are potentially useful for various analyses; however, little detailed analysis is presented herein, as the research objective was not to do a site characterization. The data has been collected and preserved for others to utilize.

The Pres-119 well, located at geographic coordinates, 39.238527, -79.571704, was drilled by the Cities Service Oil Company from 10/5/1963 to 3/17/1964, with cored depths of 7,165 to 7,438 ft. The gas well, with a total vertical depth of 9,910 ft (ground elevation 2,172 ft) was drilled to the Martinsburg Formation and plugged in 1985; the API# is 4707700119. The cored interval contains fine-grained sandstone of the Silurian age Tuscarora Sandstone and contains multiple features of interest. The core is 6 in. in diameter contained in 107 boxes.

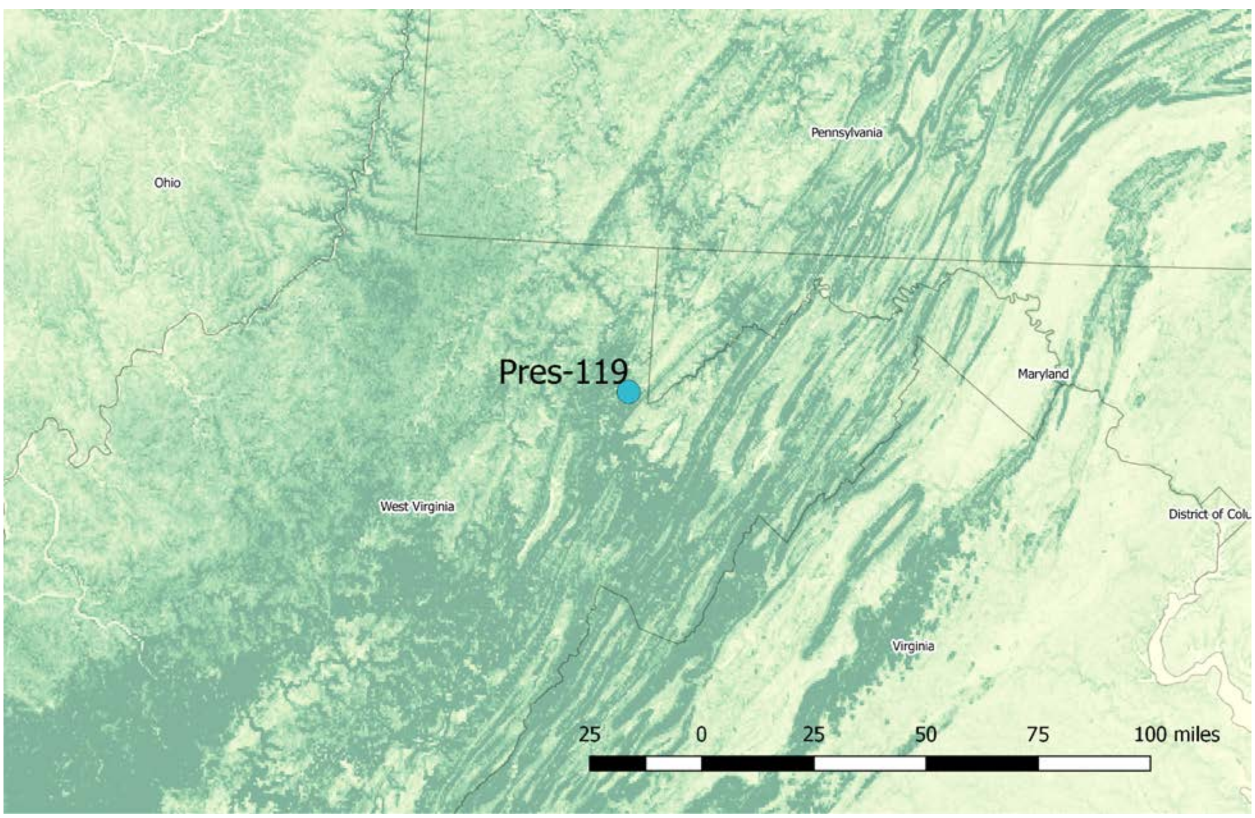

Figure 1: Location map for the Preston 119 Tuscarora well.

2. CORE DESCRIPTION

The core ranges from fine to coarse grained quartz rich sandstone (orthoquartzite or quartz arenite) tightly cemented with silica interbedded with argillaceous siliceous sandstone. Beds range from thin to thick. Some thin (6 in) layers of black shale and conglomerates alternate with the cemented sandstone. Coarse quartz grains and pebbles are found occasionally. Faint cross bedding is present throughout as well as filled and unfilled fractures. A detailed log of the core along with thin section descriptions and additional physical property measurements can be found online at http://www.wvgs.wvnet.edu/pipe2/EfileViewer.aspx (West Virginia Geological & Economic Survey, 2018)

2.1 CORE PHOTOGRAPHS

The following figures are photographs of the Preston 119 core as received at NETL.

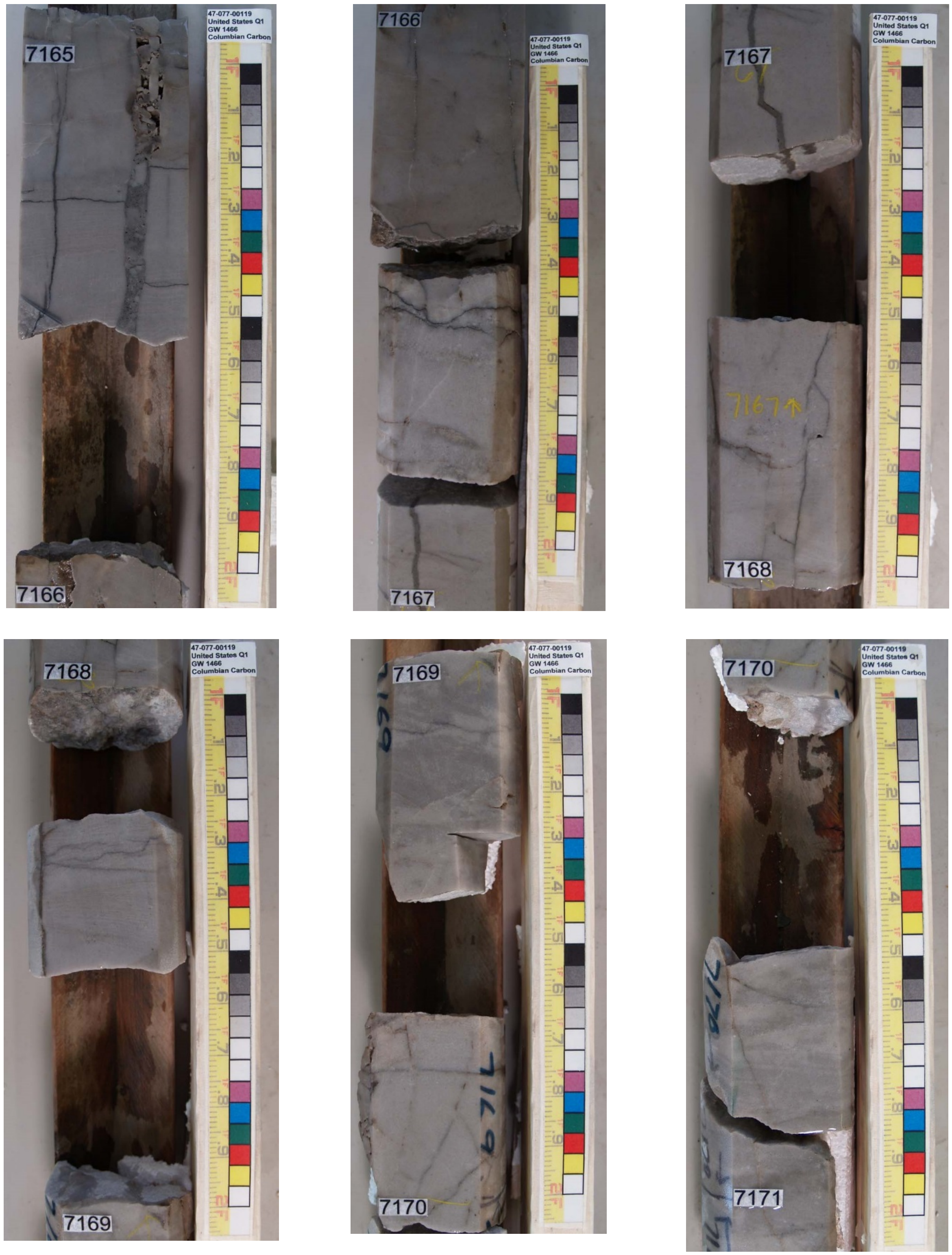

Figure 2: Pres-119 core photographs, from 7,165 to 7,171 ft.

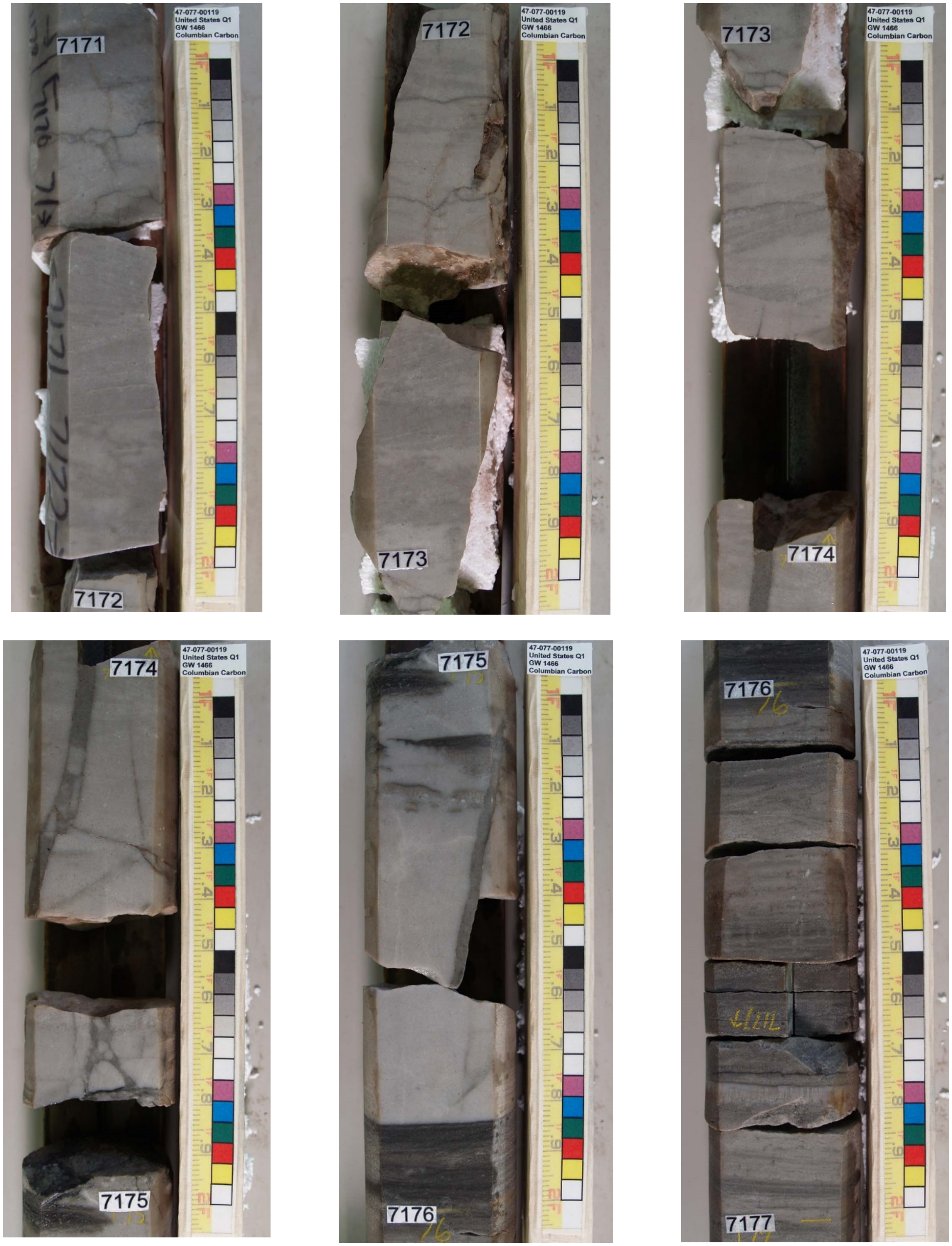

Figure 3: Pres-119 core photographs, from 7,171 to 7,177 ft.

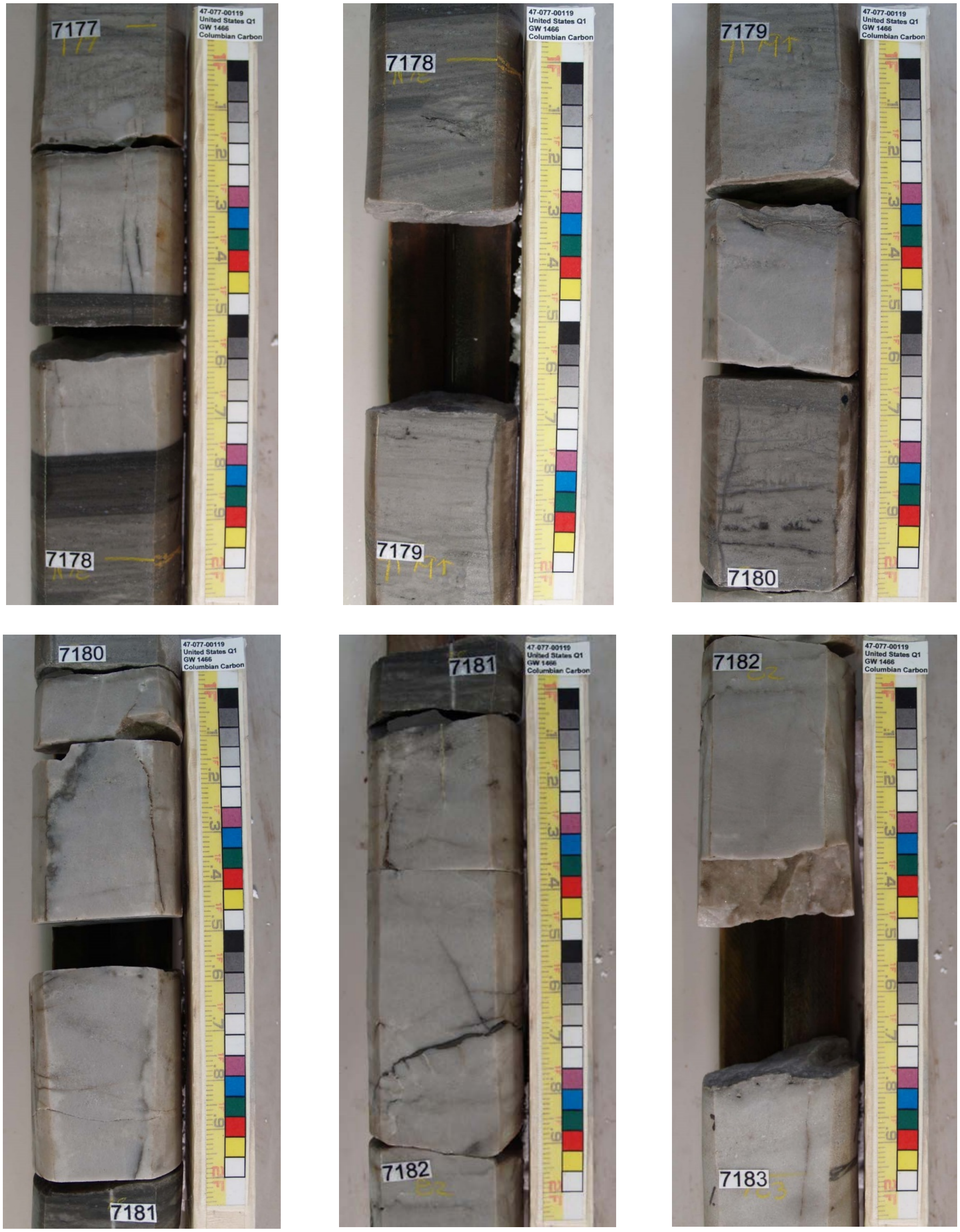

Figure 4: Pres-119 core photographs, from 7,177 to 7,182 ft.

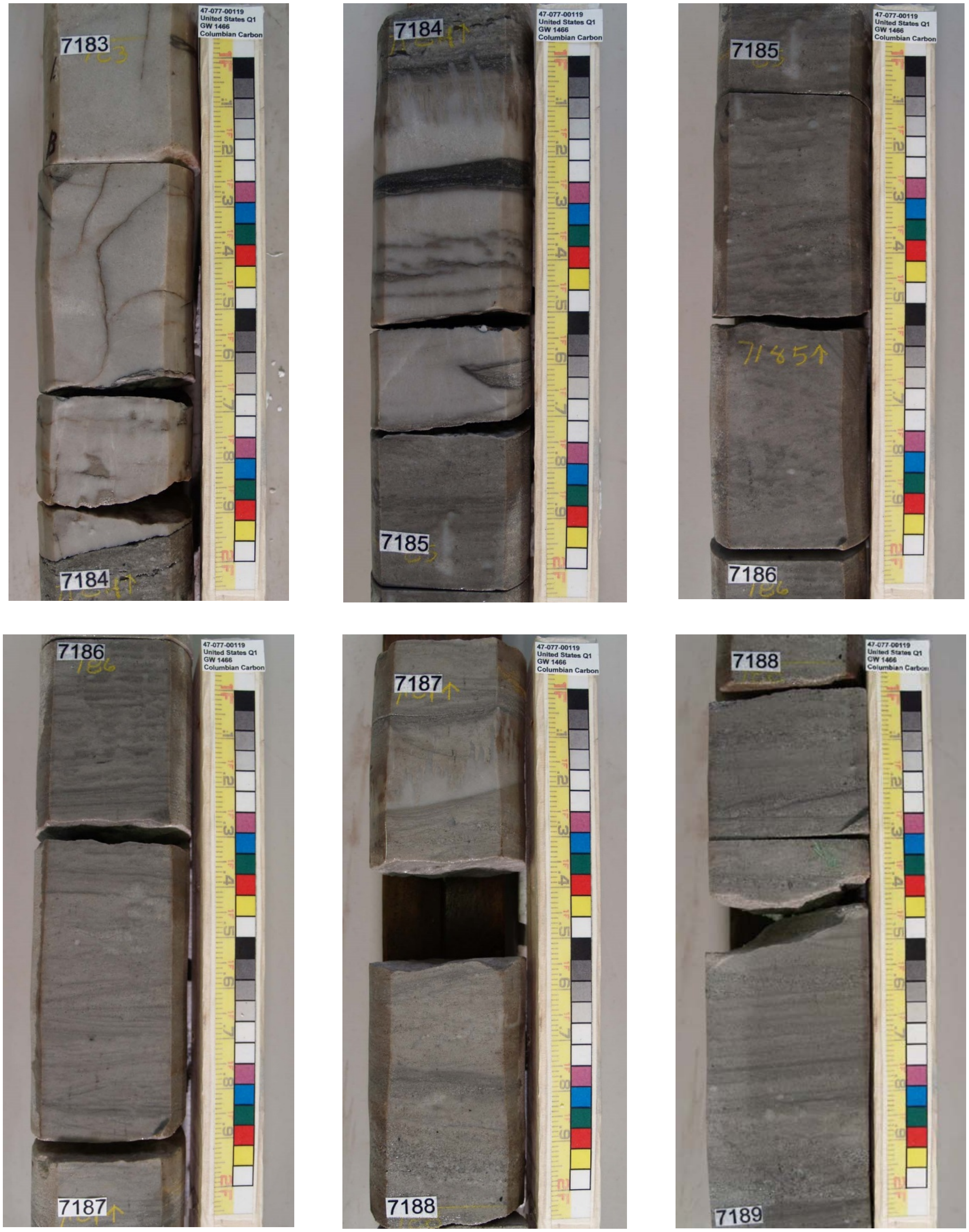

Figure 5: Pres-119 core photographs, from 7,183 to 7,189 ft.

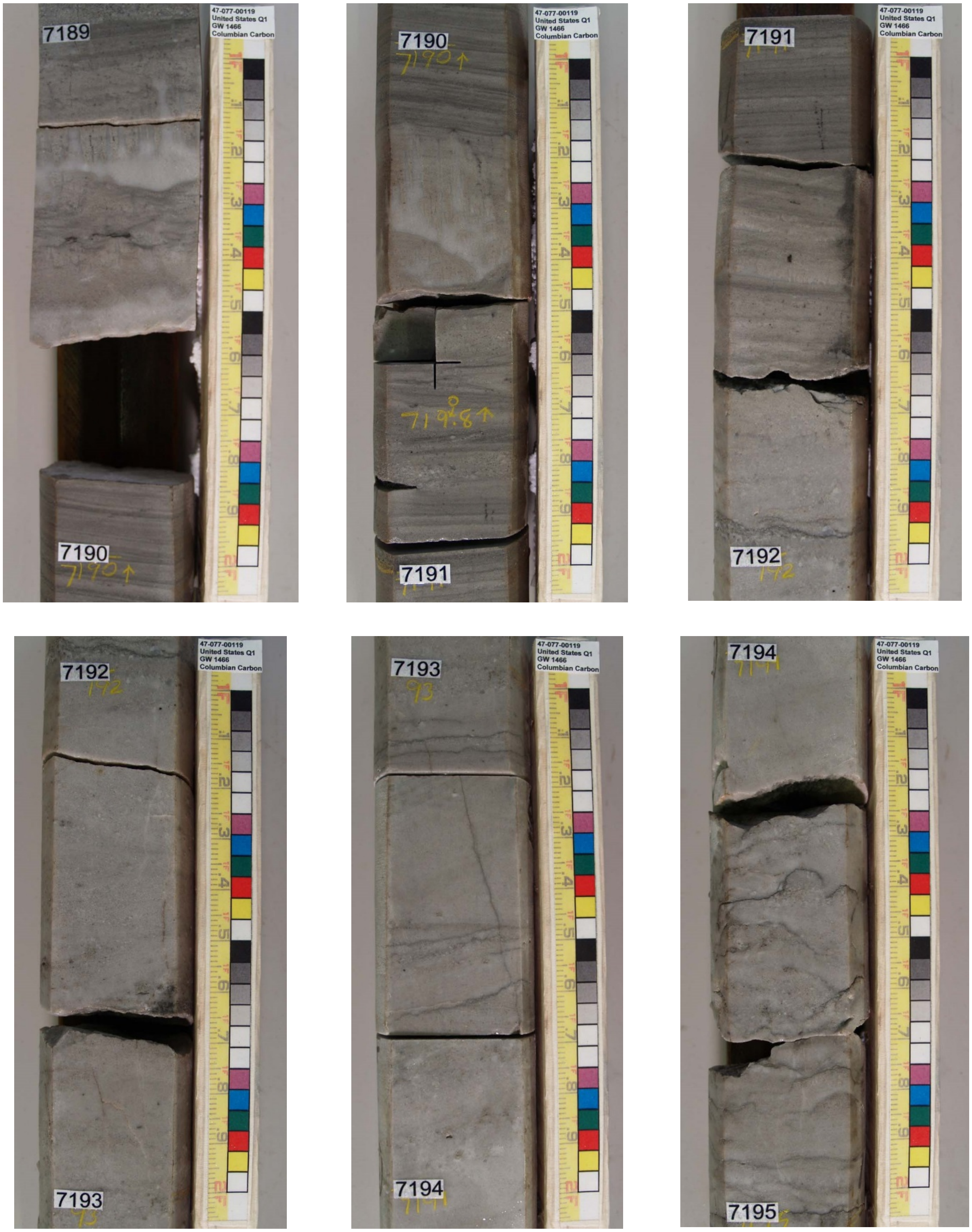

Figure 6: Pres-119 core photographs, from 7,189 to 7,195 ft.

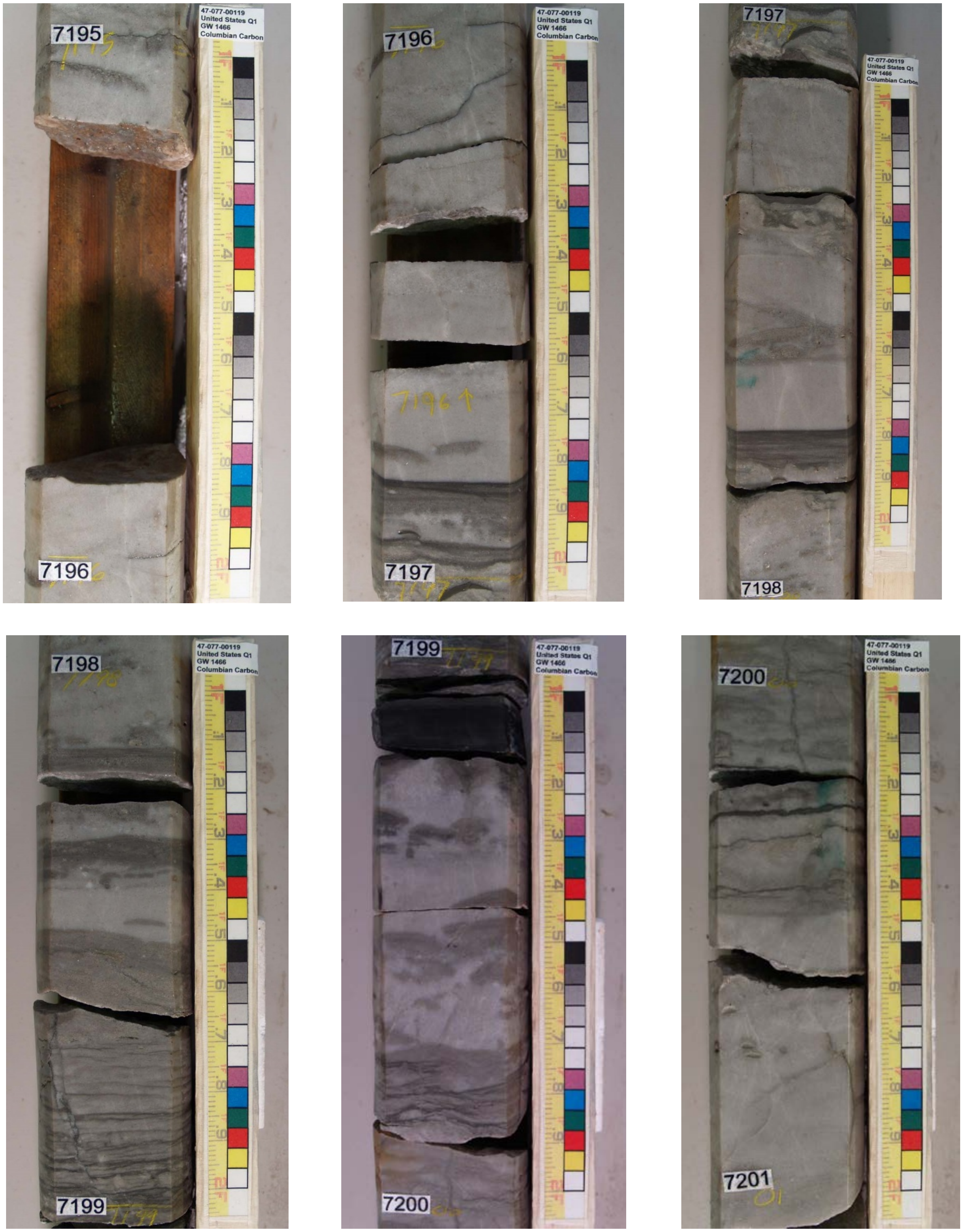

Figure 7: Pres-119 core photographs, from 7,195 to 7,201 ft.

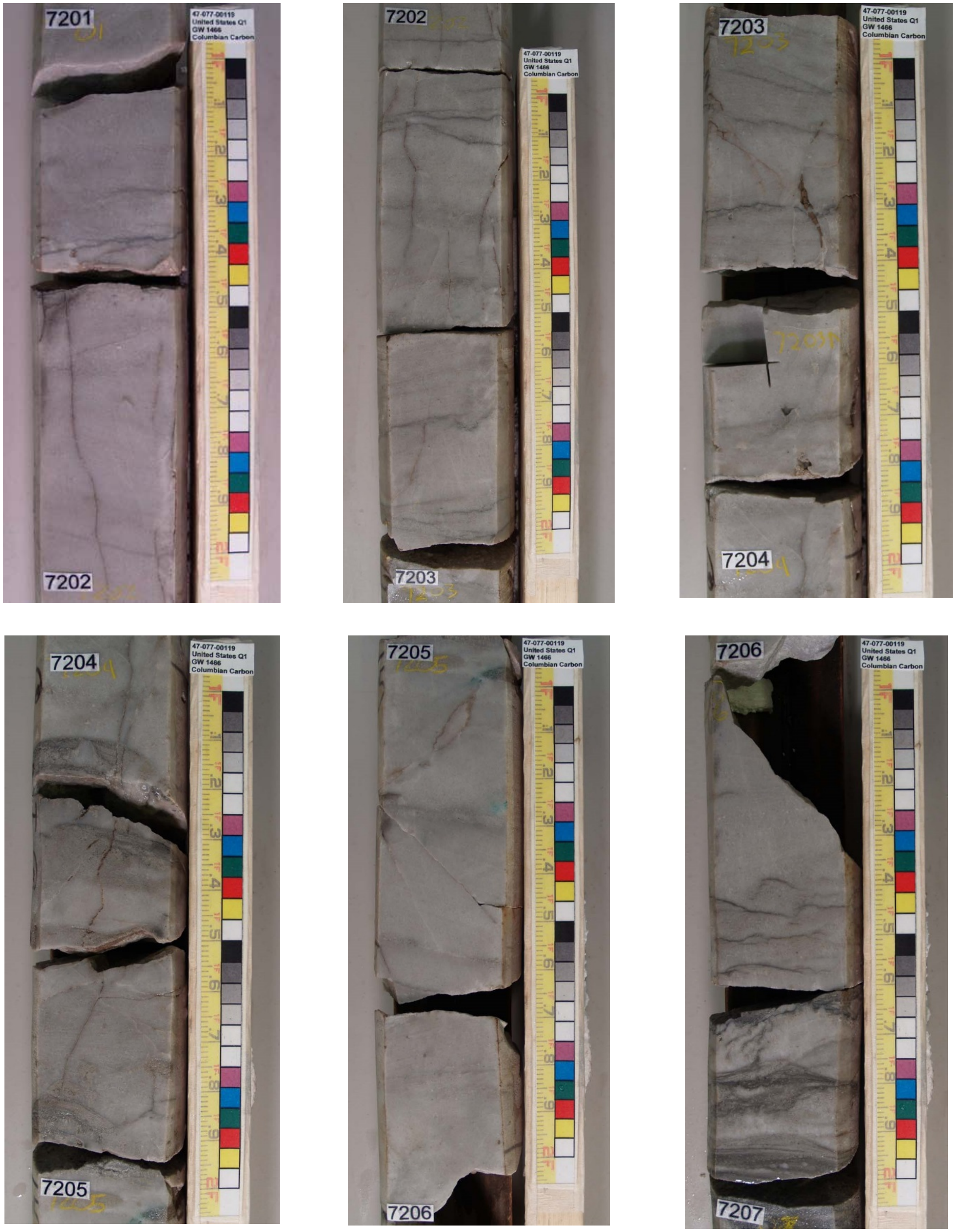

Figure 8: Pres-119 core photographs, from 7,201 to 7,207 ft.

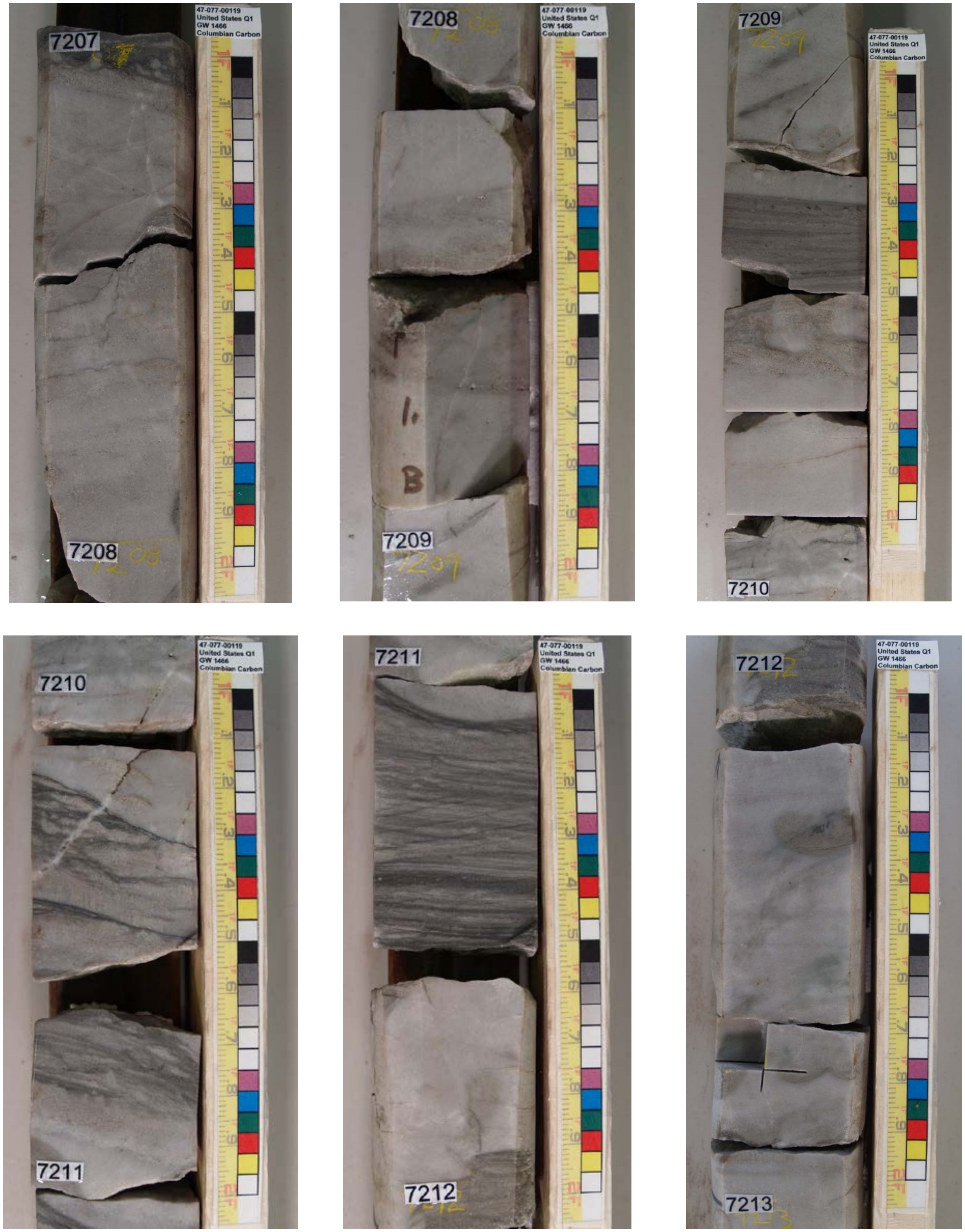

Figure 9: Pres-119 core photographs, from 7,207 to 7,213 ft.

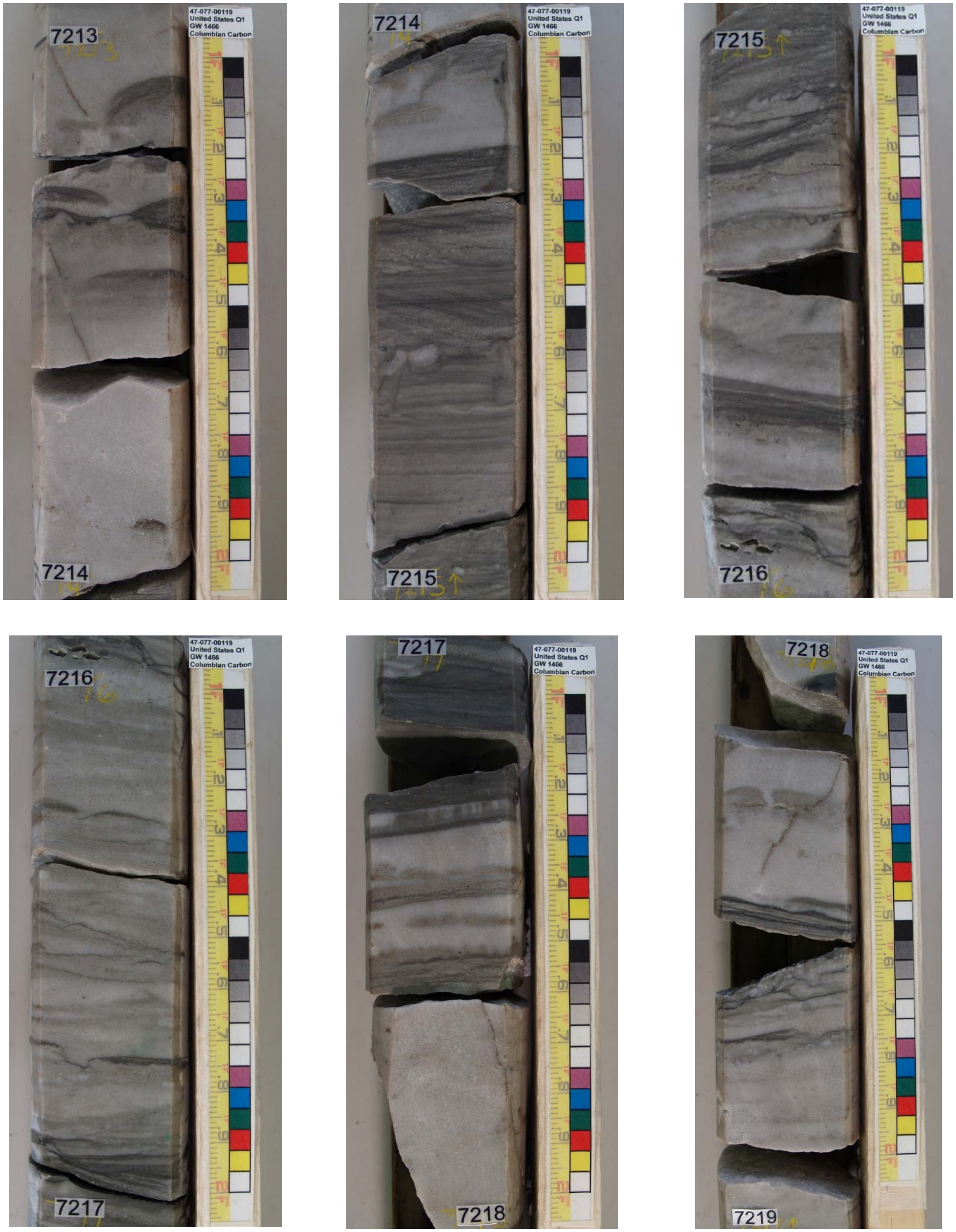

Figure 10: Pres-119 core photographs, from 7,213 to 7,219 ft.

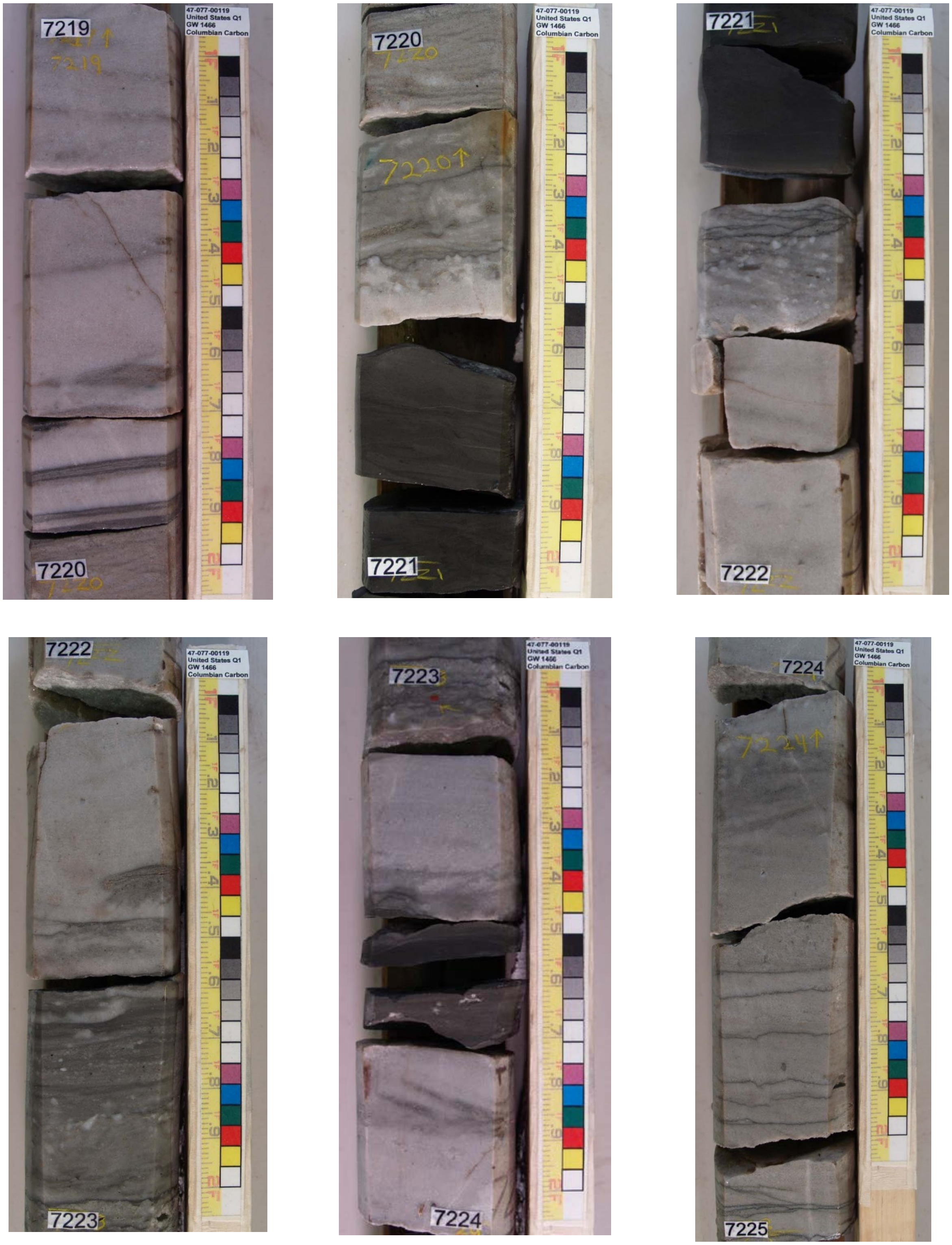

Figure 11: Pres-119 core photographs, from 7,219 to 7,225 ft.

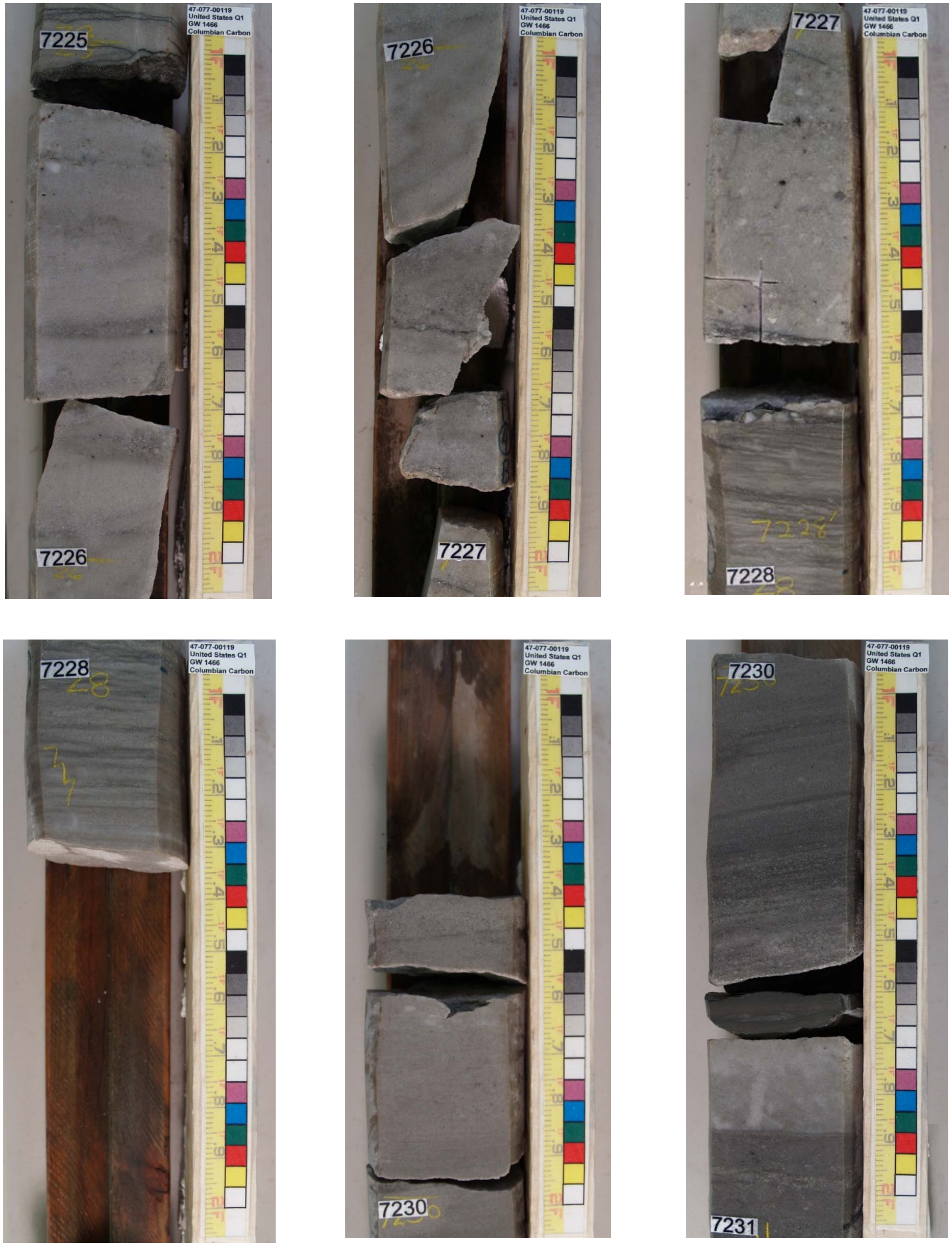

Figure 12: Pres-119 core photographs, from 7,225 to 7,231 ft.

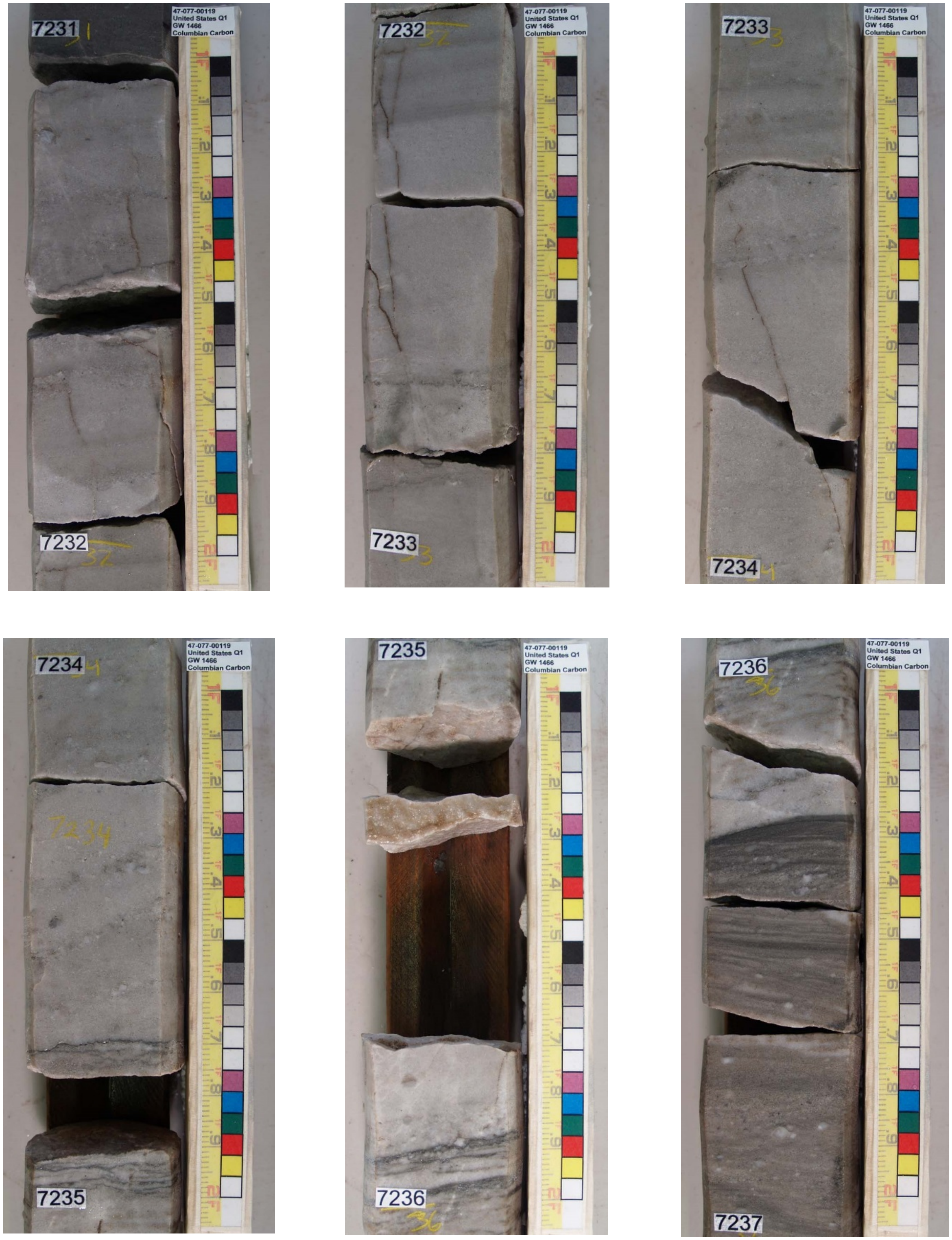

Figure 13: Pres-119 core photographs, from 7,231 to 7,237 ft.

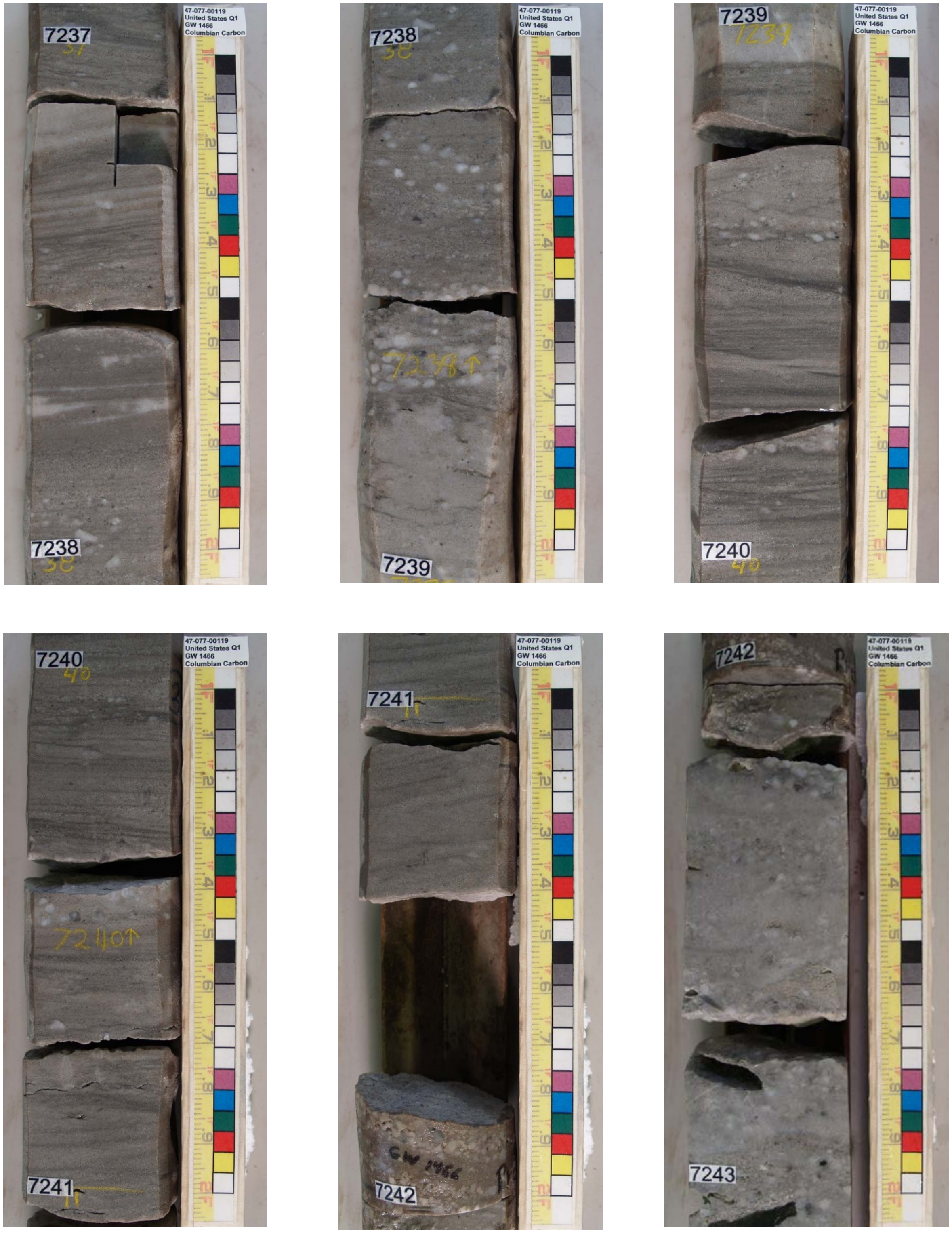

Figure 14: Pres-119 core photographs, from 7,238 to 7,243 ft.

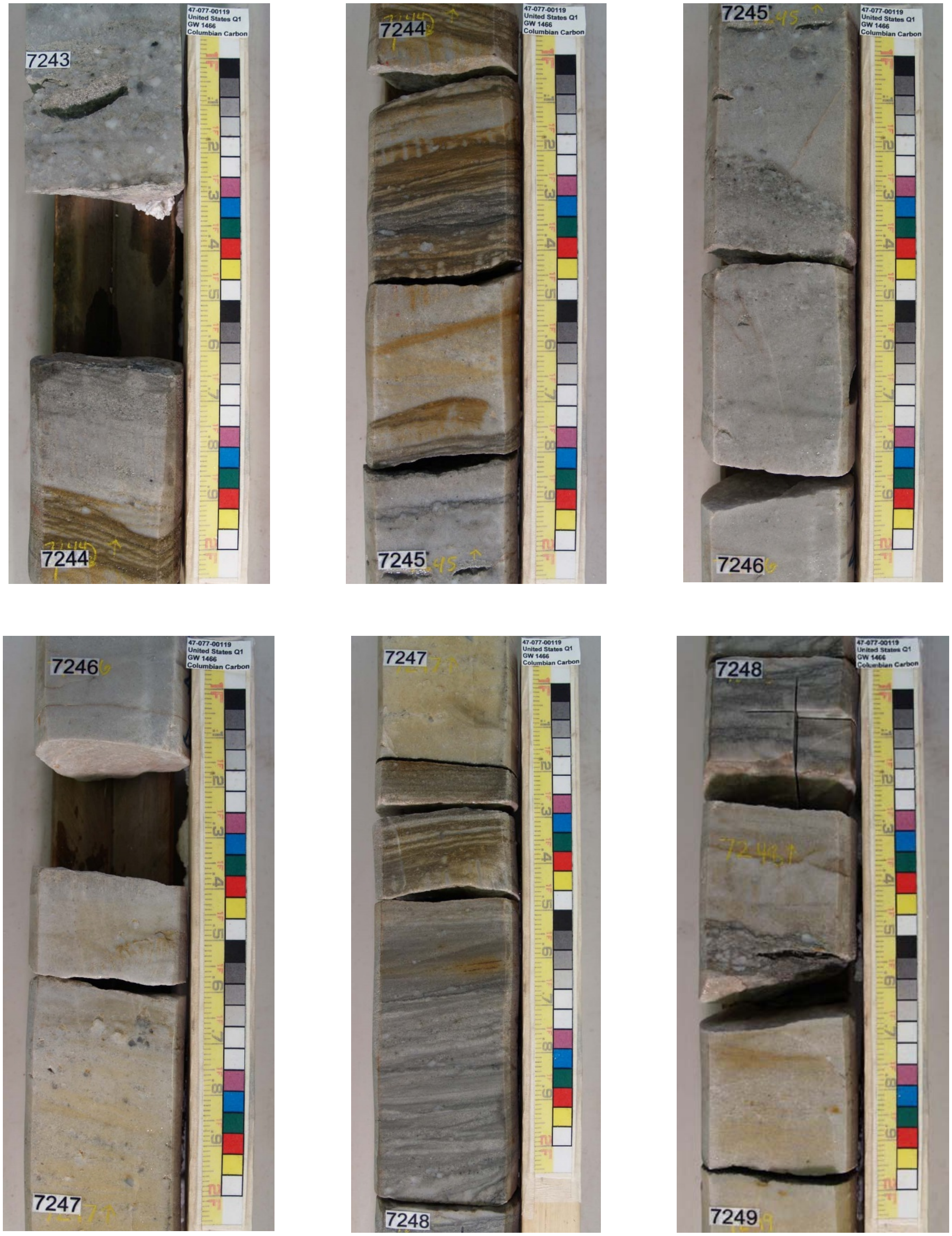

Figure 15: Pres-119 core photographs, from 7,243 to 7,249 ft.

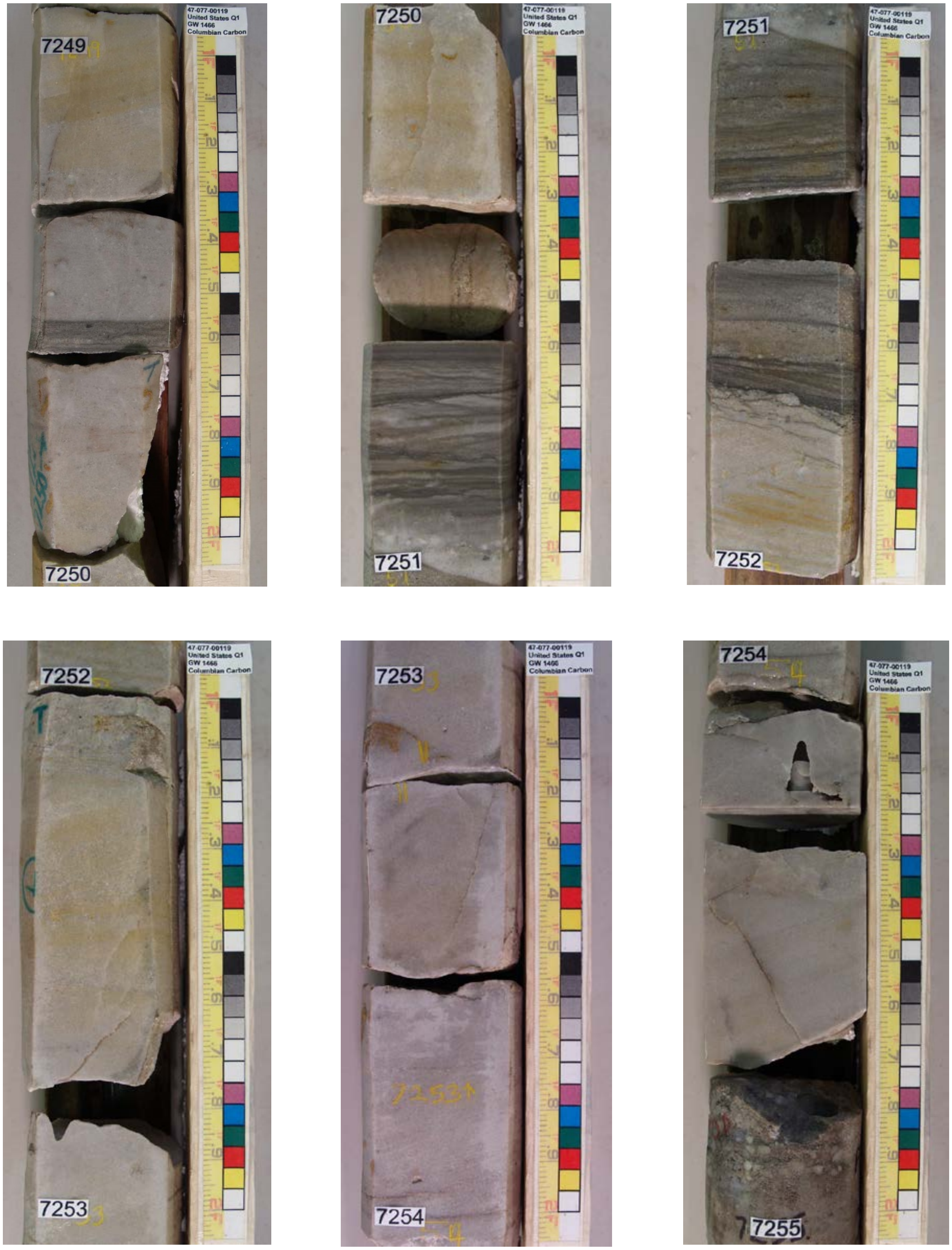

Figure 16: Pres-119 core photographs, from 7,249 to 7,255 ft.

Figure 17: Pres-119 core photographs, from 7,255 to 7,261 ft.

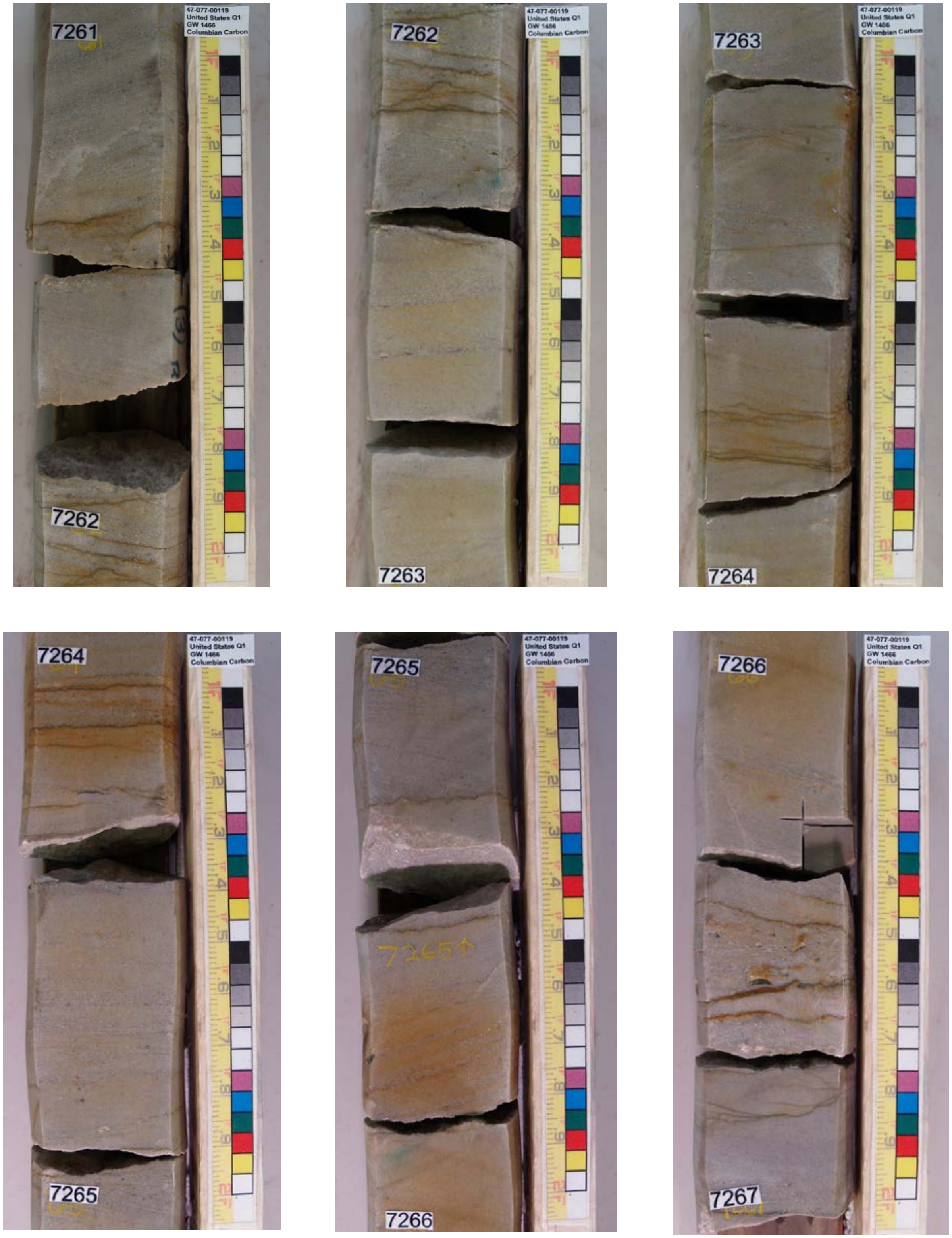

Figure 18: Pres-119 core photographs, from 7,261 to 7,267 ft.

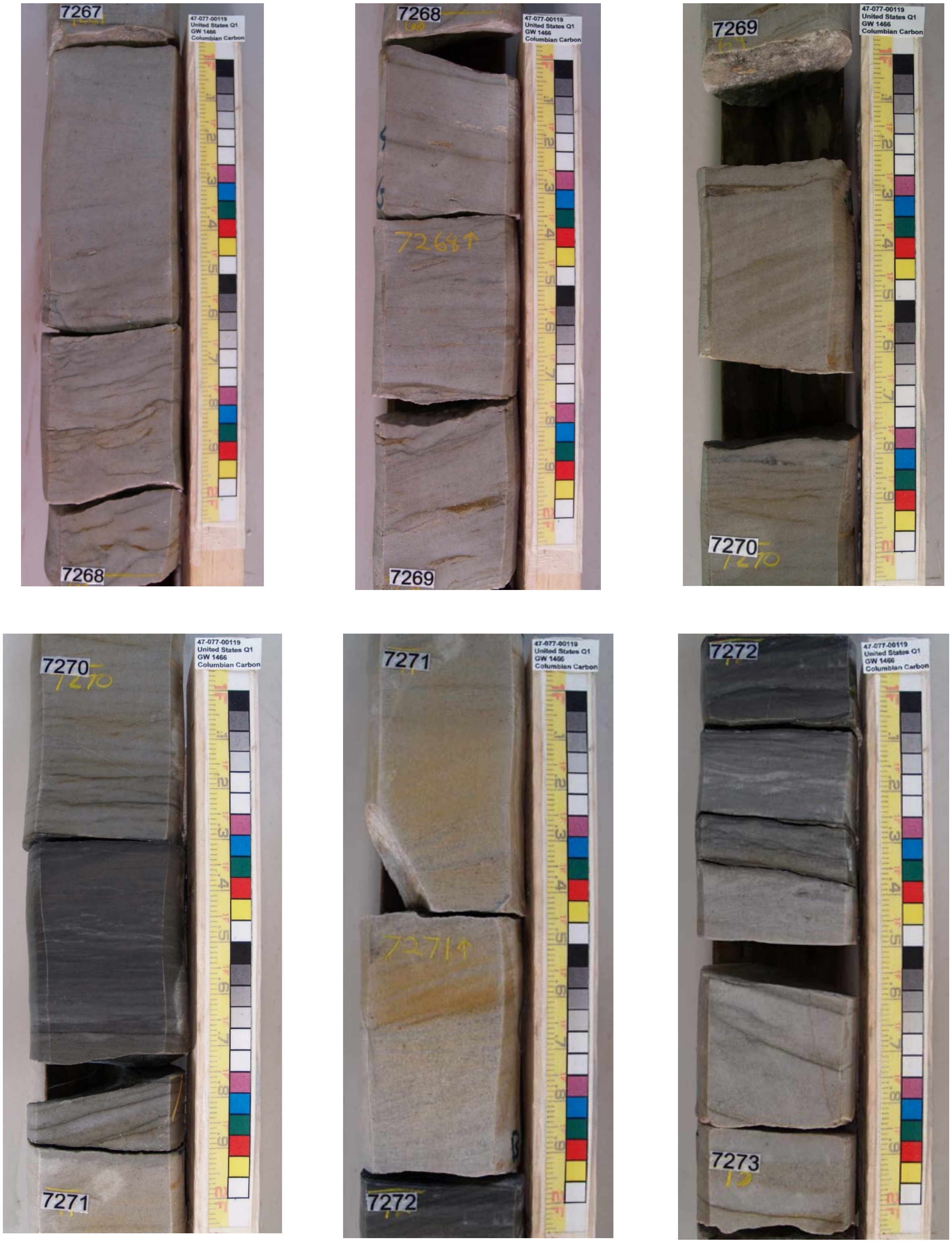

Figure 19: Pres-119 core photographs, from 7,267 to 7,273 ft.

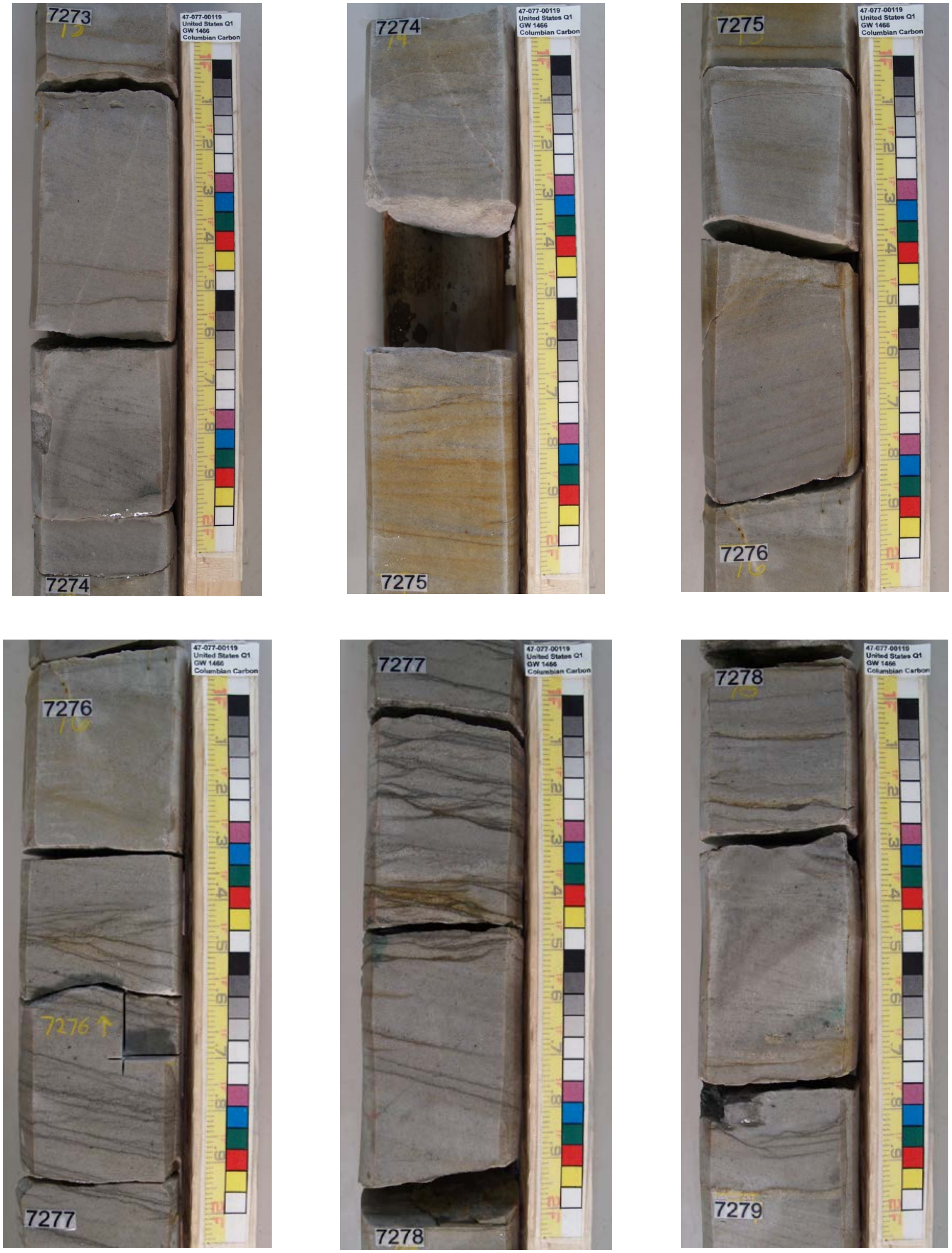

Figure 20: Pres-119 core photographs, from 7,273 to 7,279 ft.

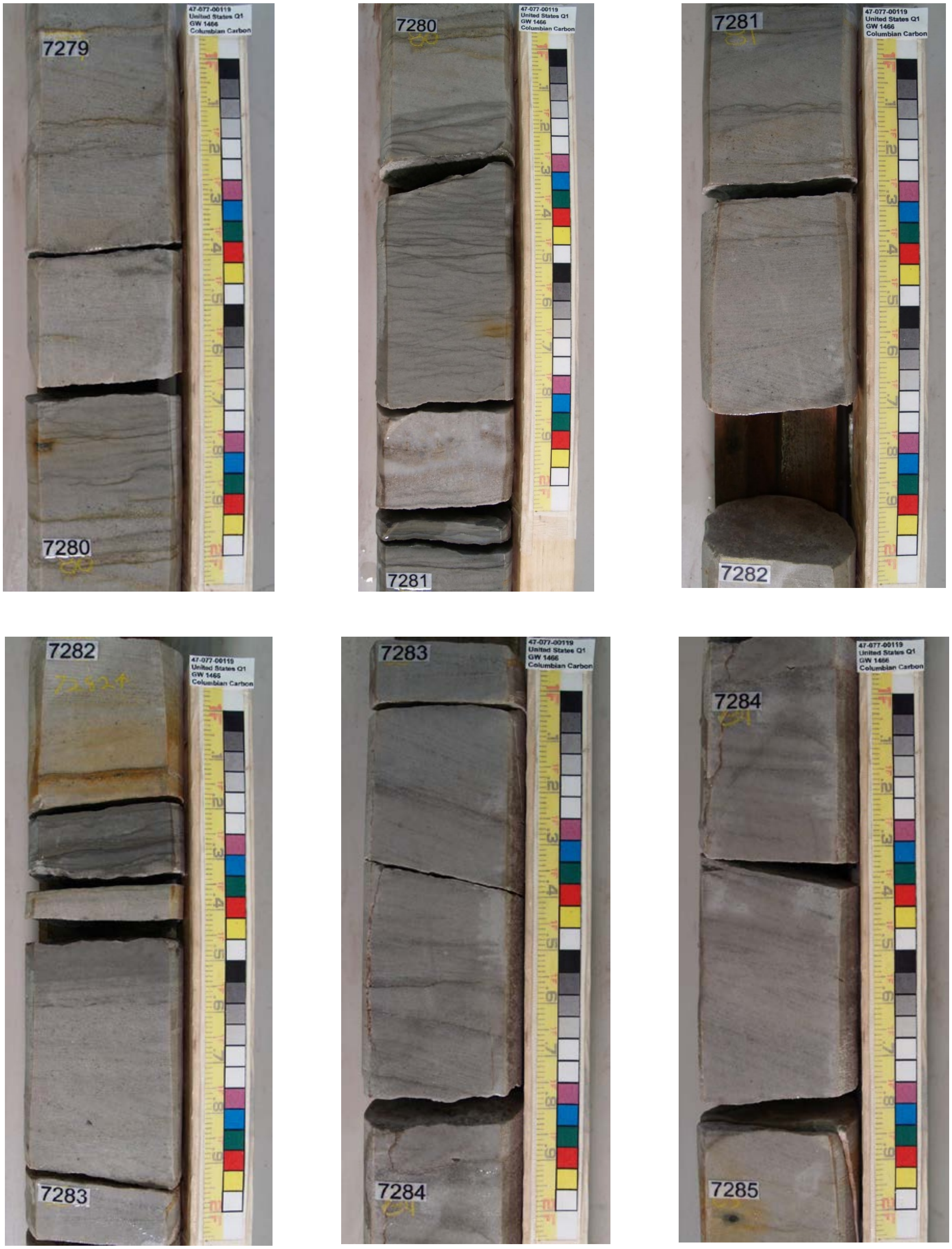

Figure 21: Pres-119 core photographs, from 7,279 to 7,285 ft.

Figure 22: Pres-119 core photographs, from 7,286 to 7,291 ft.

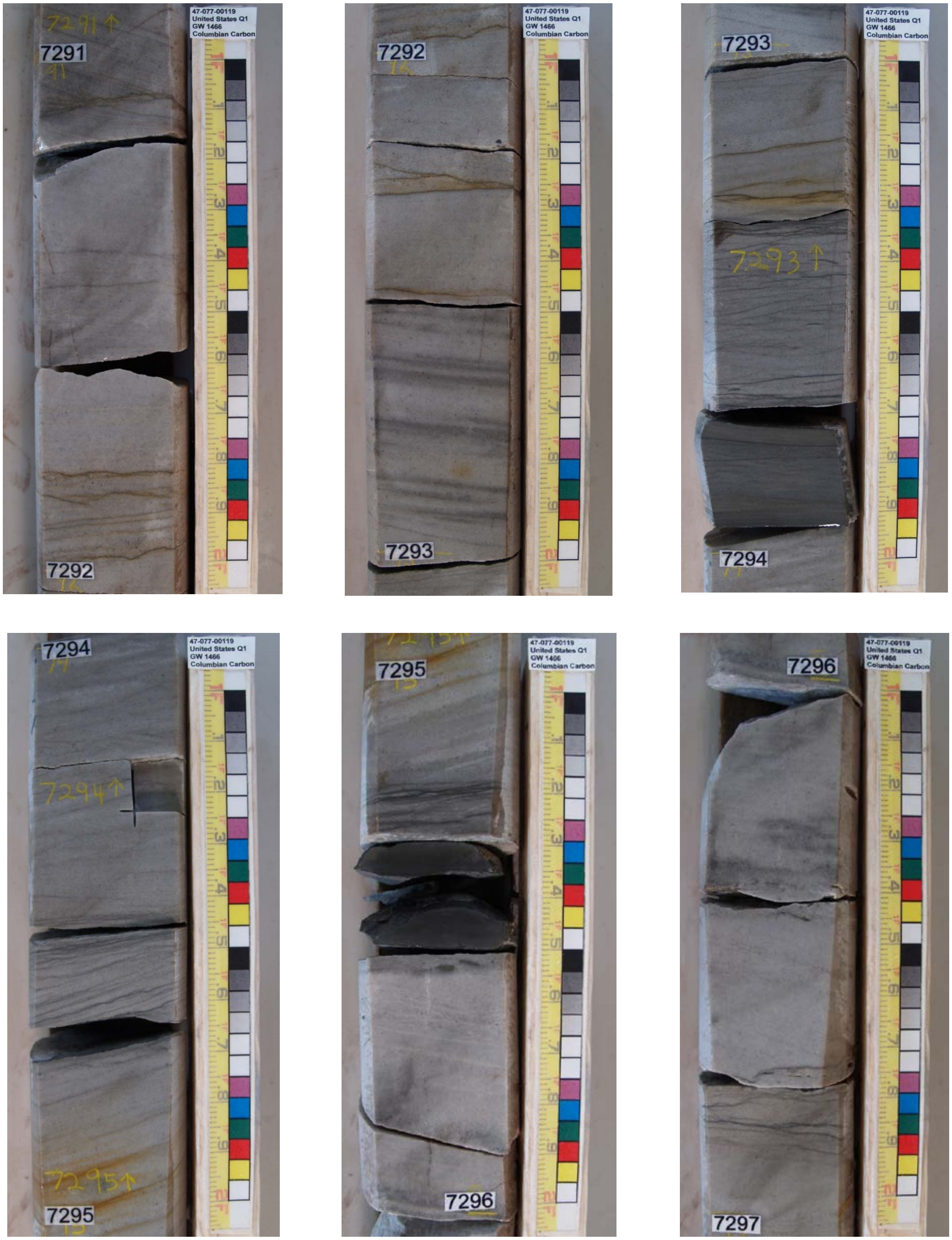

Figure 23: Pres-119 core photographs, from 7,291 to 7,297 ft.

Figure 24: Pres-119 core photographs, from 7,297 to 7,302 ft.

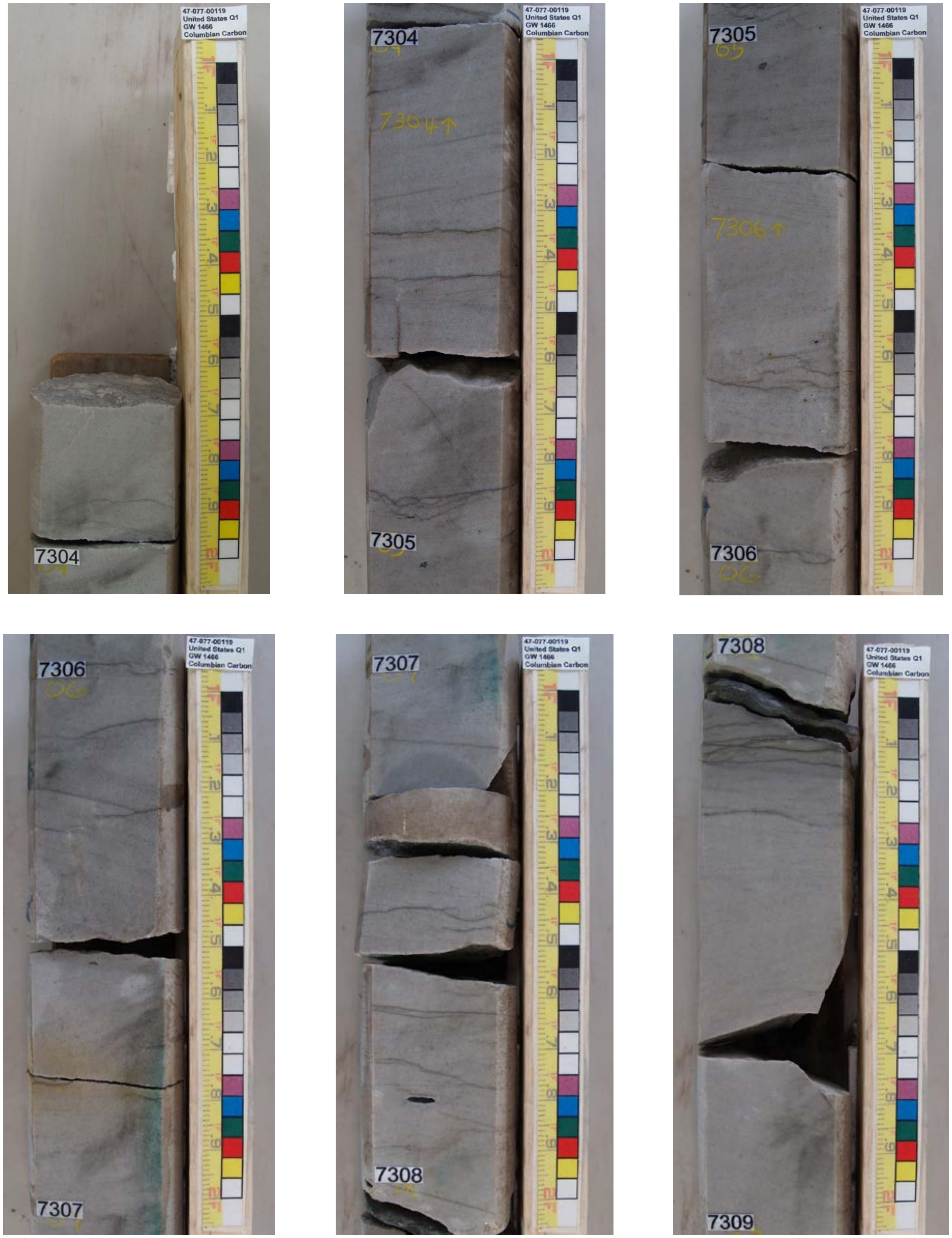

Figure 25: Pres-119 core photographs, from 7,303 to 7,309 ft.

Figure 26: Pres-119 core photographs, from 7,310 to 7,315 ft.

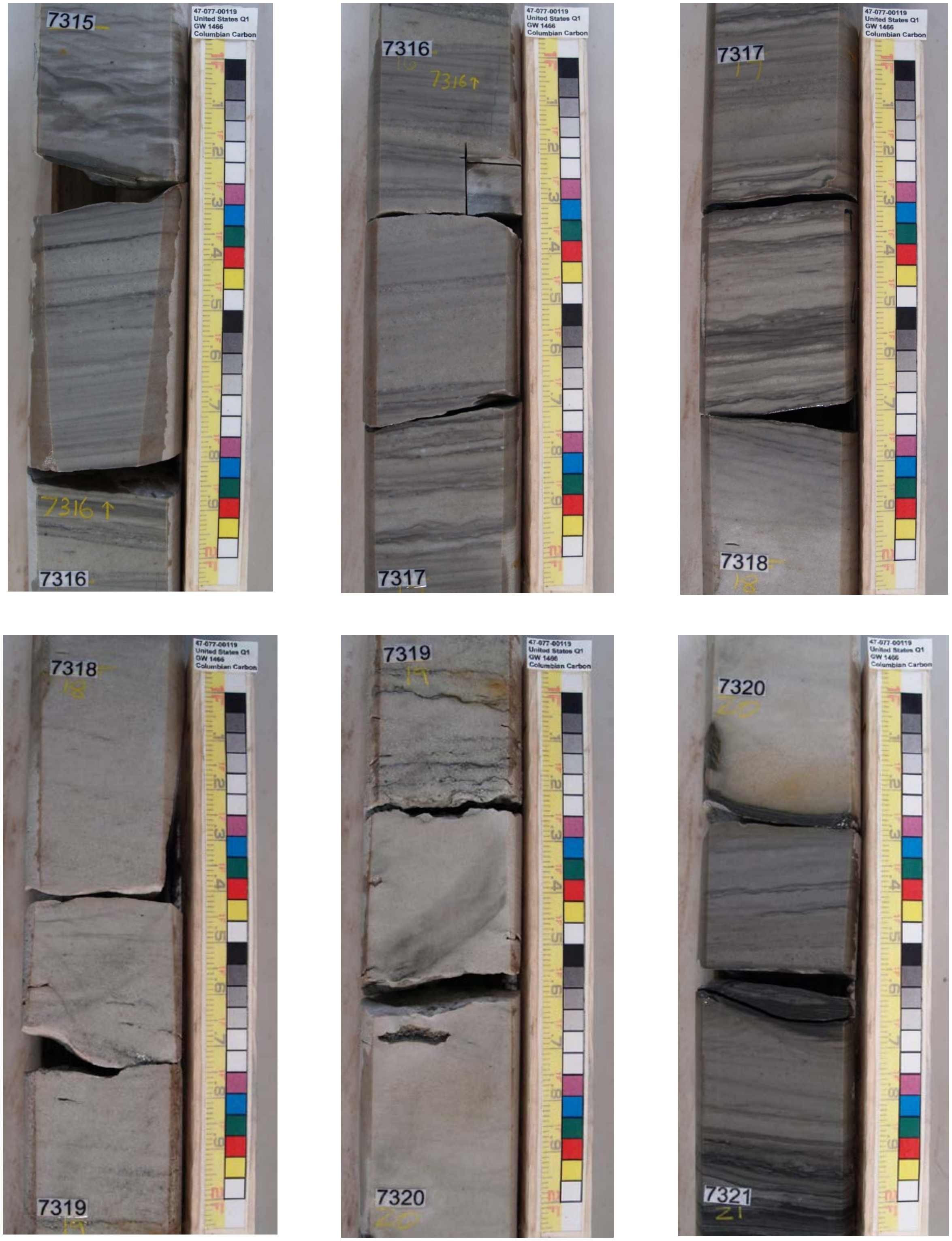

Figure 27: Pres-119 core photographs, from 7,315 to 7,321 ft.

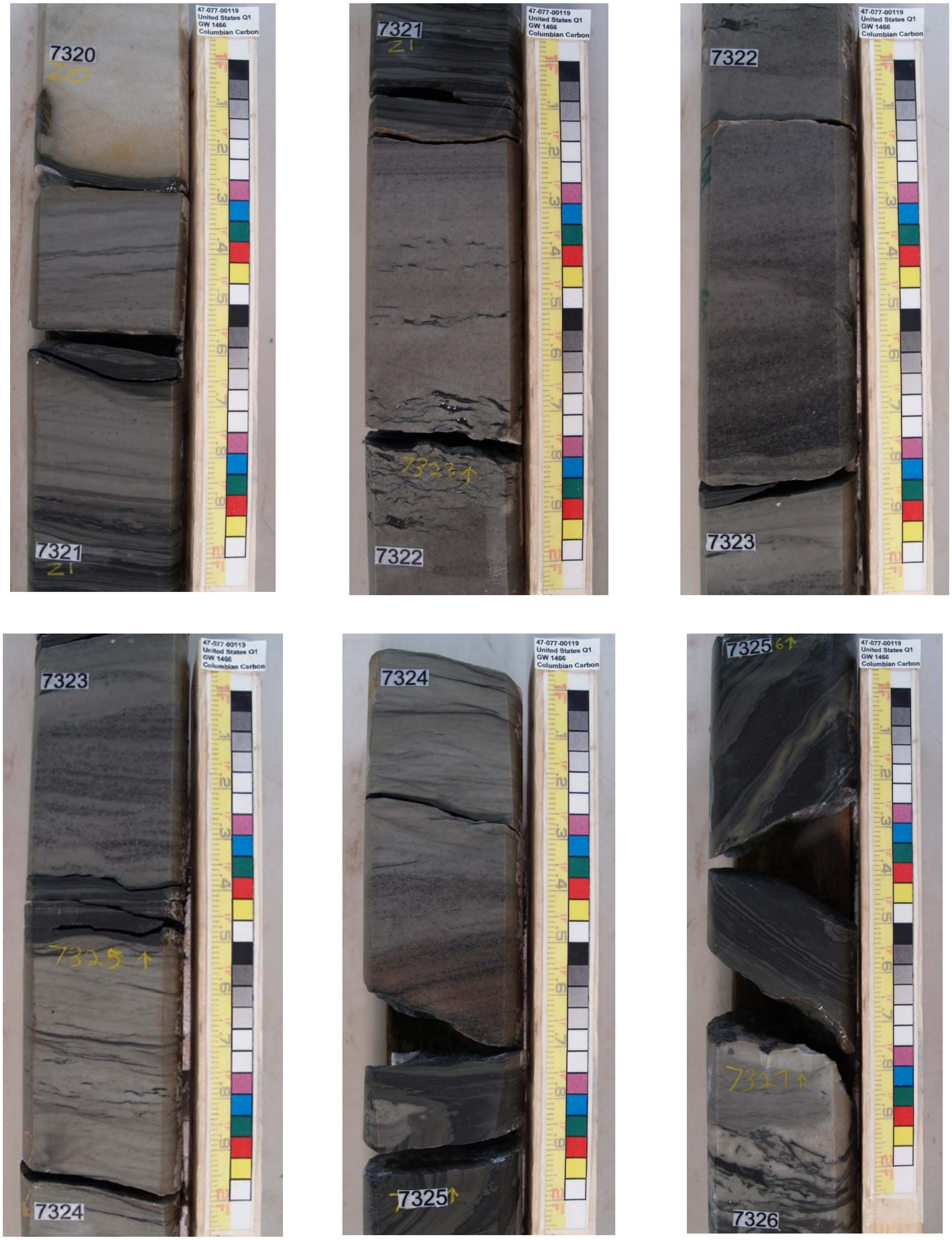

Figure 28: Pres-119 core photographs, from 7,320 to 7,326 ft.

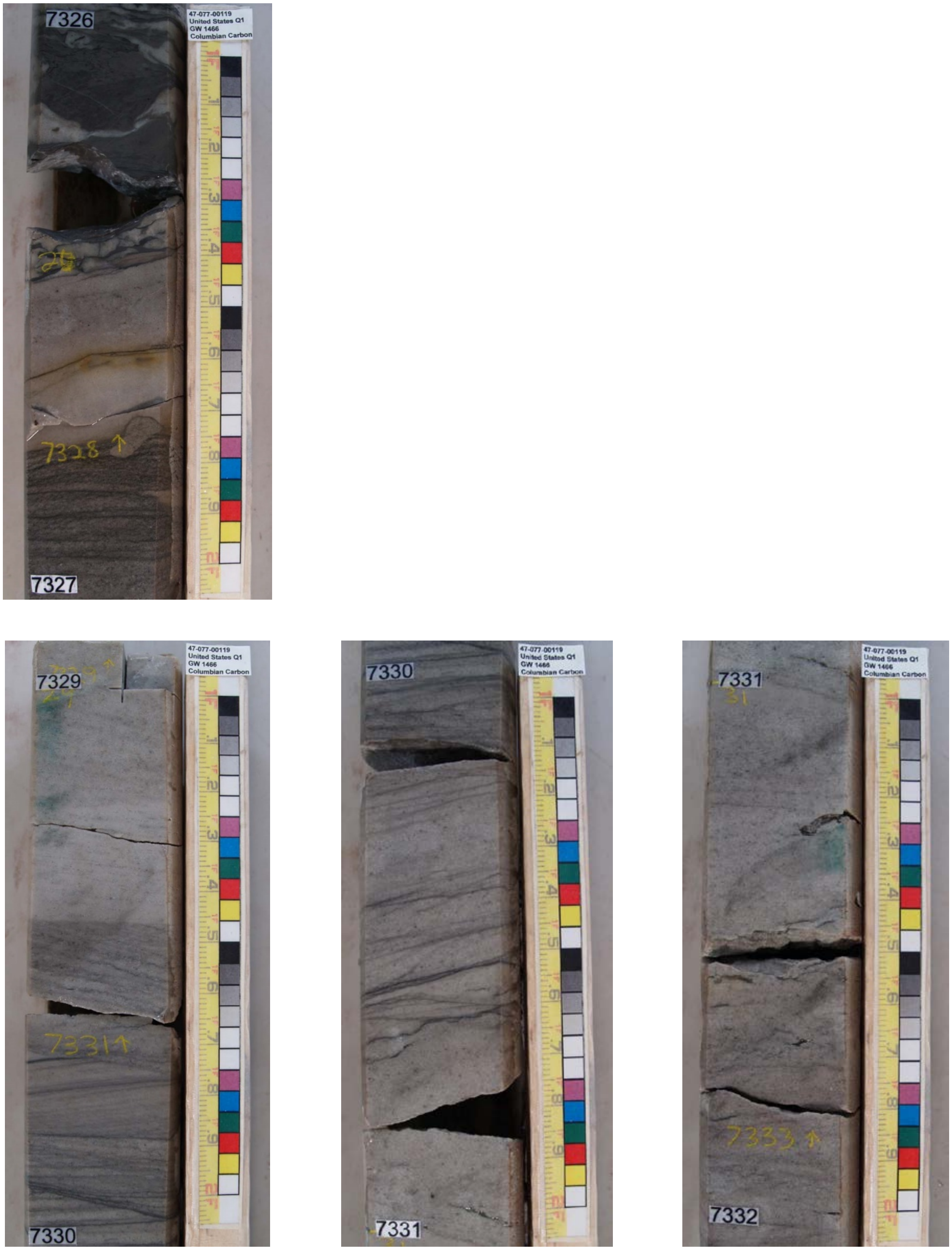

Figure 29: Pres-119 core photographs, from 7,326 to 7,332 ft.

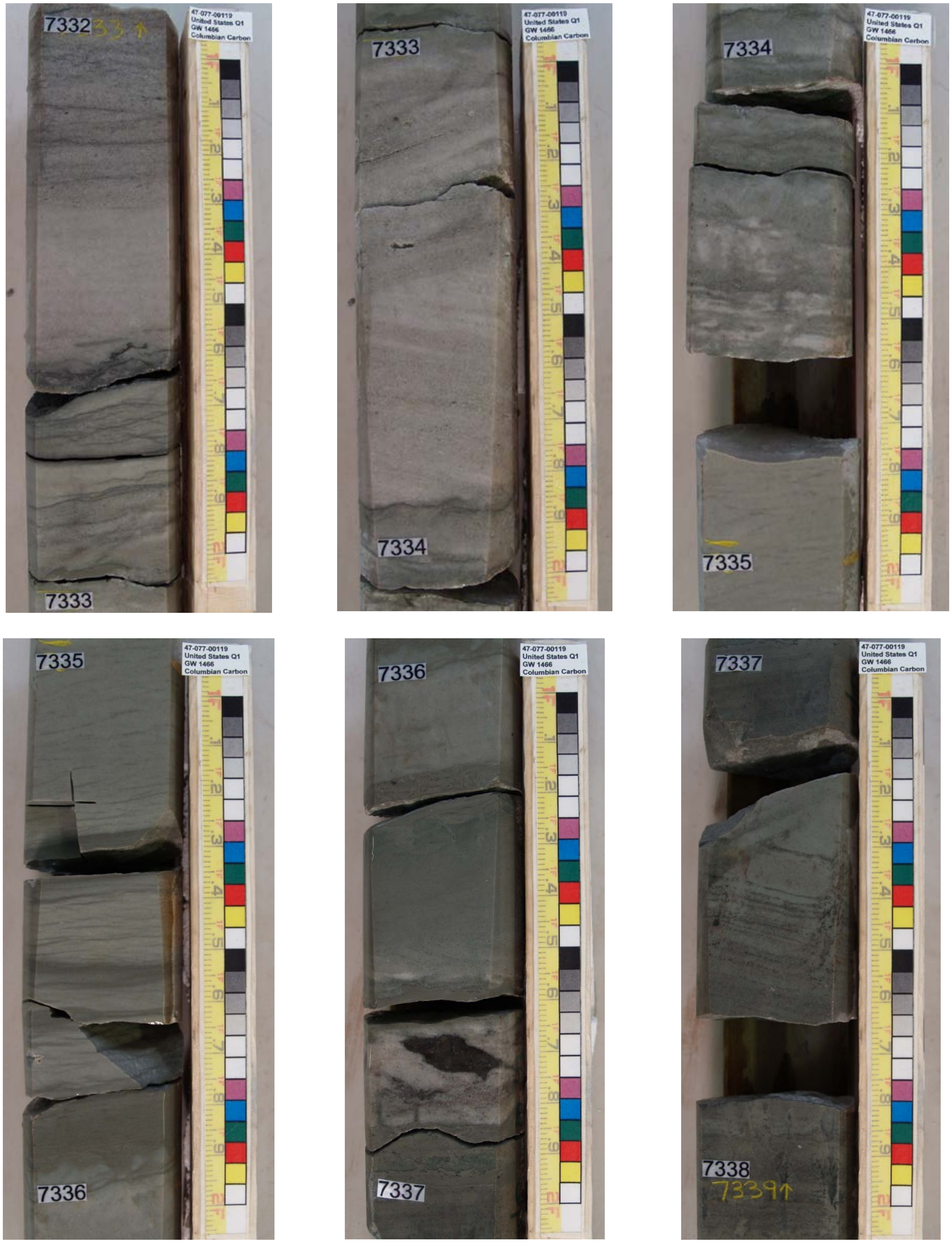

Figure 30: Pres-119 core photographs, from 7,332 to 7,338 ft.

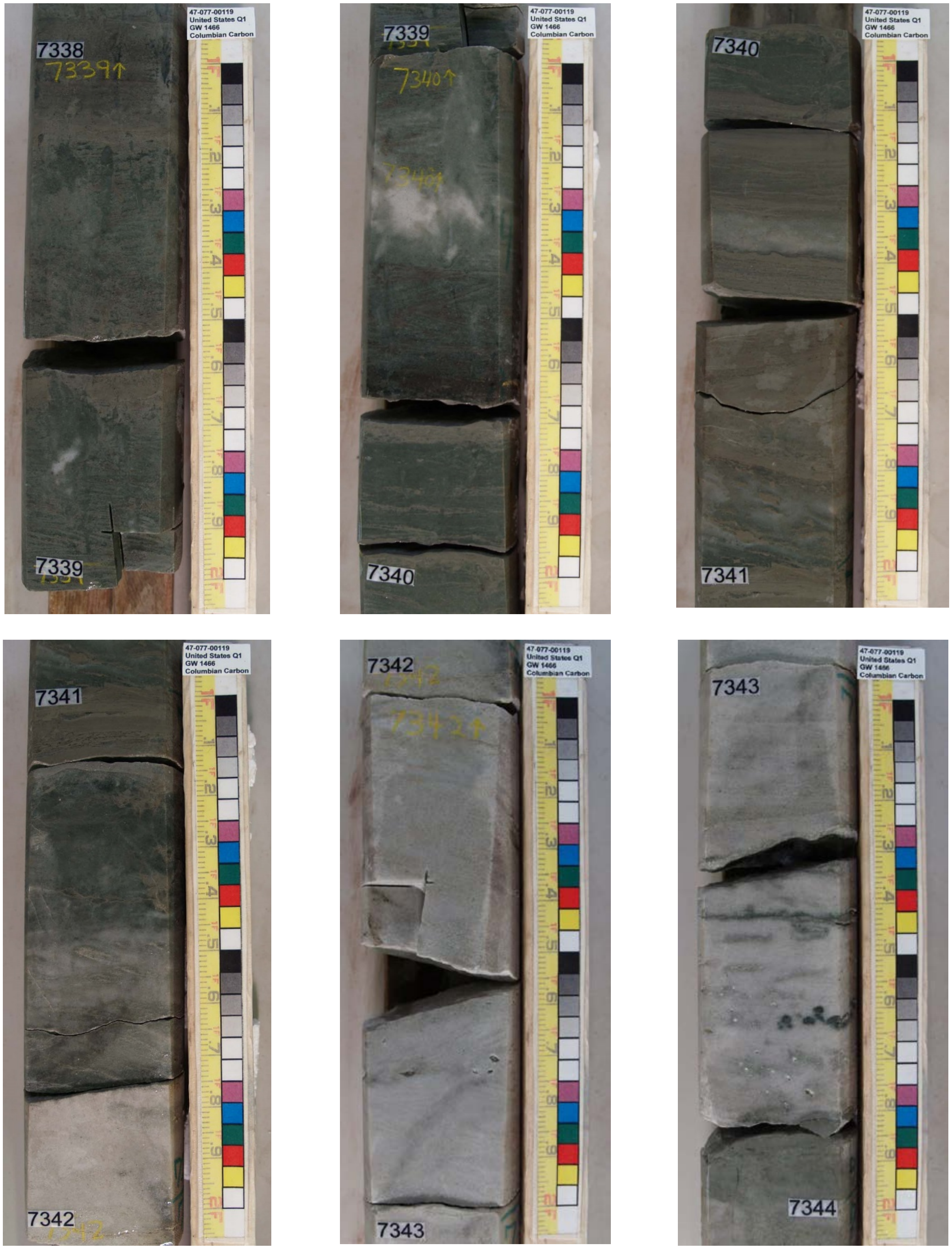

Figure 31: Pres-119 core photographs, from 7,338 to 7,344 ft.

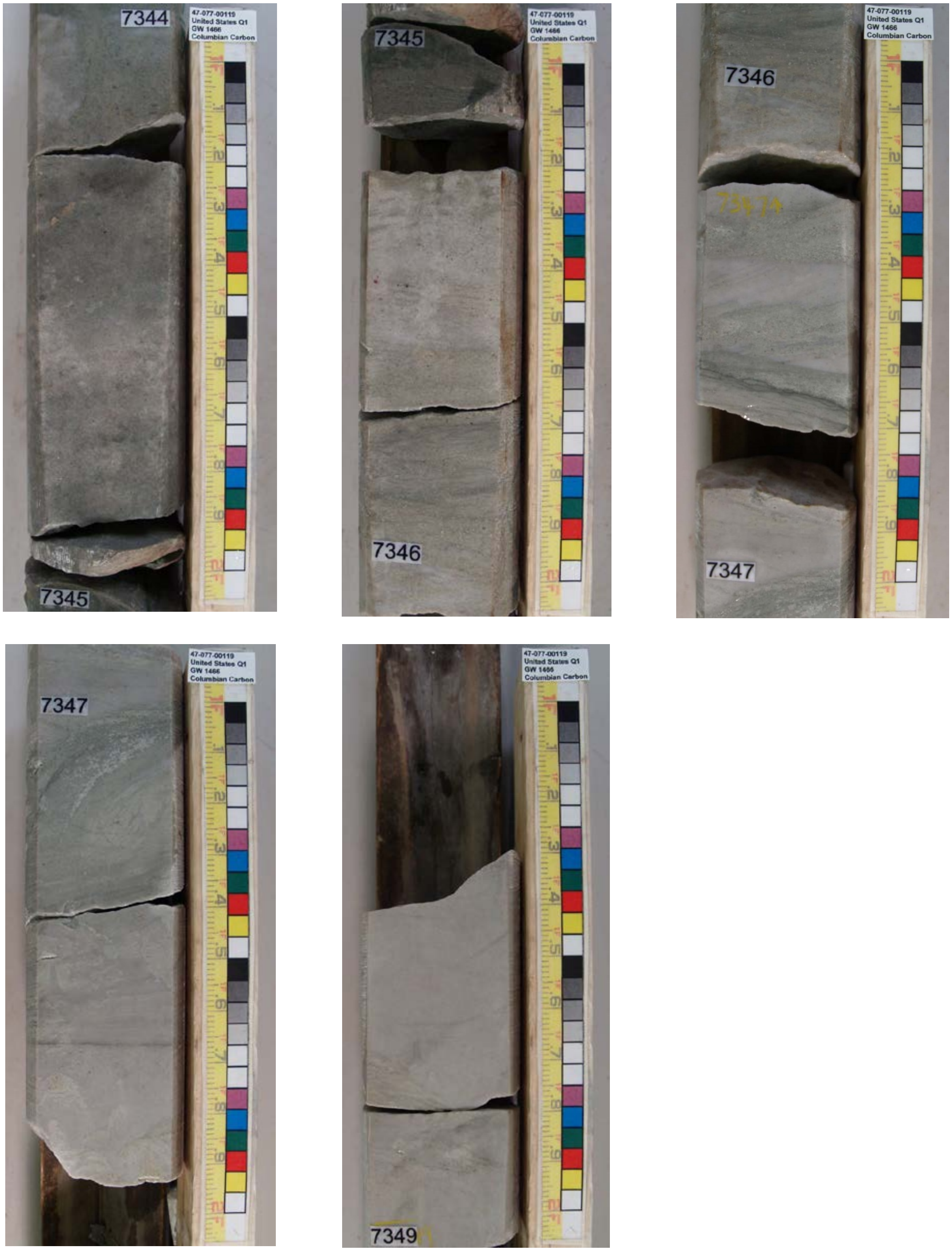

Figure 32: Pres-119 core photographs, from 7,344 to 7,349 ft.

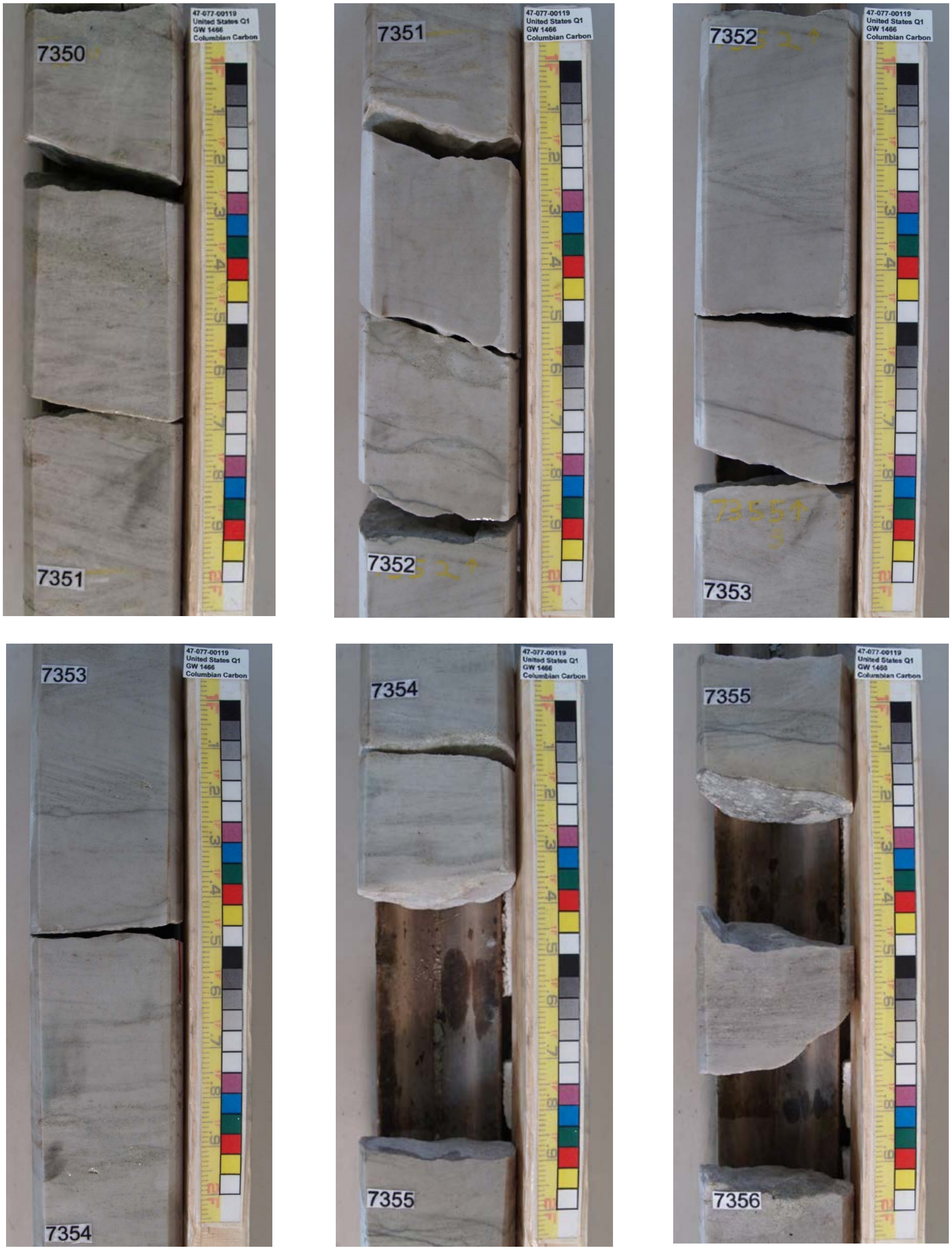

Figure 33: Pres-119 core photographs, from 7,350 to 7,356 ft.

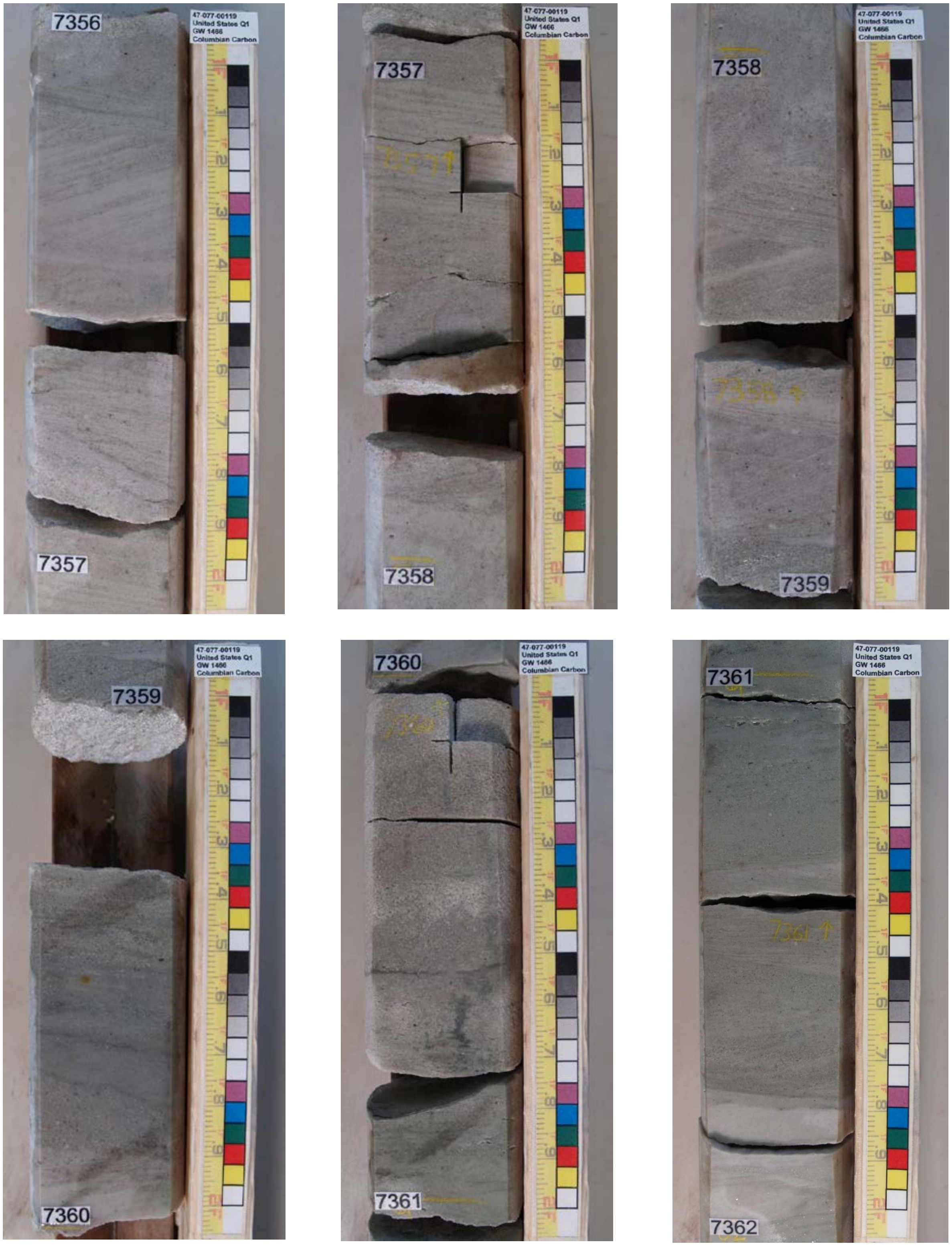

Figure 34: Pres-119 core photographs, from 7,356 to 7,362 ft.

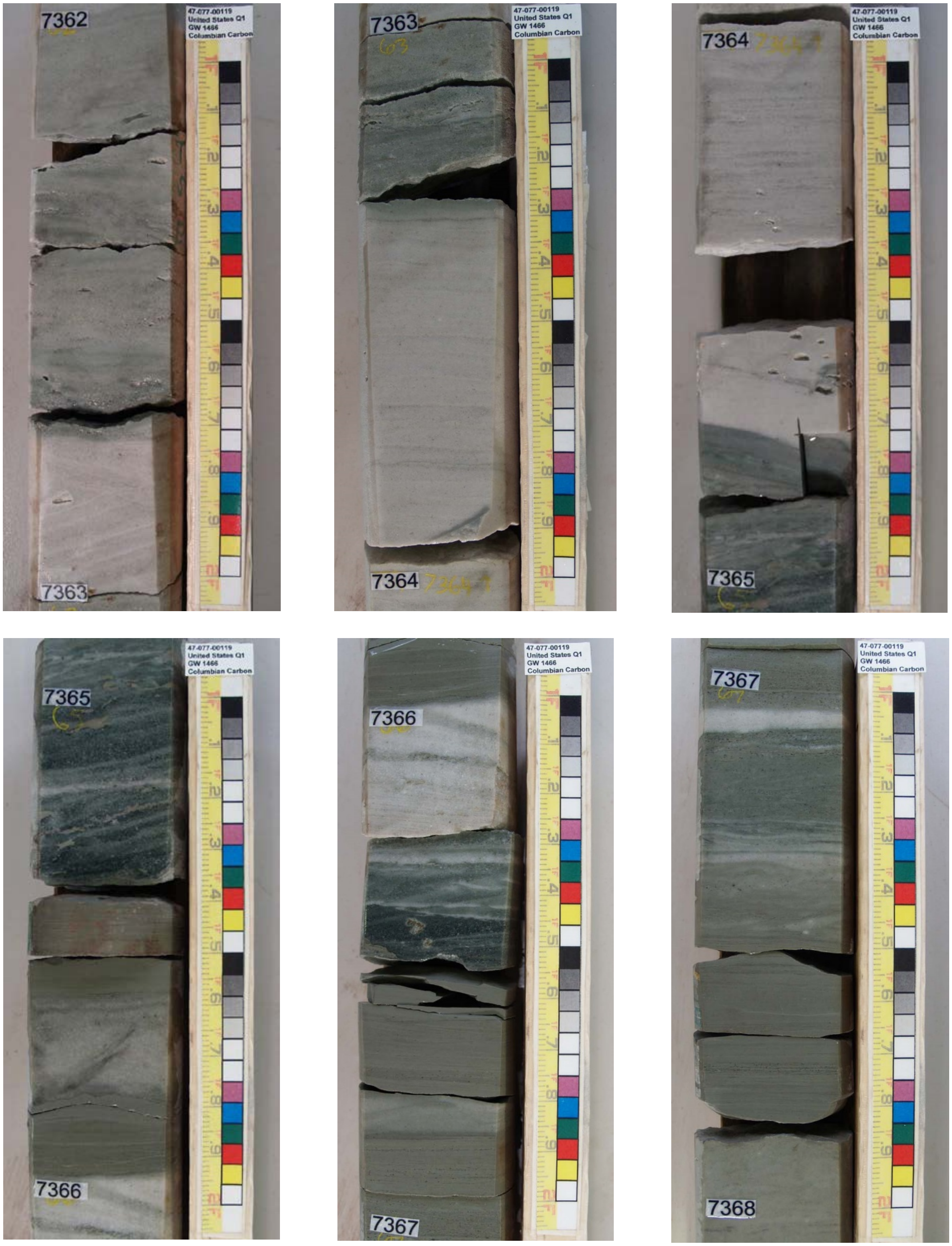

Figure 35: Pres-119 core photographs, from 7,362 to 7,368 ft.

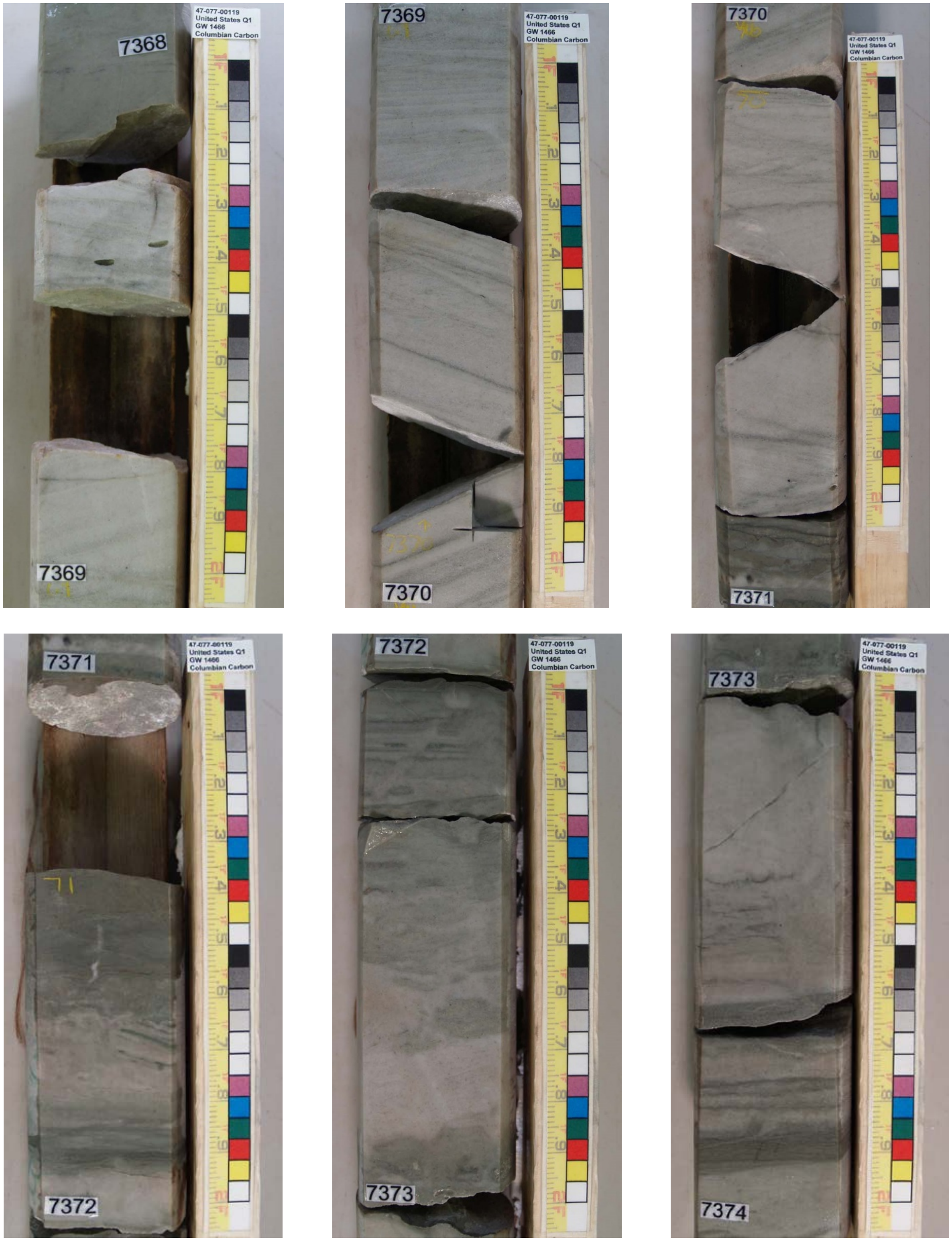

Figure 36: Pres-119 core photographs, from 7,368 to 7,374 ft.

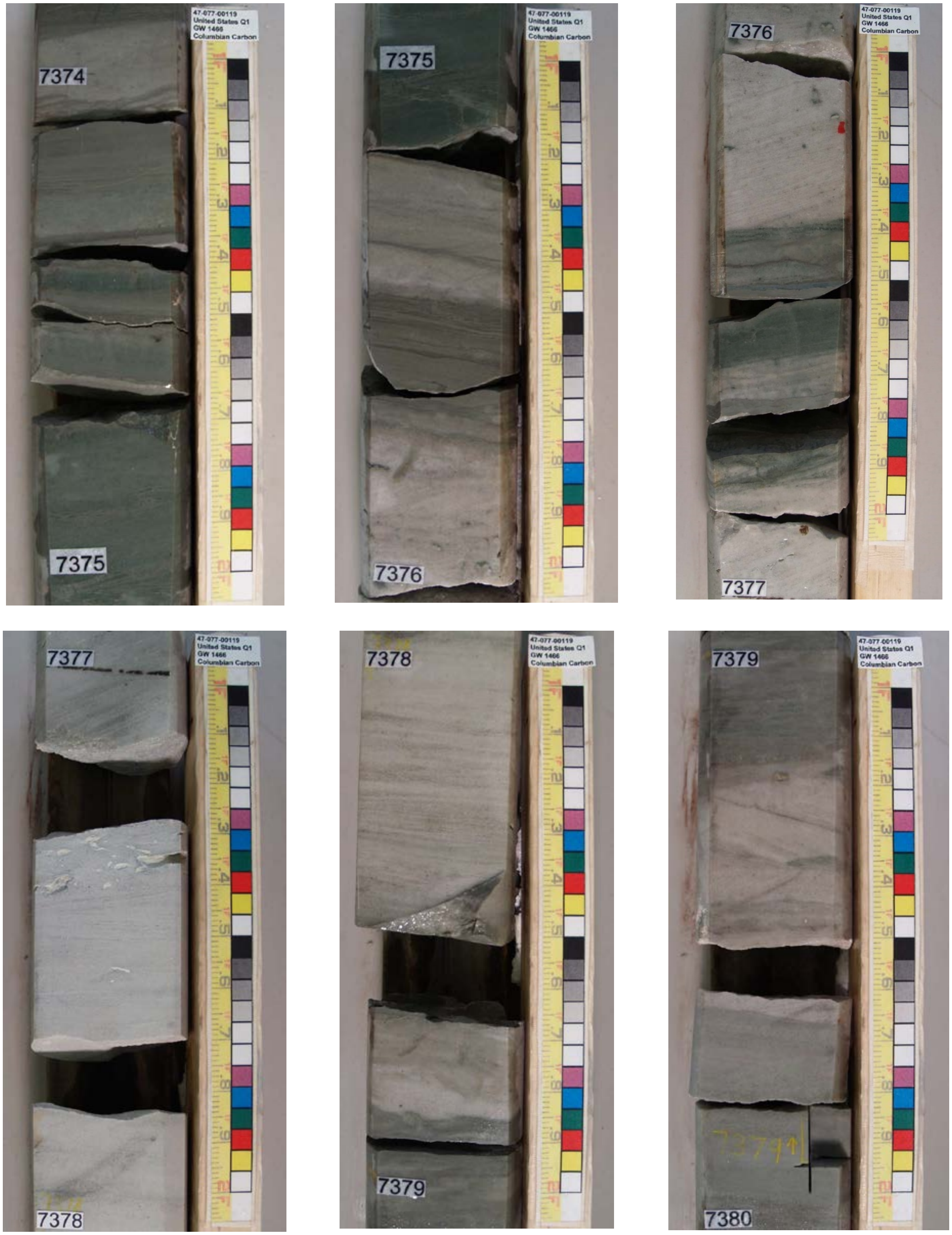

Figure 37: Pres-119 core photographs, from 7,374 to 7,380 ft.

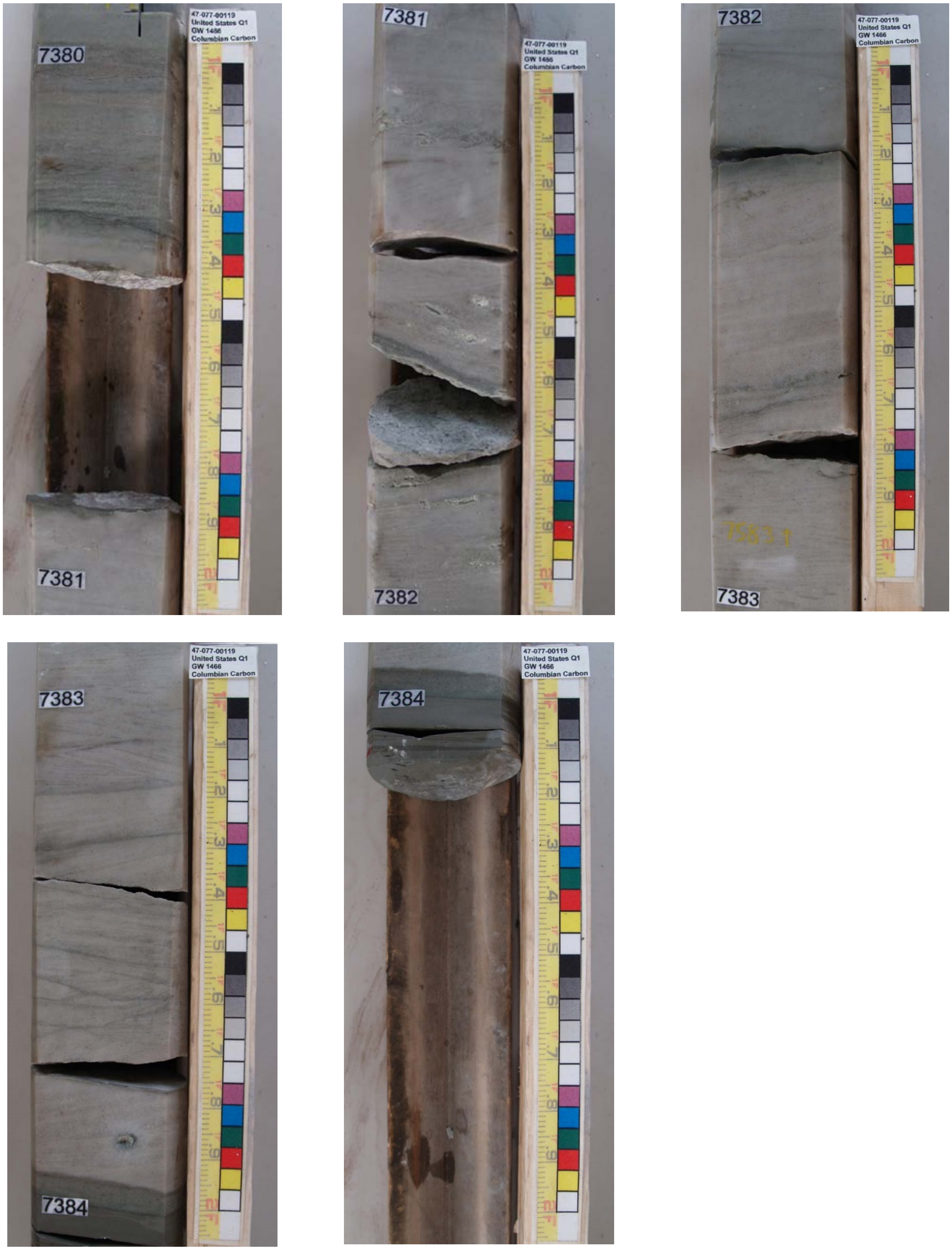

Figure 38: Pres-119 core photographs, from 7,380 to 7,385 ft.

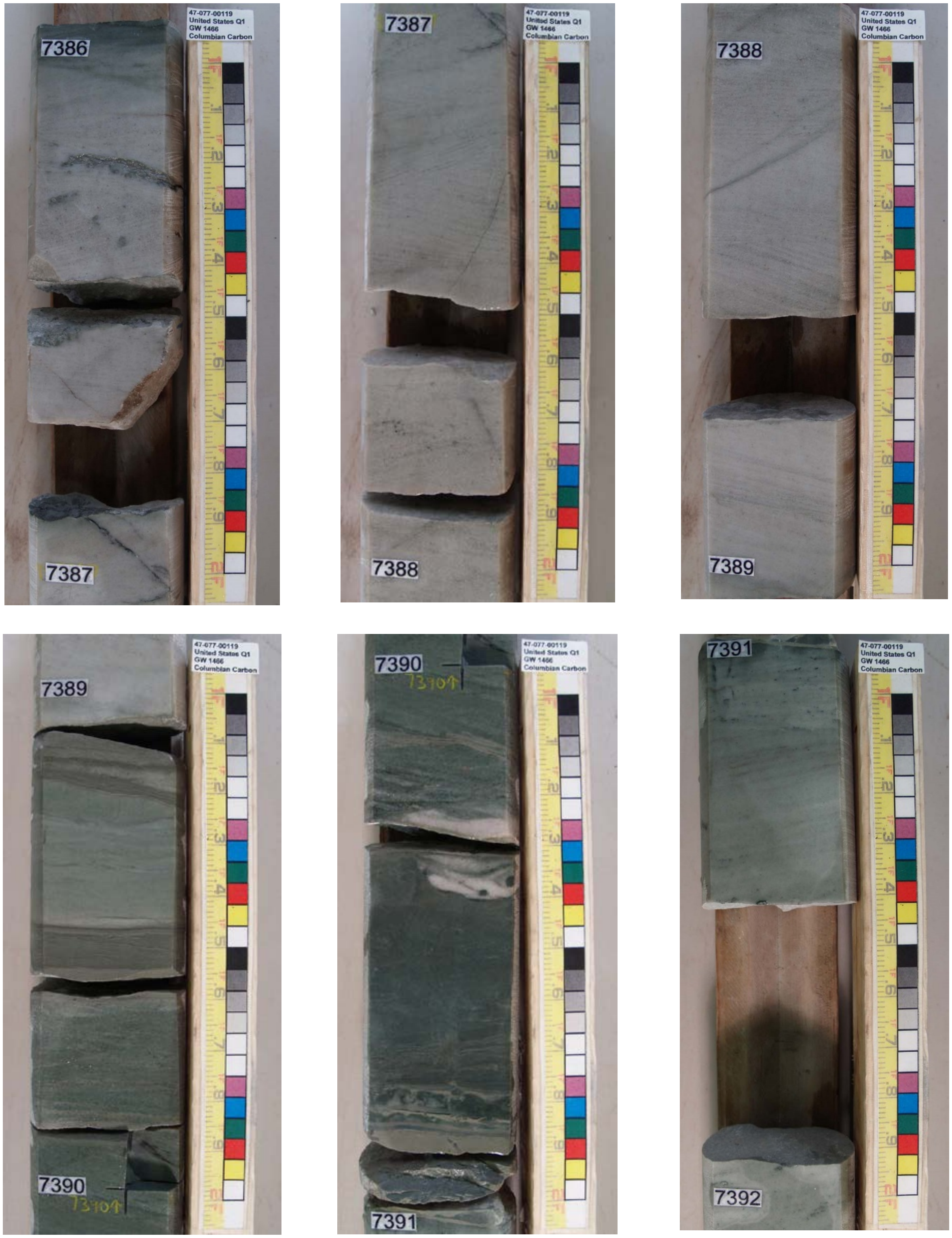

Figure 39: Pres-119 core photographs, from 7,386 to 7,392 ft.

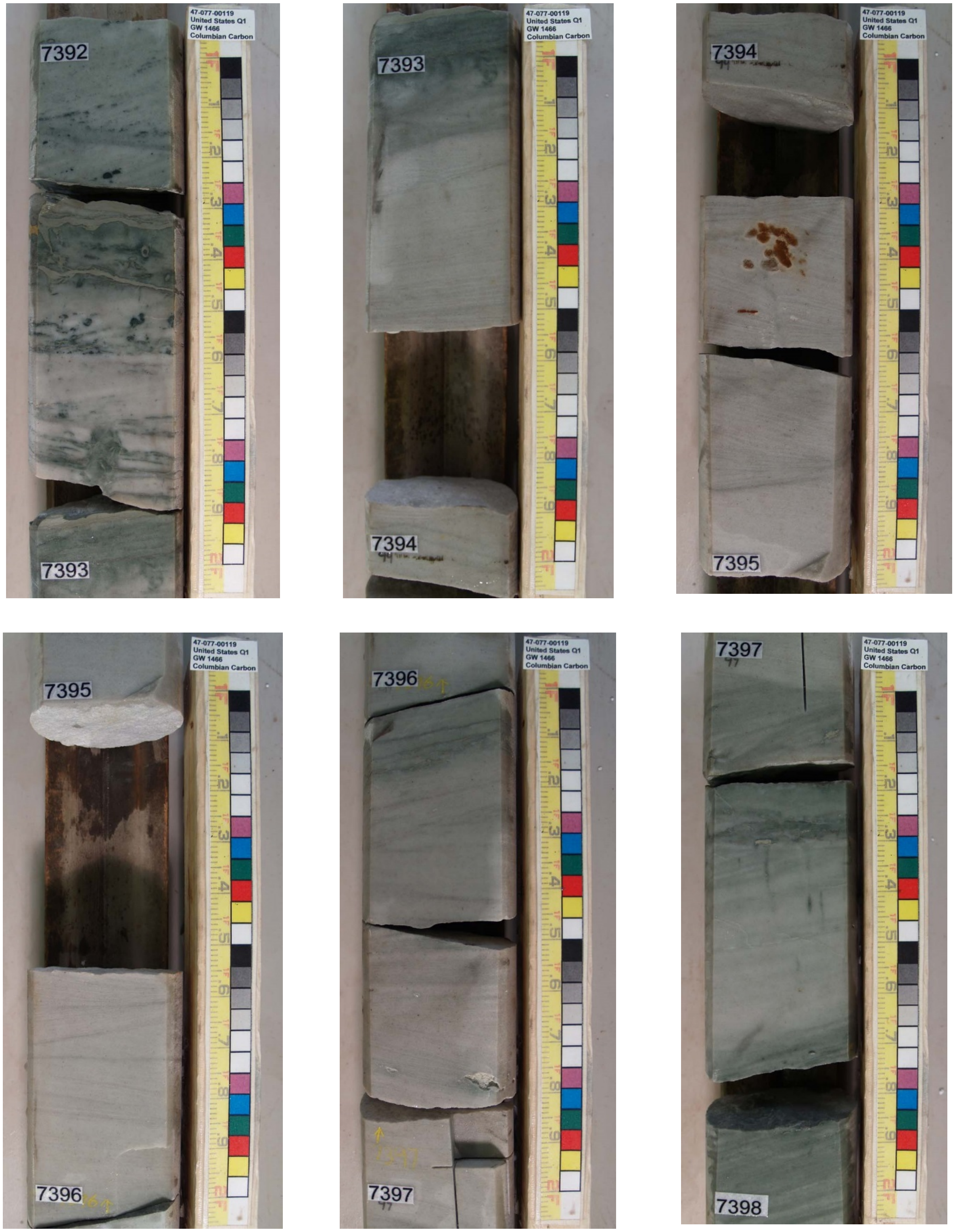

Figure 40: Pres-119 core photographs, from 7,392 to 7,398 ft.

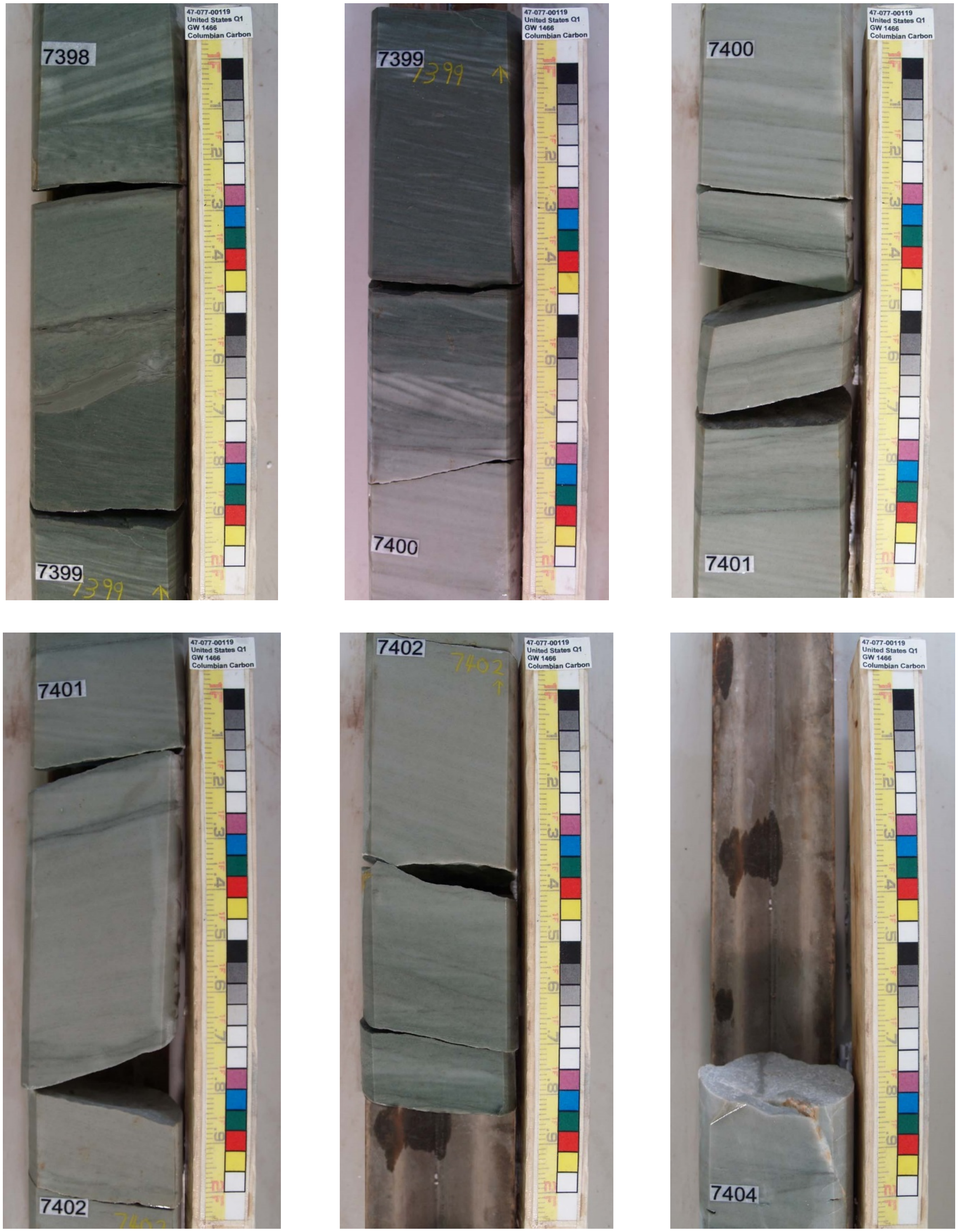

Figure 41: Pres-119 core photographs, from 7,398 to 7,404 ft.

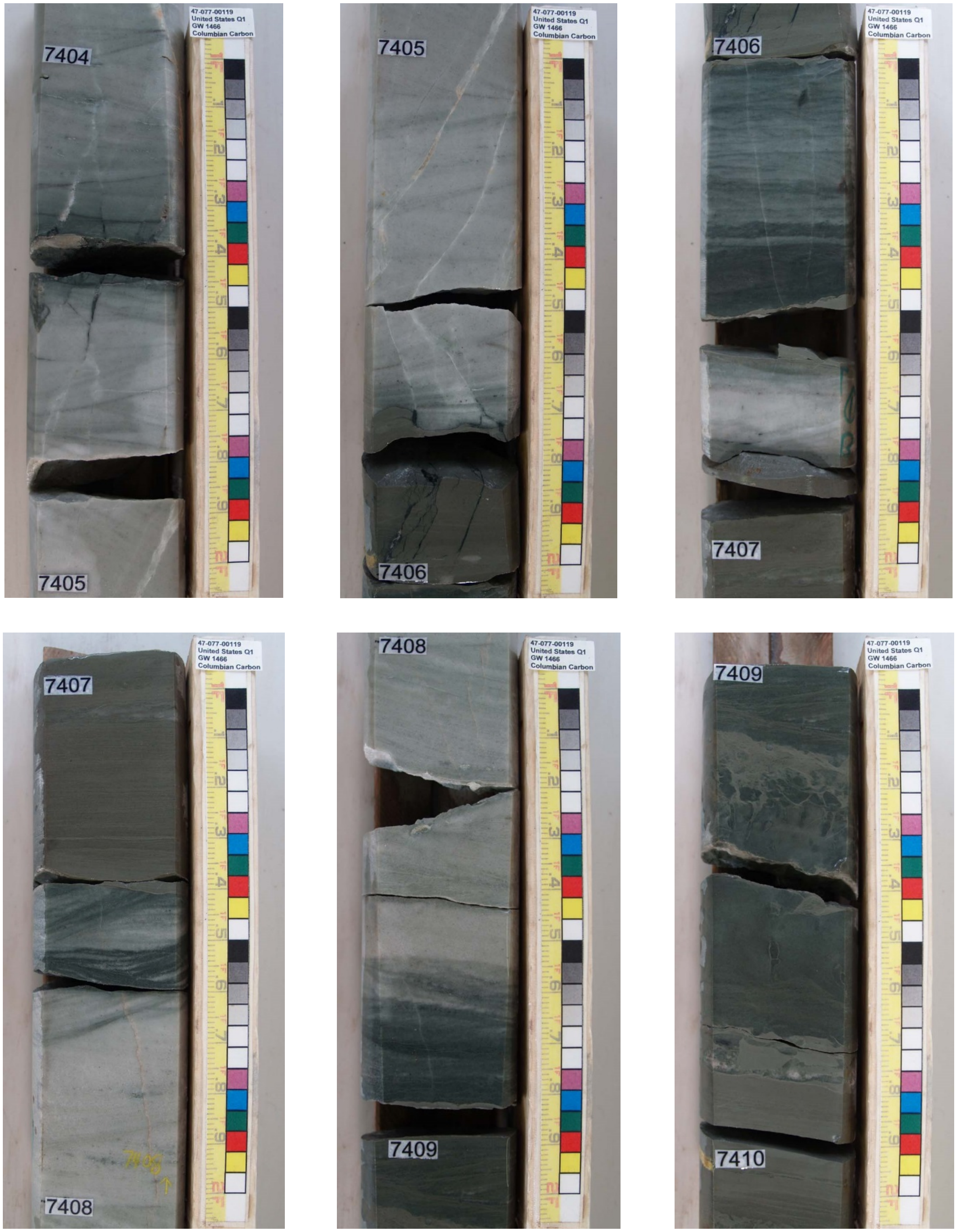

Figure 42: Pres-119 core photographs, from 7,404 to 7,410 ft.

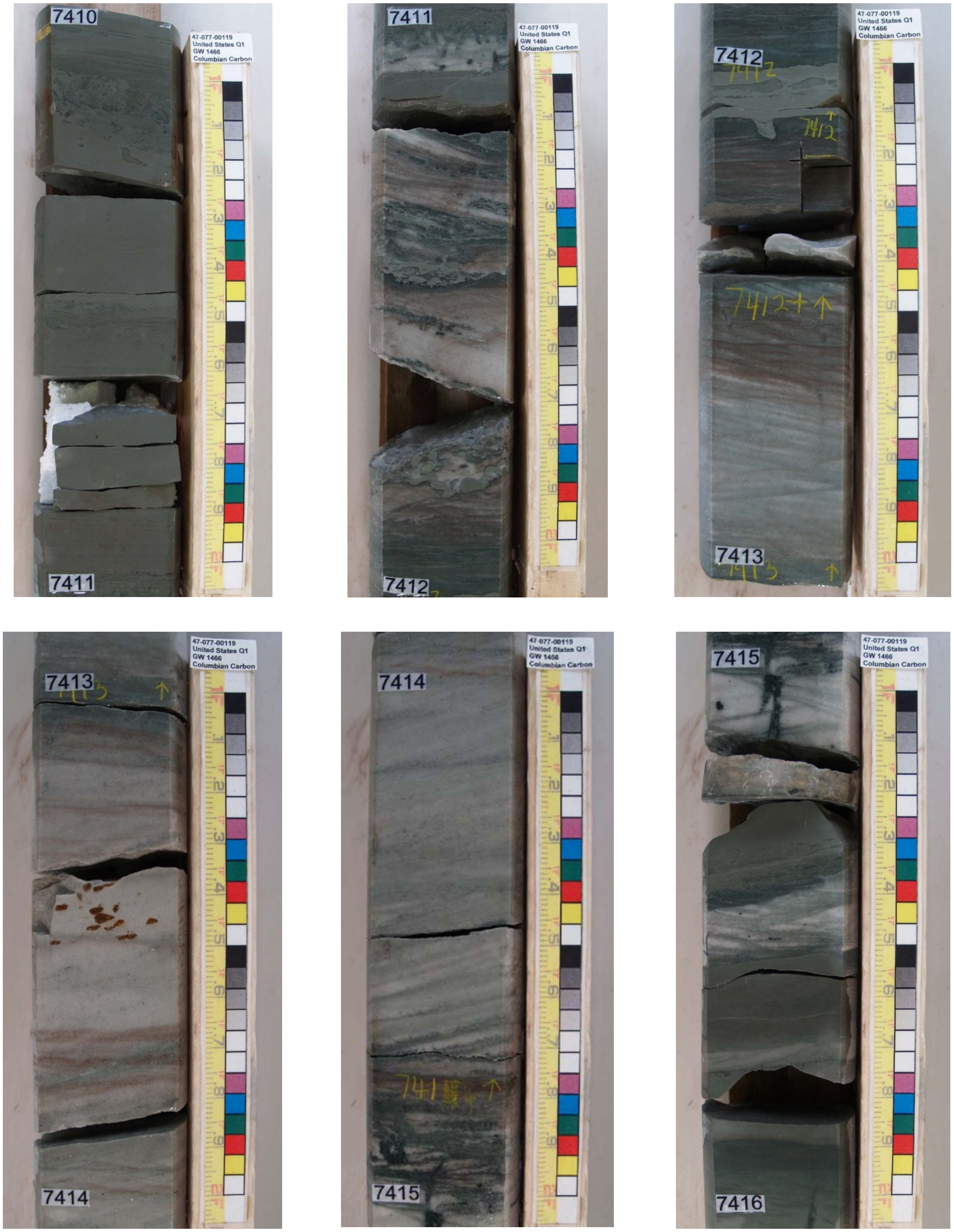

Figure 43: Pres-119 core photographs, from 7,411 to 7,416 ft.

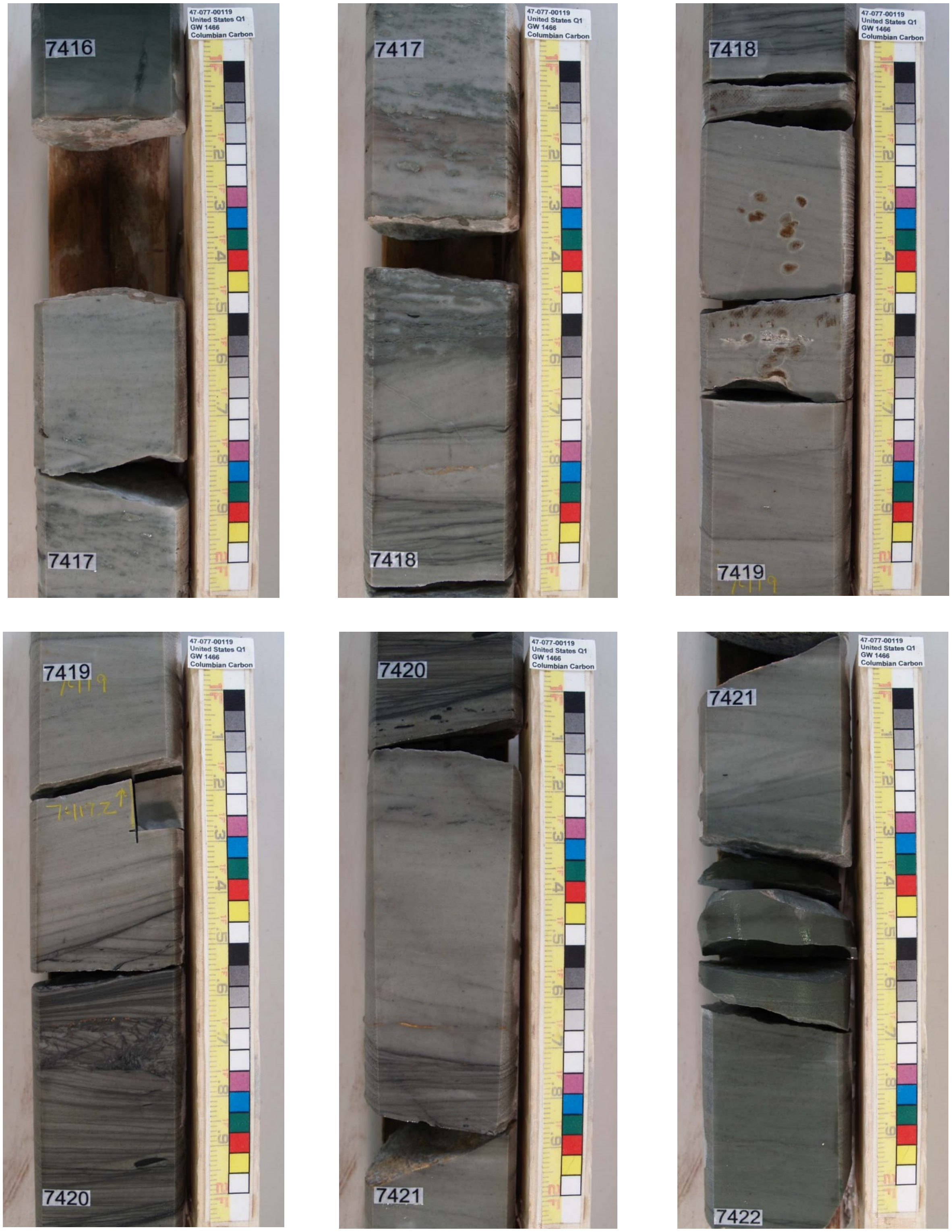

Figure 44: Pres-119 core photographs, from 7,416 to 7,422 ft.

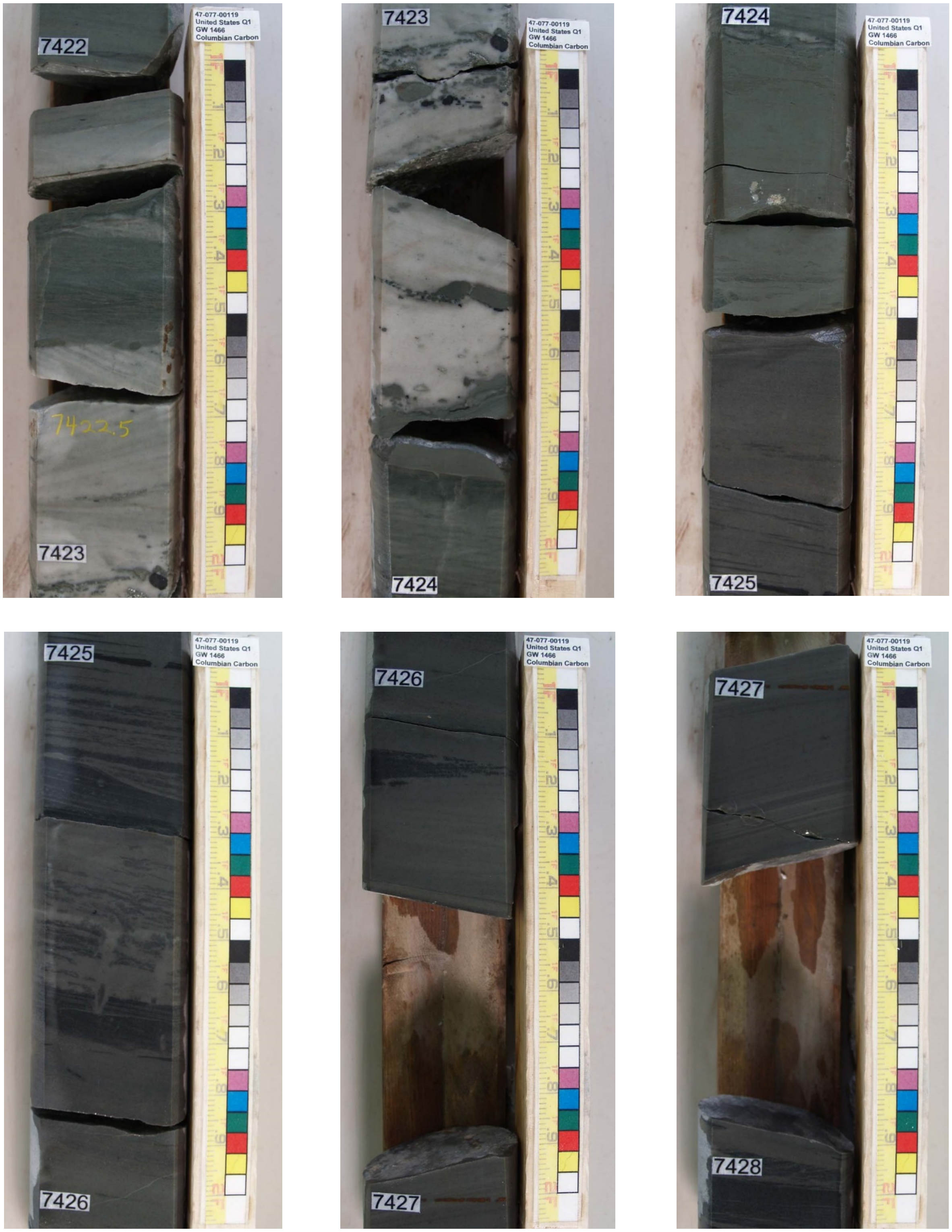

Figure 45: Pres-119 core photographs, from 7,422 to 7,428 ft.

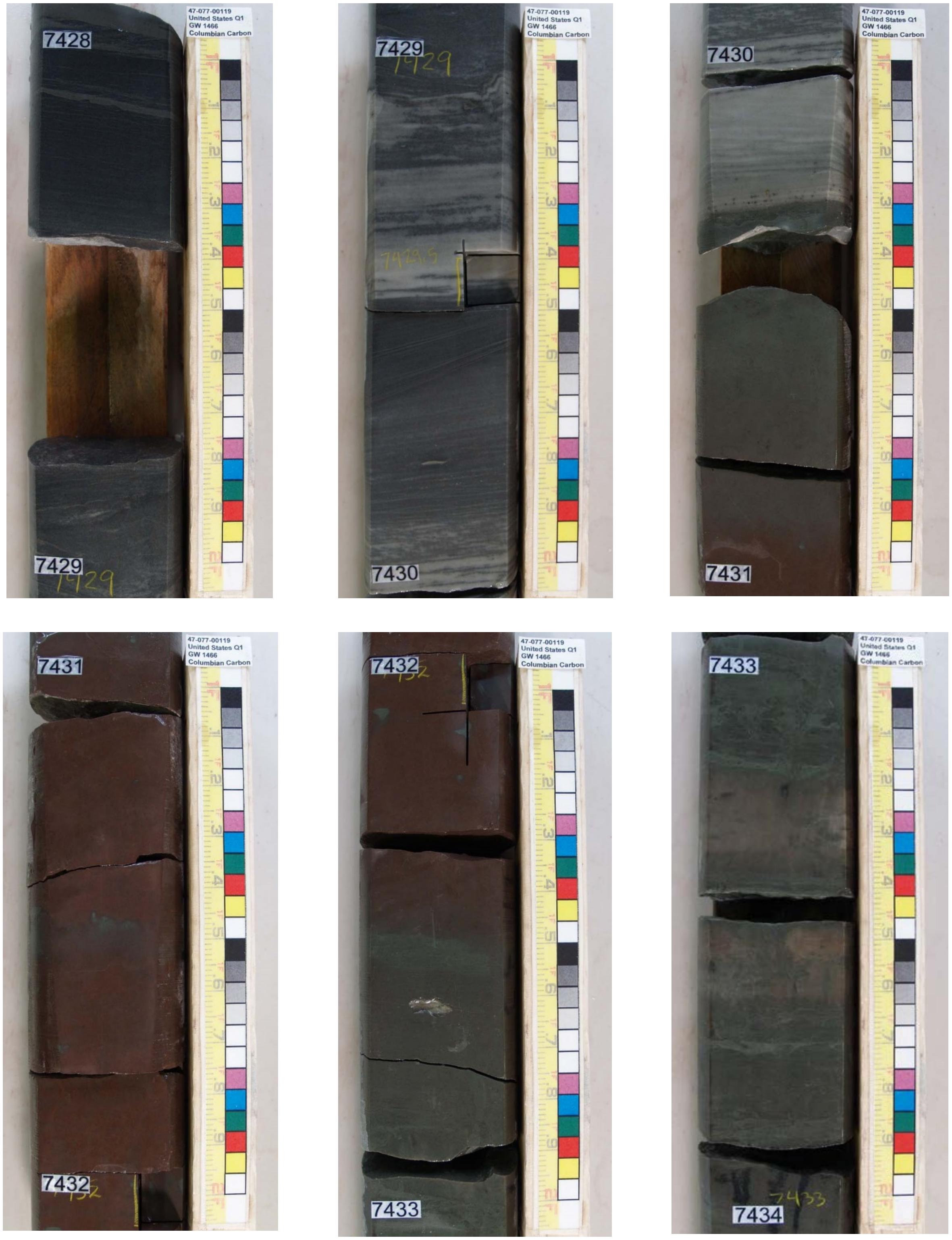

Figure 46: Pres-119 core photographs, from 7,428 to 7,434 ft.

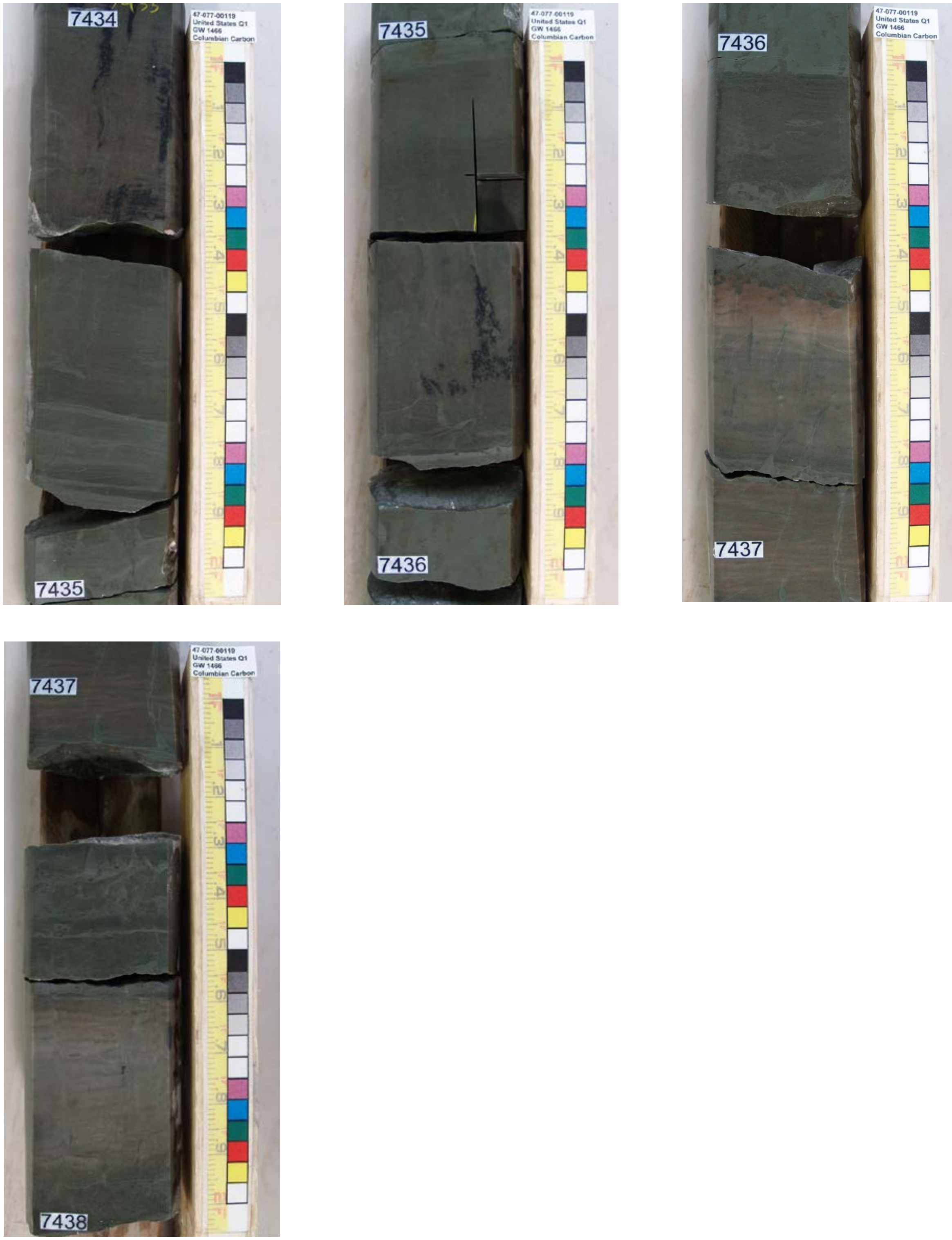

Figure 47: Pres-119 core photographs, from 7,434 to 7,438 ft.

3. DATA ACQUISITION AND METHODOLOGY

The core was evaluated using CT scanning and traditional core logging. CT scans and core logging were performed on the 2/3 slabbed cores shown in the previous photographs to maximize the internal area of the core that could be visualized.

3.1 MEDICAL CT SCANNING

Core scale CT scanning was done with a medical Toshiba® Aquilion TSX-101A/R medical Scanner as shown in Figure 48. The medical CT scanner generates images with a resolution in the millimeter range, with scans having voxel resolutions of 0.43 x 0.43 mm in the XY plane and 0.50 mm along the core axis. The scans were conducted at a voltage of 135 kV and at 200 mA. Subsequent processing and combining of stacks was performed to create three-dimensional (3D) volumetric representations of the cores and a two-dimensional (2D) cross-section through the middle of the core samples using ImageJ (Rasband, 2018). The variation in greyscale values observed in the CT images indicates changes in the CT number obtained from the CT scans, which is directly proportional to changes in the attenuation and density of the scanned rock. Darker regions are less dense. While the medical CT scanner was not used for detailed characterization in this study, it allowed for non-destructive bulk characterization of the core, and thus complimented the MSCL data on the resultant logs.

Figure 48: Toshiba® Aquilion™ Multislice Helical Computed Tomography Scanner at the NETL used for core analysis.

3.2 DUAL ENERGY SCANS

This data can be accessed from NETL's Energy Data eXchange (EDX) online system using the following link: https://edx.netl.doe.gov/dataset/preston-119-well.

4. RESULTS

Processed 2D slices of the medical CT scans through the cores are shown first, followed by the dual energy scans.

4.1 MEDICAL CT SCANS

As previously discussed, the variation in greyscale values observed in the medical CT images indicates changes in the CT number obtained, which is directly proportional to changes in the attenuation and density of the scanned rock (i.e. darker regions are less dense).

Core was scanned in 3 ft or smaller sections due to the limitation of how many images could be generated for each scan. In highly-fractured core, sections in excess of 3 ft were often scanned. Detailed information in log books and photographs of cores were used to merge multiple scans of cores when this occurred. In the following images, the reported depth (top and bottom) for each scanned sub-section of core is listed. Scans marked with an asterisk(*) were named as received from the original study, but have significant overlap and redundancy. Since the cores were scanned as received, there is no way to differentiate which depths are correct.

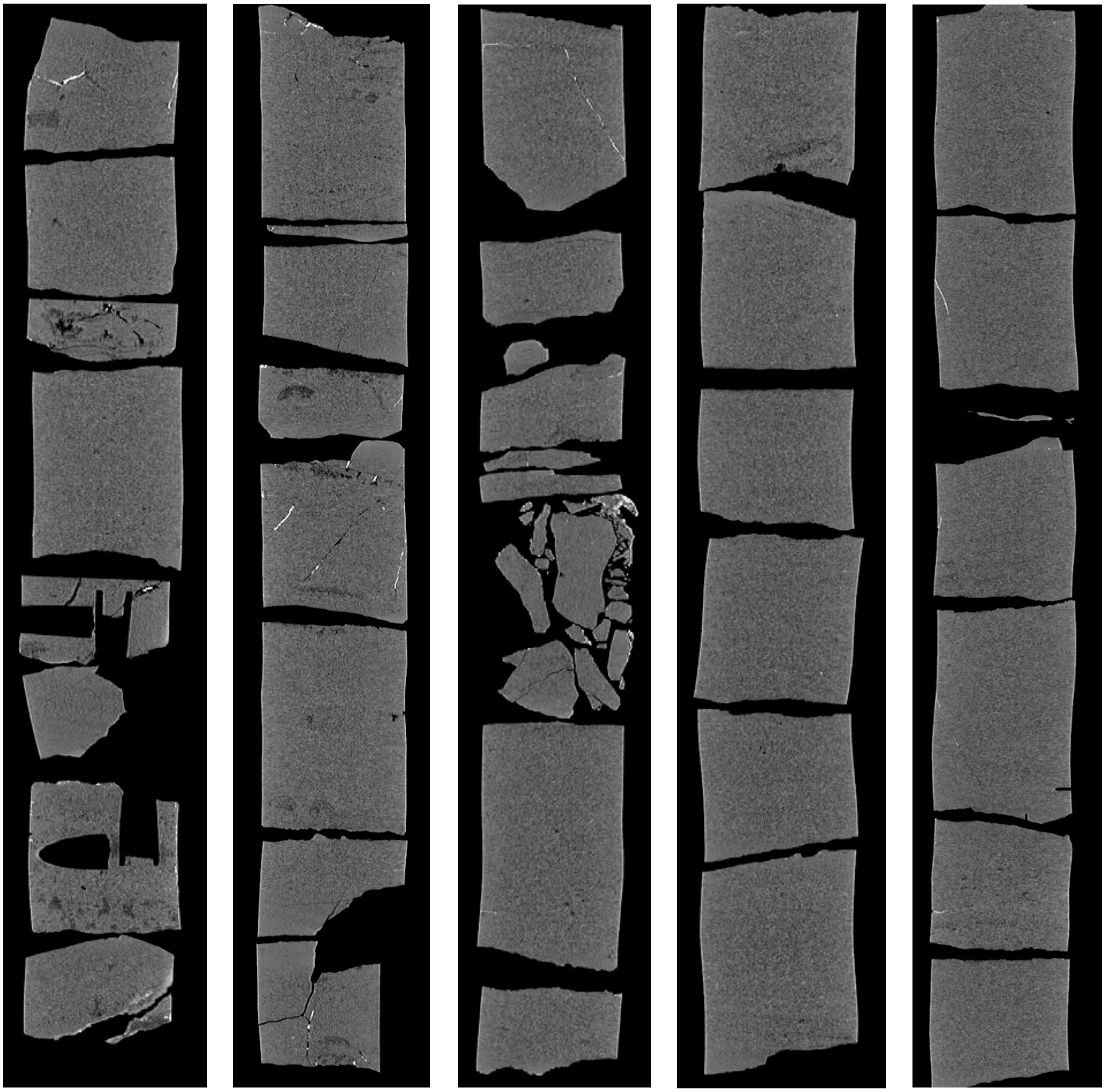

7,153–7,156 **7,156–7,159** **7,159–7,161** **7,161–7,164** **7,164–7,167***

Figure 49: 2D isolated planes through the vertical center of the medical CT scans of the Pres-119 core from 7,153 to 7,167 ft.

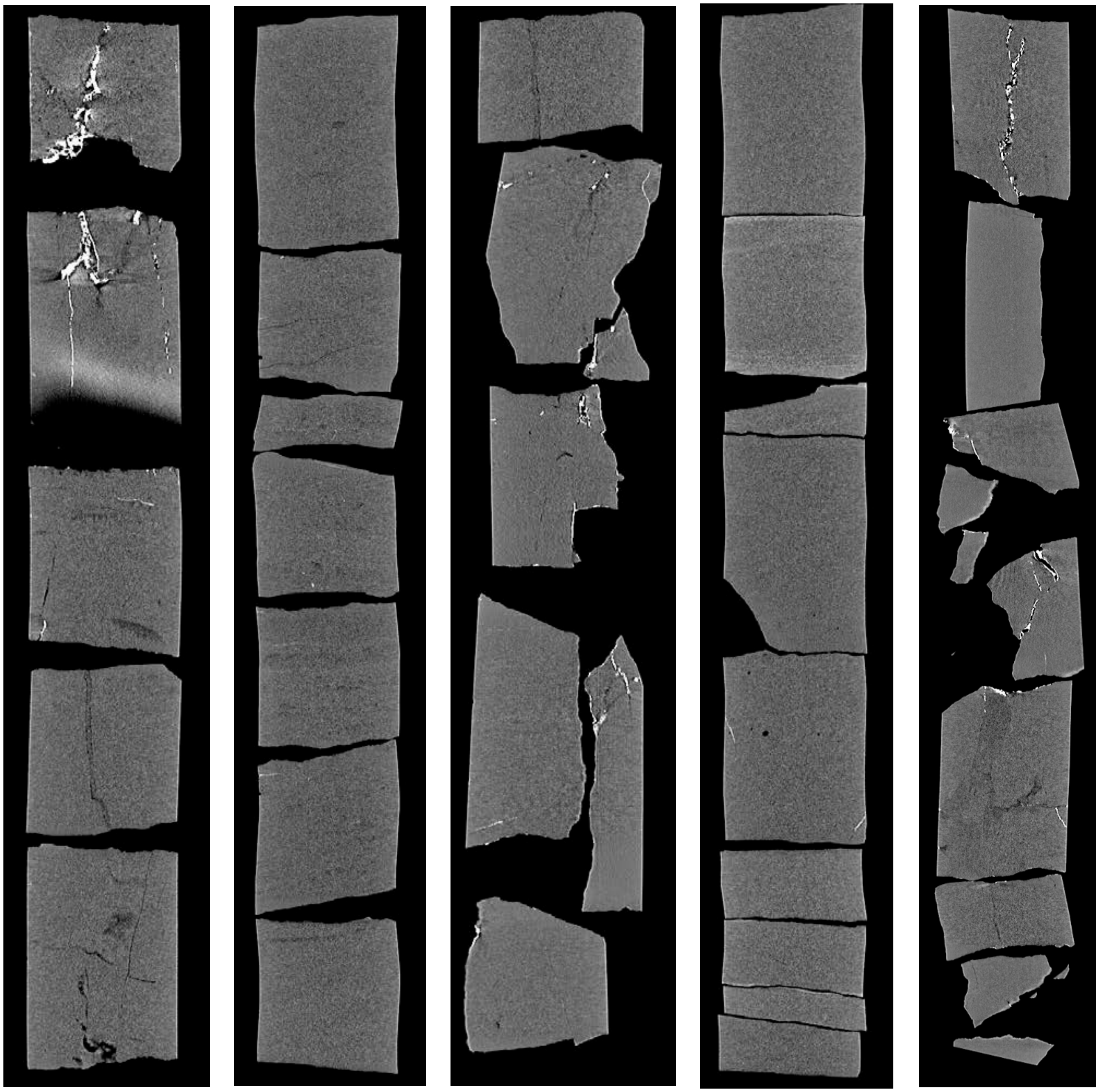

7,164–7,167* **7,167–7,170*** **7,168–7,170*** **7,170–7,173*** **7,170–7,175***

Figure 50: 2D isolated planes through the vertical center of the medical CT scans of the Pres-119 core from 7,164 to 7,175 ft.

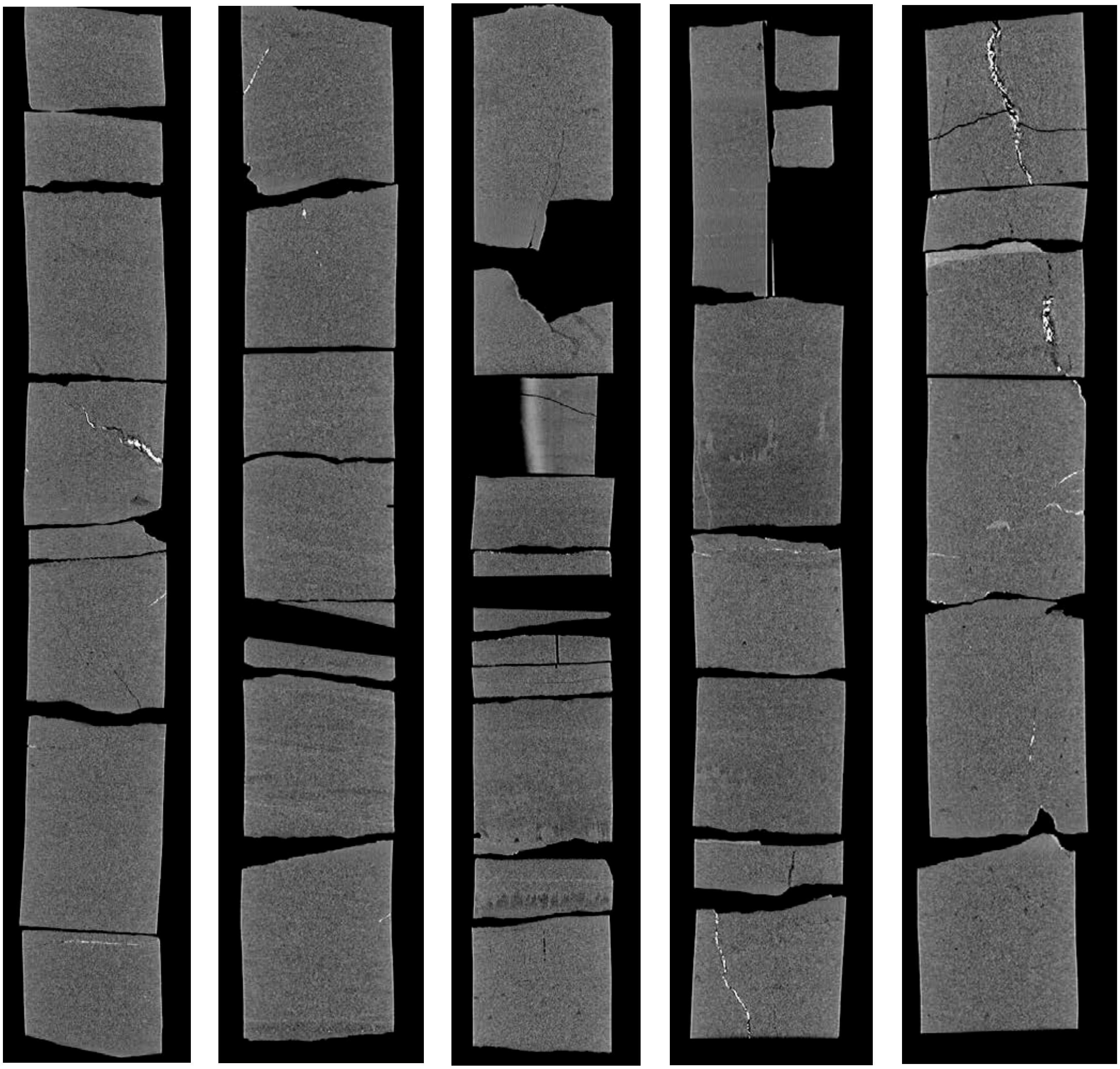

7,173–7,175.5*　**7,175.5–7,178***　**7,175–7,178***　**7,178–7,180**　**7,180–7,183**

Figure 51: 2D isolated planes through the vertical center of the medical CT scans of the Pres-119 core from 7,173 to 7,183 ft.

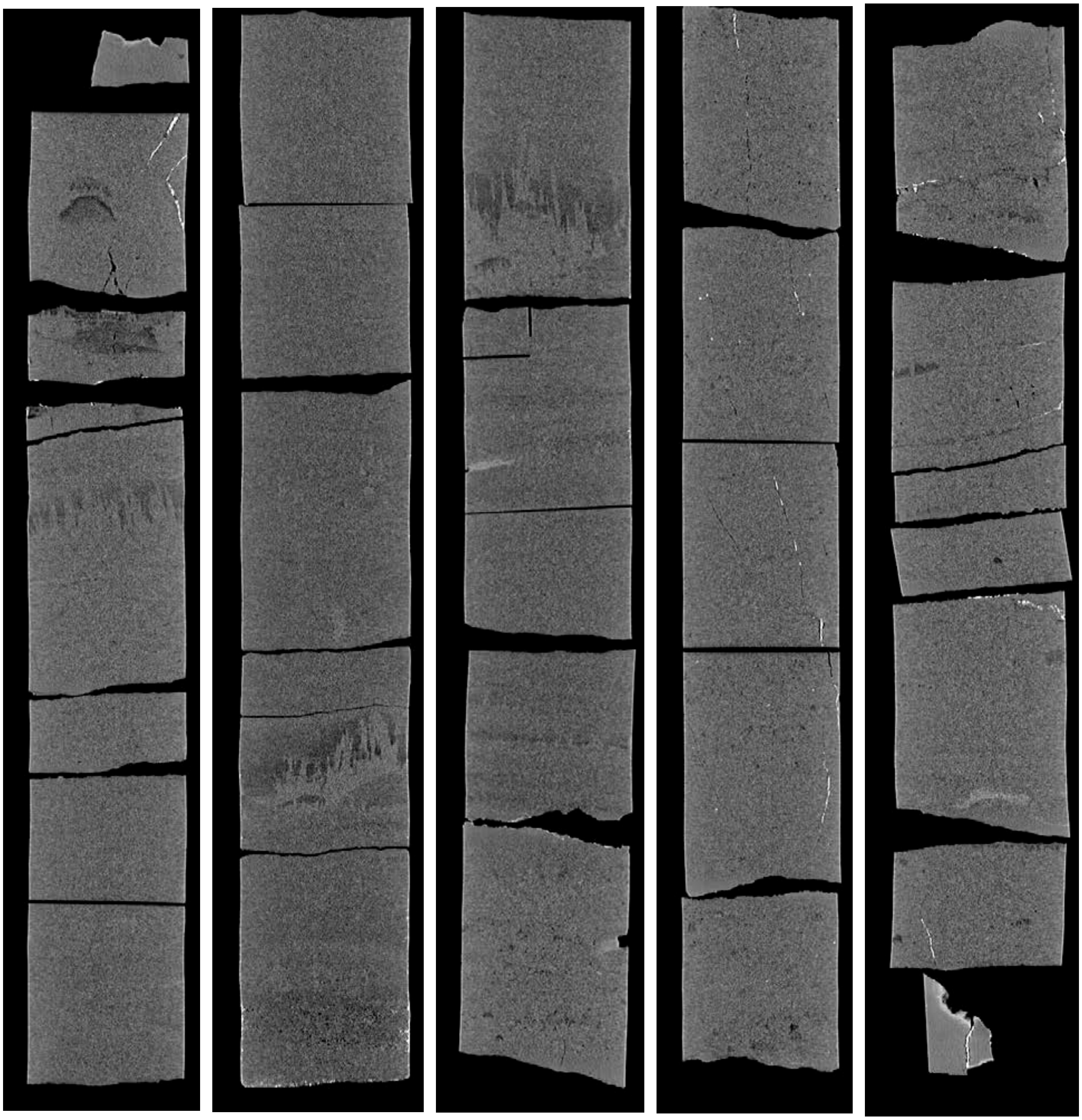

7,183–7,186 7,186–7,188 7,188–7,192.5 7,192.5–7,194.5 7,194.5–7,197.5

Figure 52: 2D isolated planes through the vertical center of the medical CT scans of the Pres-119 core from 7,183 to 7,197.5 ft.

7,197.5–7,200 7,200–7,202 7,202–7,204 7,204–7,206 7,206–7,208

Figure 53: 2D isolated planes through the vertical center of the medical CT scans of the Pres-119 core from 7,197.5 to 7,208 ft.

7,208–7,211 7,211–7,213 7,213–7,215 7,215–7,218 7,218–7,221

Figure 54: 2D isolated planes through the vertical center of the medical CT scans of the Pres-119 core from 7,208 to 7,221 ft.

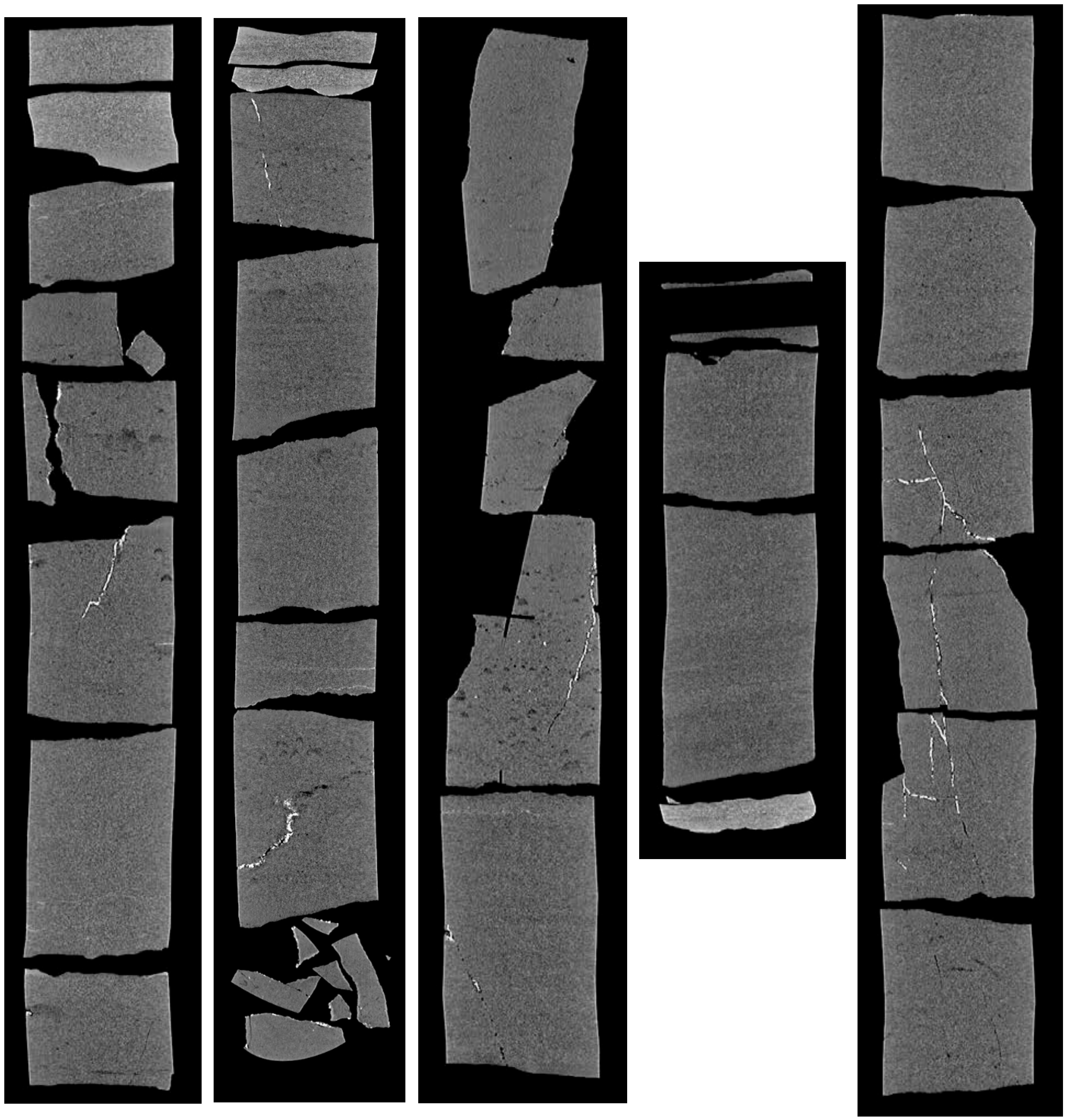

Figure 55: 2D isolated planes through the vertical center of the medical CT scans of the Pres-119 core from 7,221 to 7,233 ft.

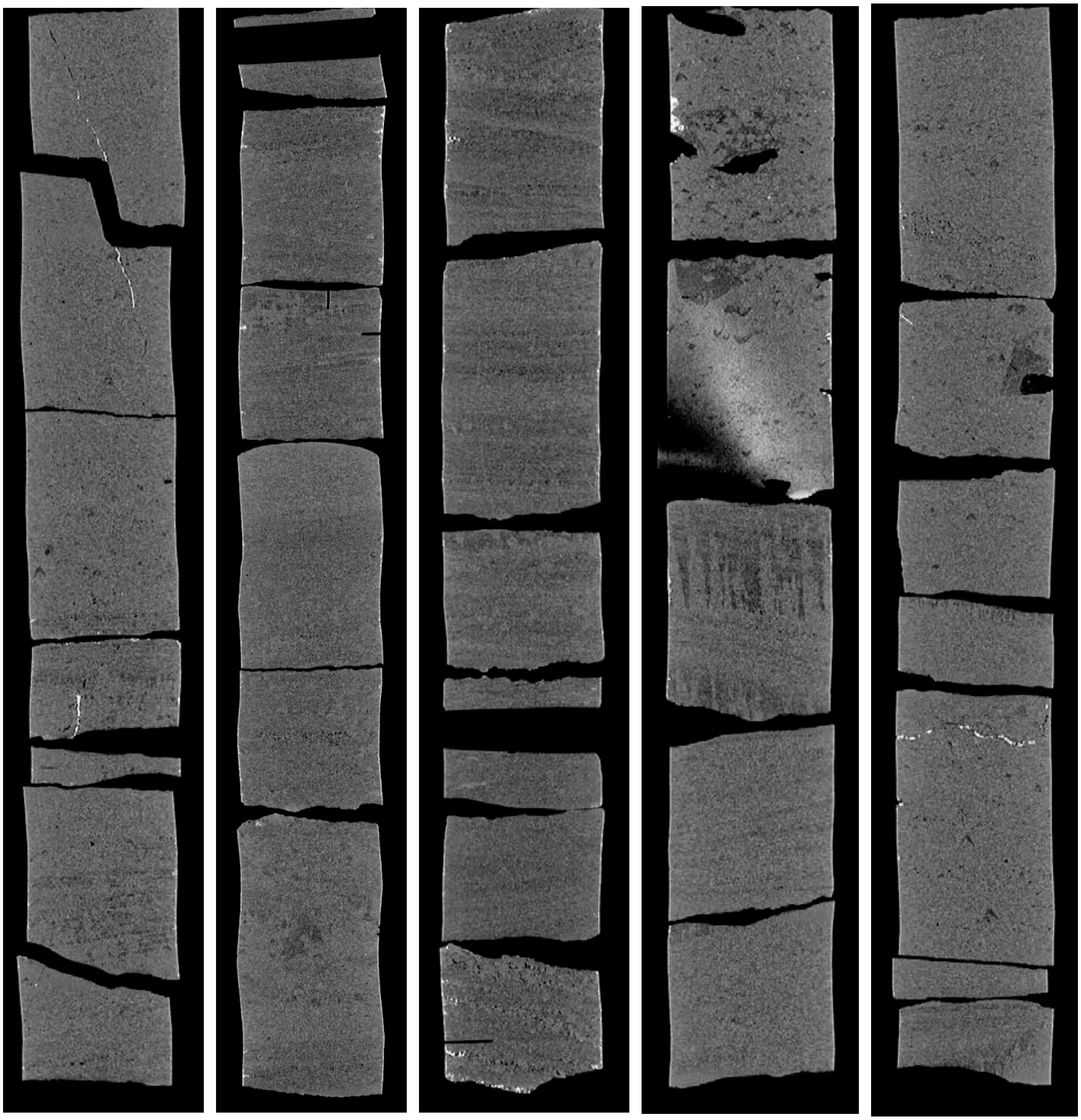

7,233–7,236 7,236–7,239 7,239–7,241.5 7,241.5–7,244 7,244–7,247

Figure 56: 2D isolated planes through the vertical center of the medical CT scans of the Pres-119 core from 7,233 to 7,247 ft.

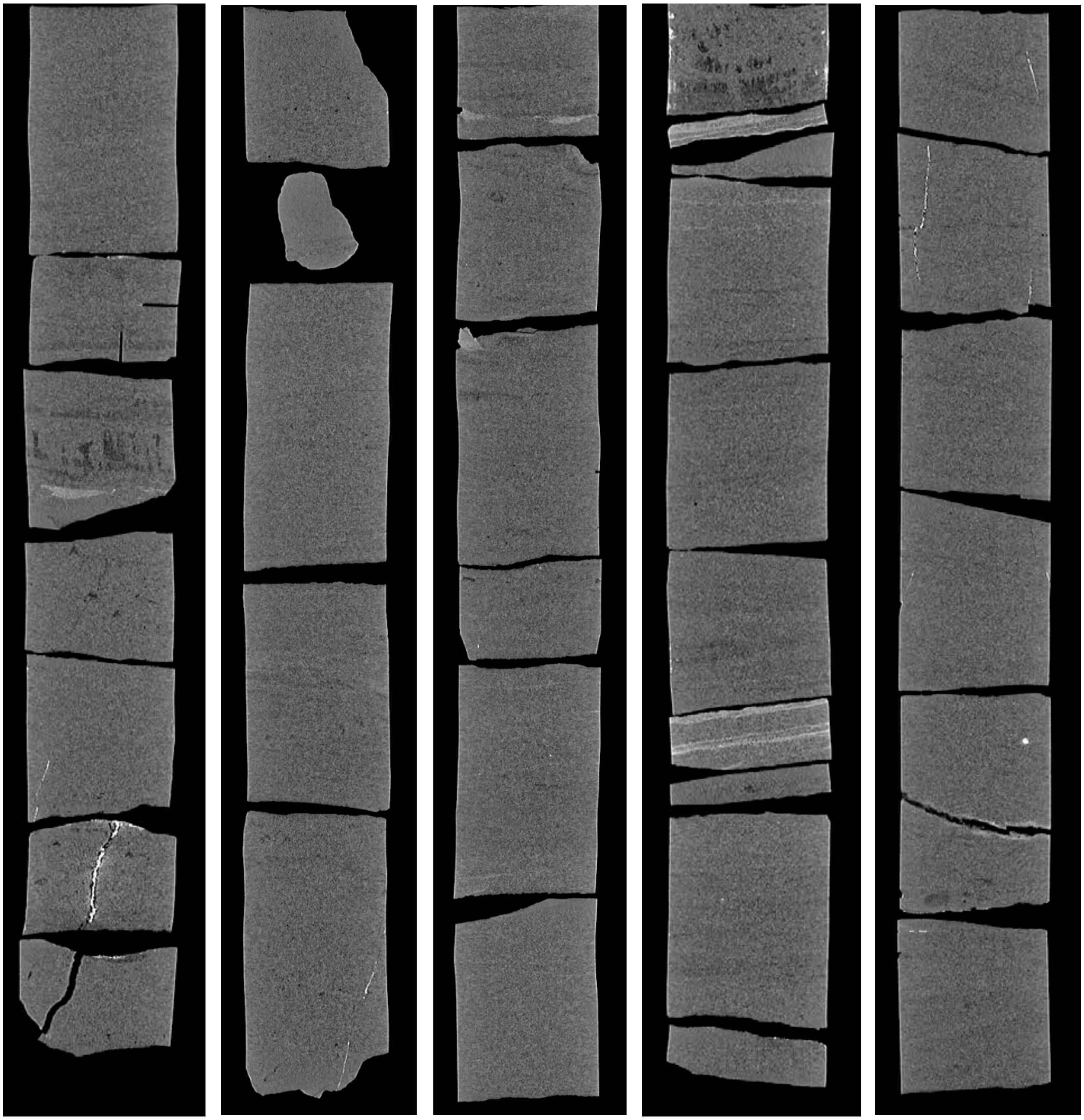

7,247–7,250 7,250–7,253 7,278–7,281 7,281–7,283 7,283–7,286

Figure 57: 2D isolated planes through the vertical center of the medical CT scans of the Pres-119 core from 7,247 to 7,286 ft, with a gap.

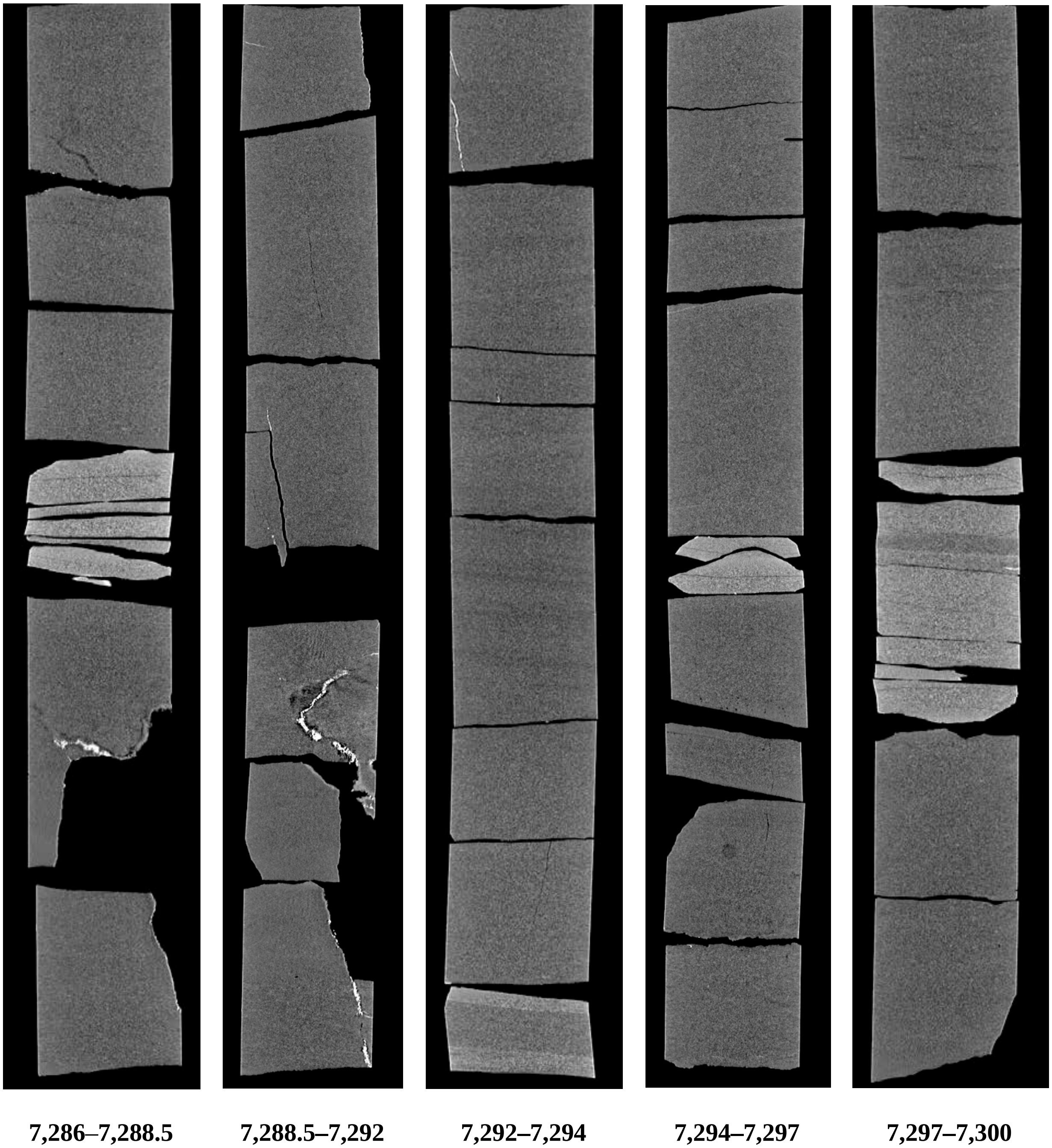

Figure 58: 2D isolated planes through the vertical center of the medical CT scans of the Pres-119 core from 7,286 to 7,300 ft.

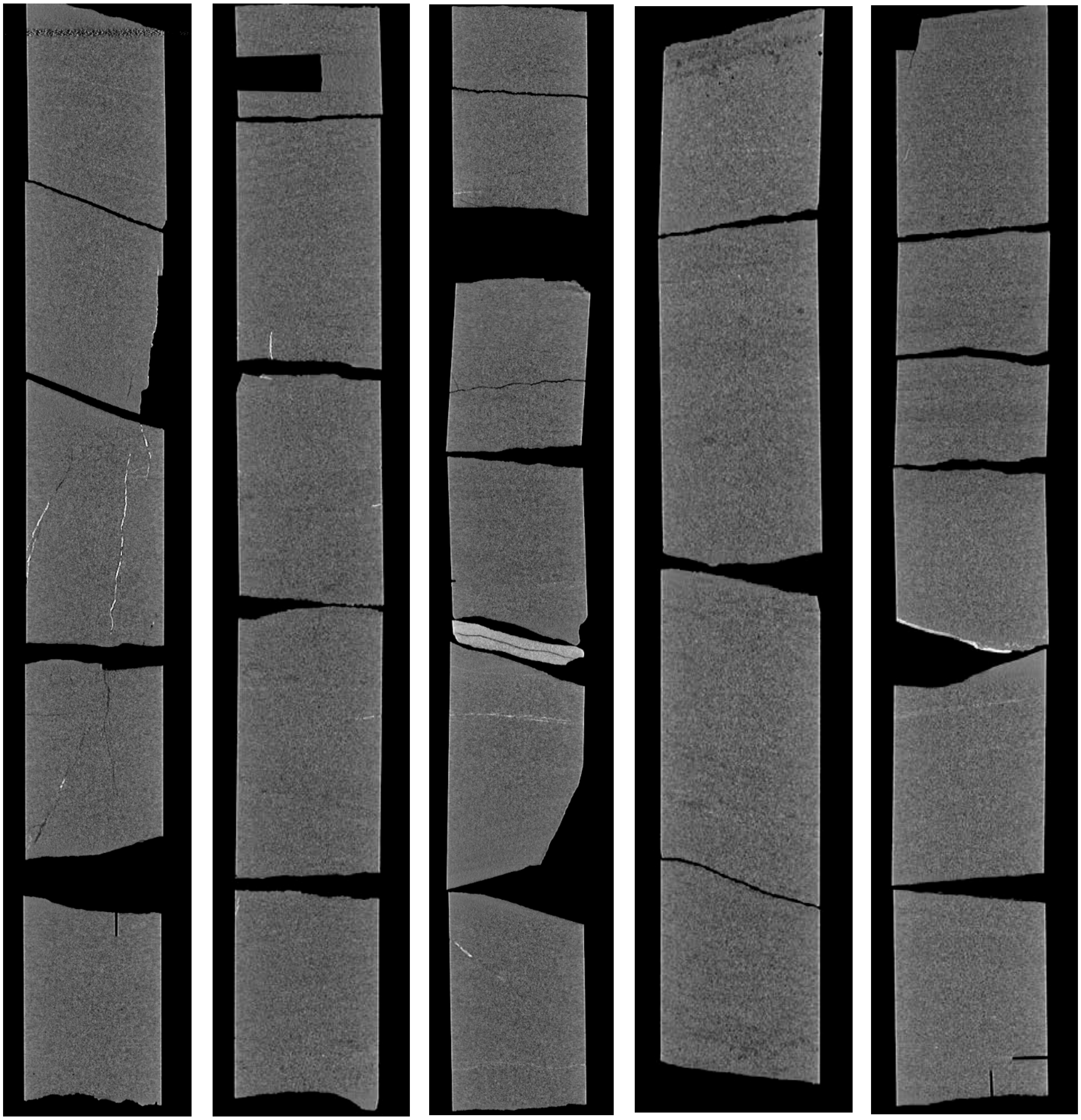

7,301–7,304 **7,304–7,307** **7,307–7,309** **7,310–7,313** **7,313.5–7,316.5**

Figure 59: 2D isolated planes through the vertical center of the medical CT scans of the Pres-119 core from 7,301 to 7,316.5 ft.

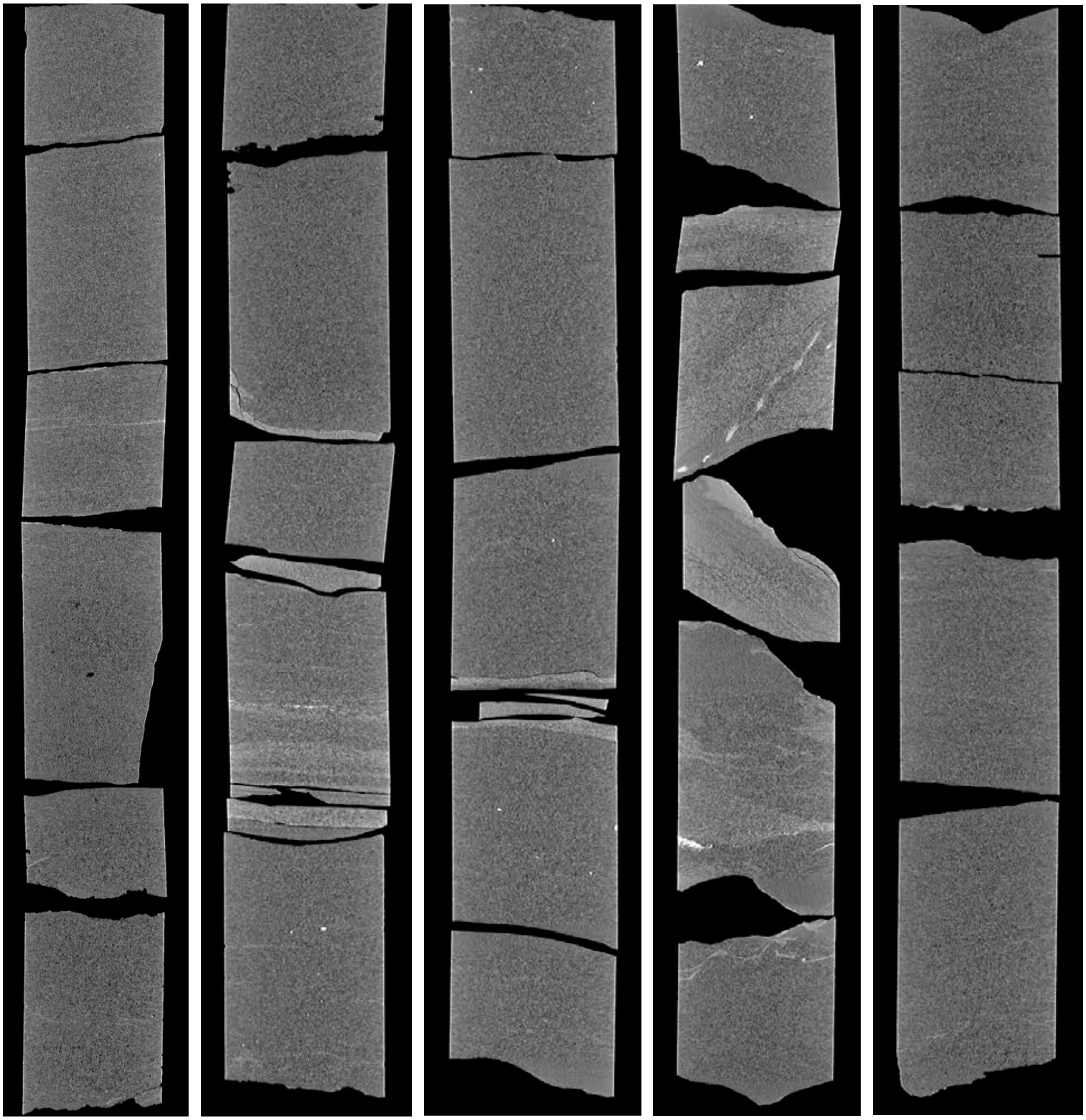

7,316.5–7,319.5 **7,319.5–7,322** **7,323–7,325.5** **7,325.5–7,328** **7,328–7,331**

Figure 60: 2D isolated planes through the vertical center of the medical CT scans of the Pres-119 core from 7,316.5 to 7,331 ft.

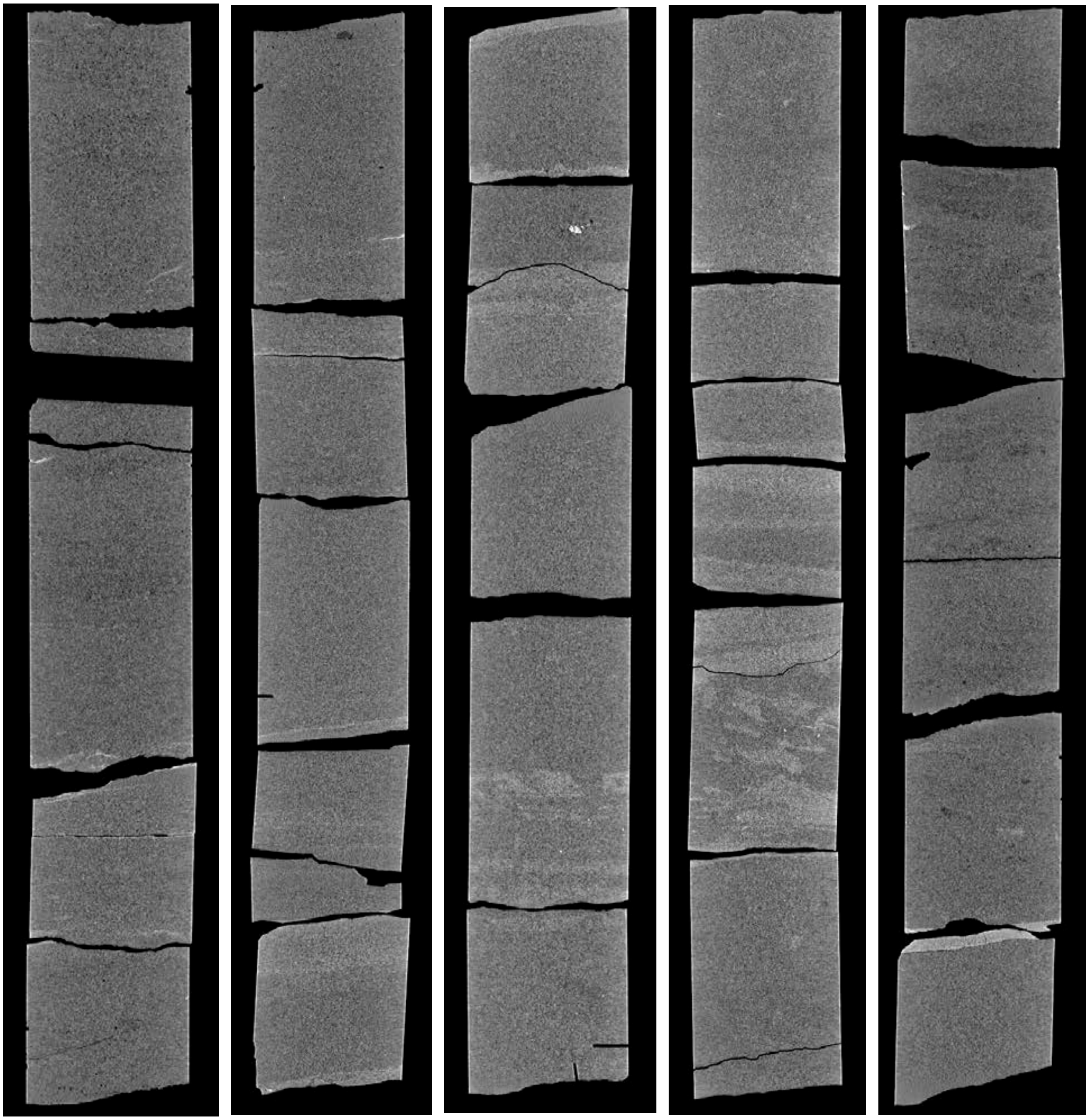

7,331–7,333.5 7,333.5–7,336 7,336–7,339 7,339–7,342 7,342–7,344.5

Figure 61: 2D isolated planes through the vertical center of the medical CT scans of the Pres-119 core from 7,331 to 7,344.5 ft.

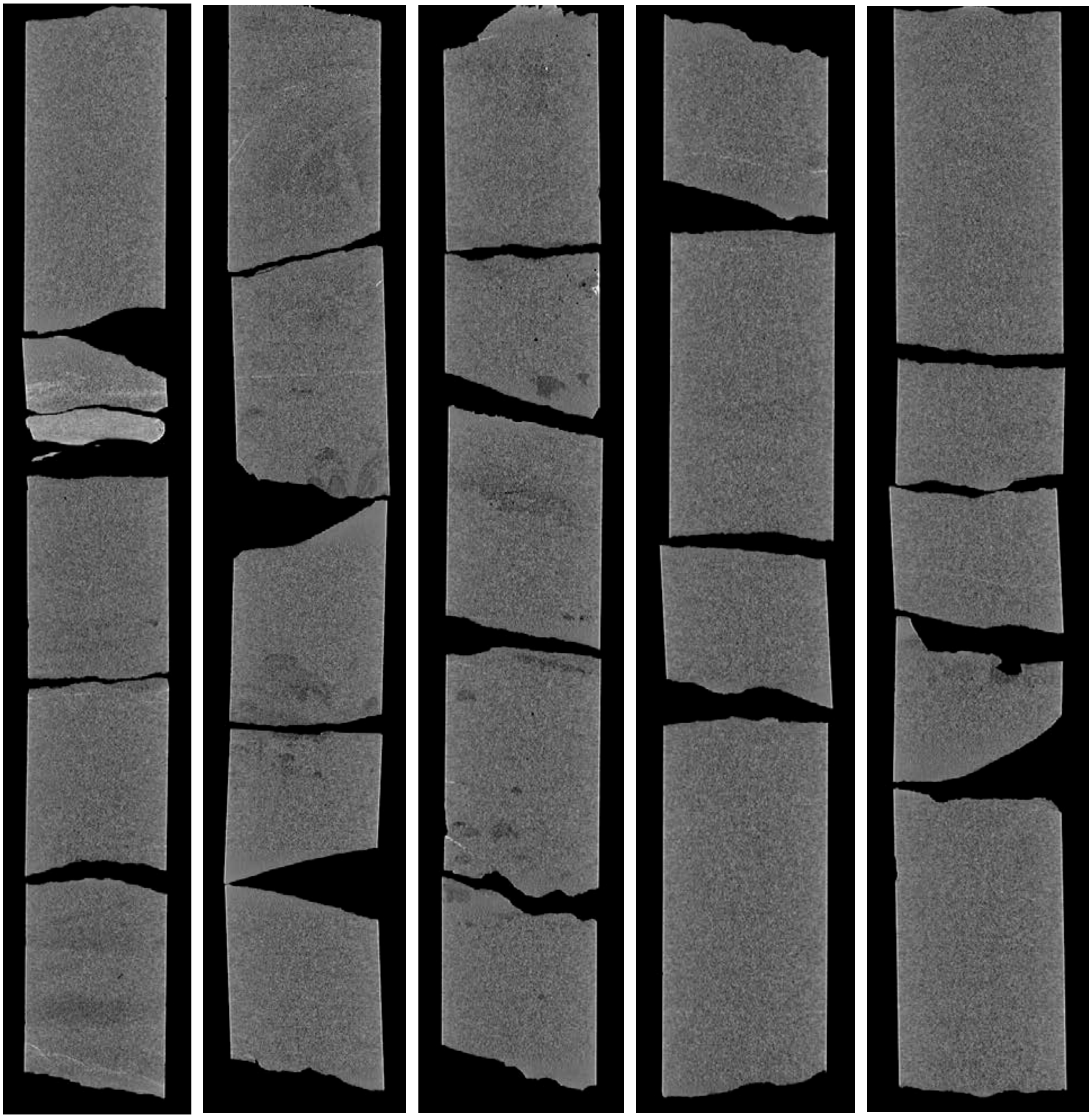

7,344.5–7,347 7,347–7,349 7,349–7,351 7,351–7,353 7,354–7,356.5

Figure 62: 2D isolated planes through the vertical center of the medical CT scans of the Pres-119 core from 7,344.5 to 7,356.5 ft.

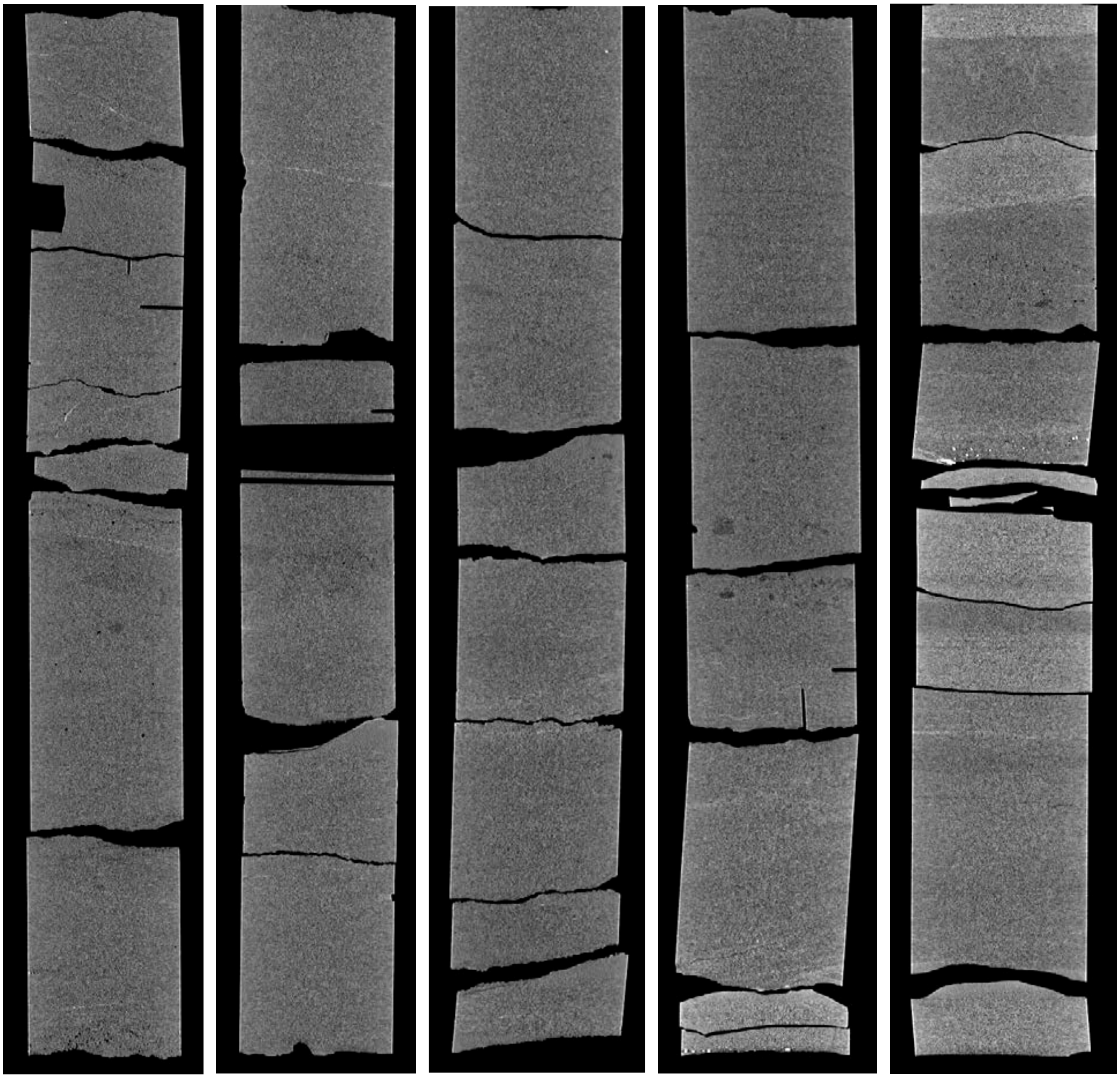

7,357–7,359 7,359–7,361.5 7,361.5–7,363 7,363–7,365 7,365–7,367.5

Figure 63: 2D isolated planes through the vertical center of the medical CT scans of the Pres-119 core from 7,344.5 to 7,356.5 ft.

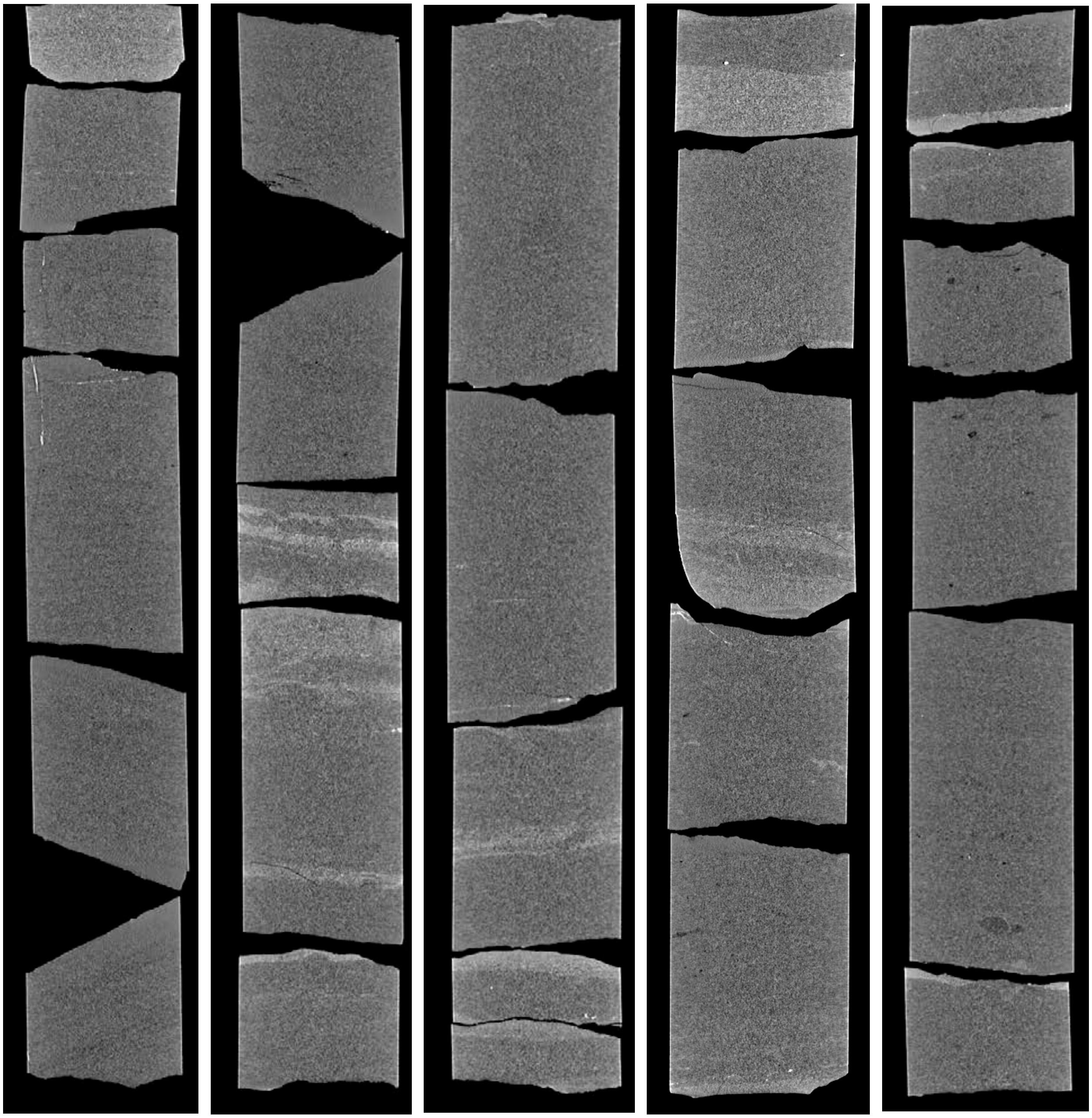

7,367.5–7,370 7,370–7,372 7,372–7,374 7,374–7,376.5 7,376.5–7,379

Figure 64: 2D isolated planes through the vertical center of the medical CT scans of the Pres-119 core from 7,367.5 to 7,379 ft.

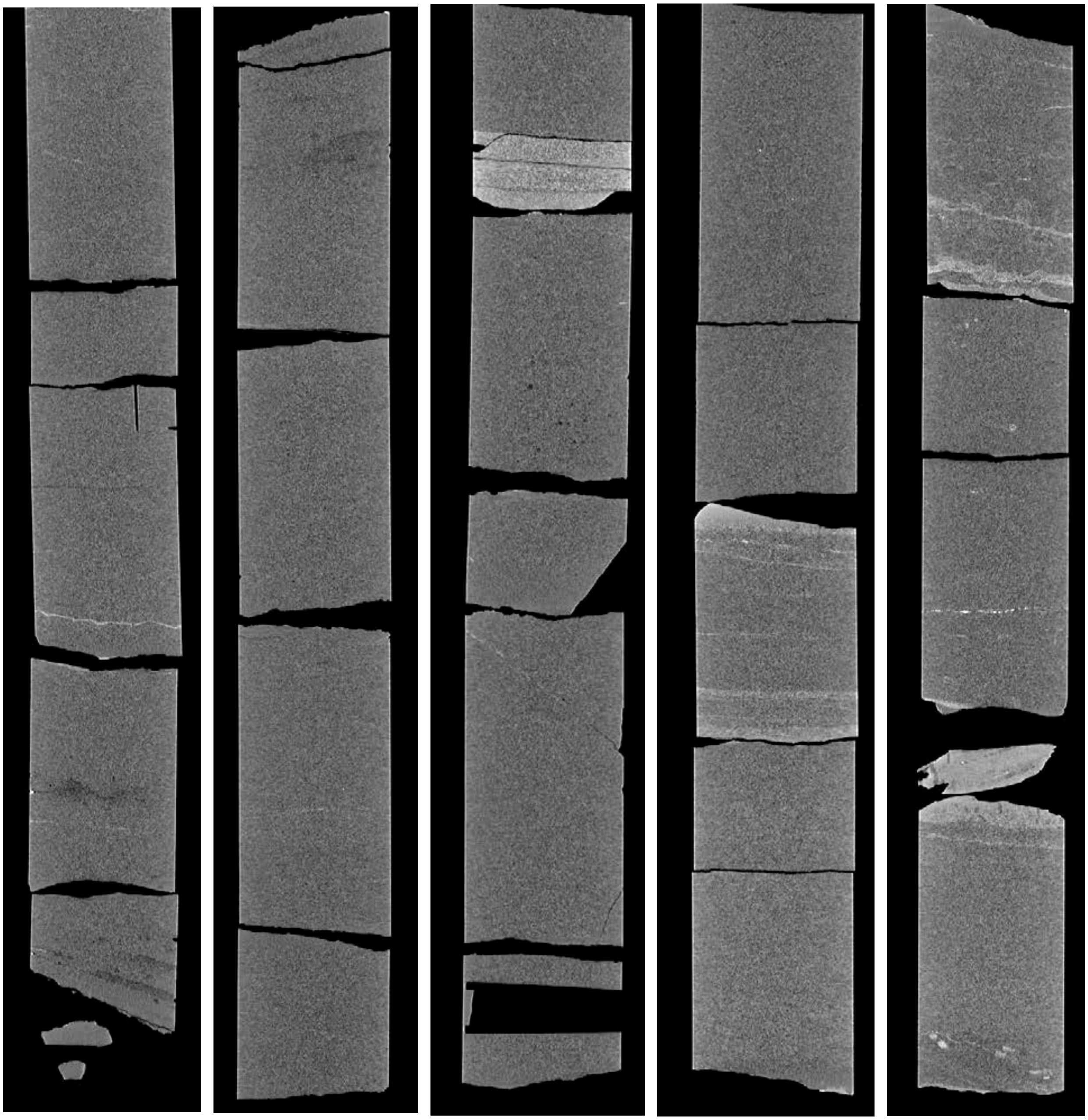

7,379–7,382 **7,382–7,384** **7,384–7,388** **7,388–7,390** **7,390–7,393**

Figure 65: 2D isolated planes through the vertical center of the medical CT scans of the Pres-119 core from 7,367.5 to 7,379 ft.

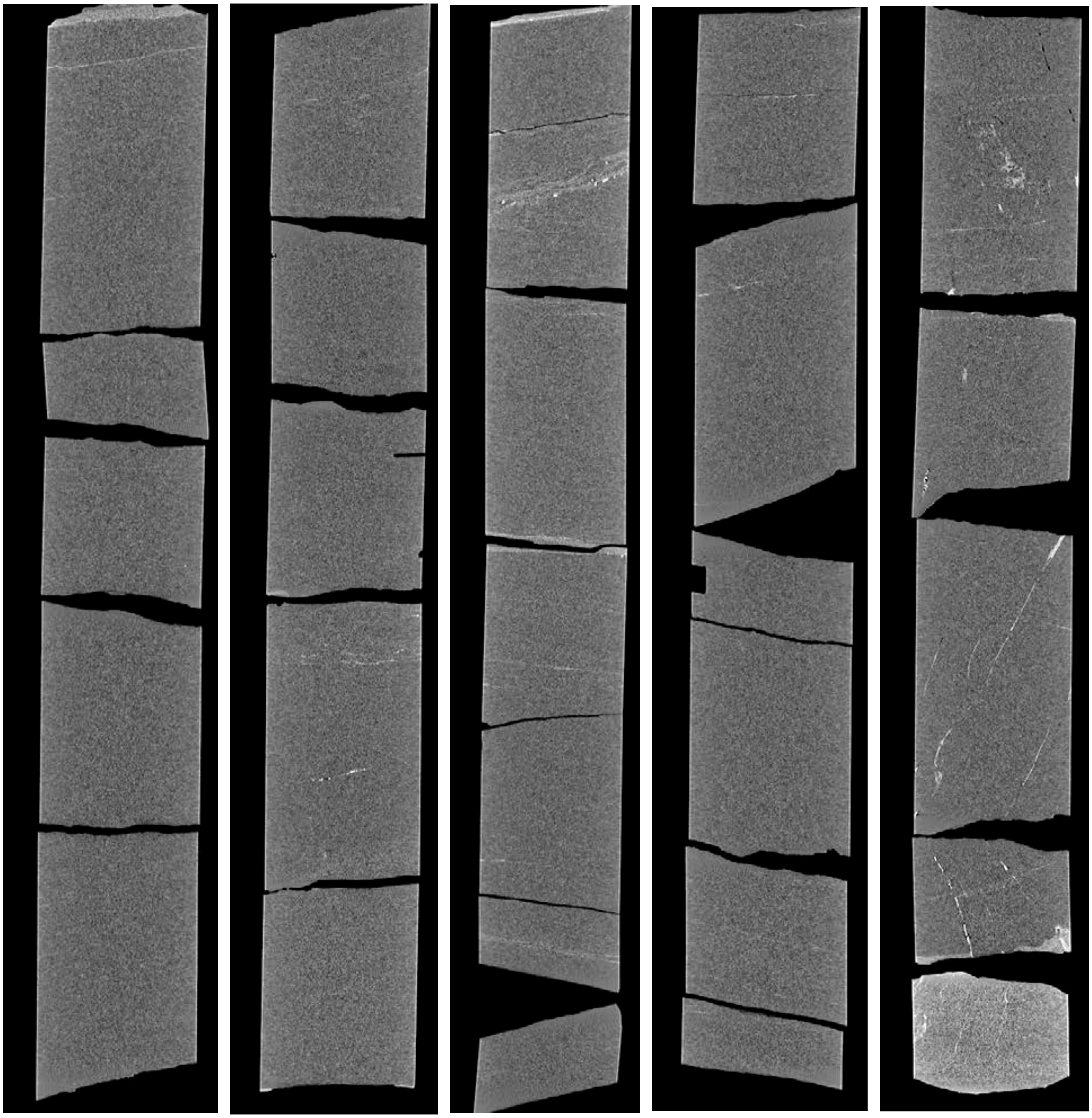

Figure 66: 2D isolated planes through the vertical center of the medical CT scans of the Pres-119 core from 7,393 to 7,406 ft.

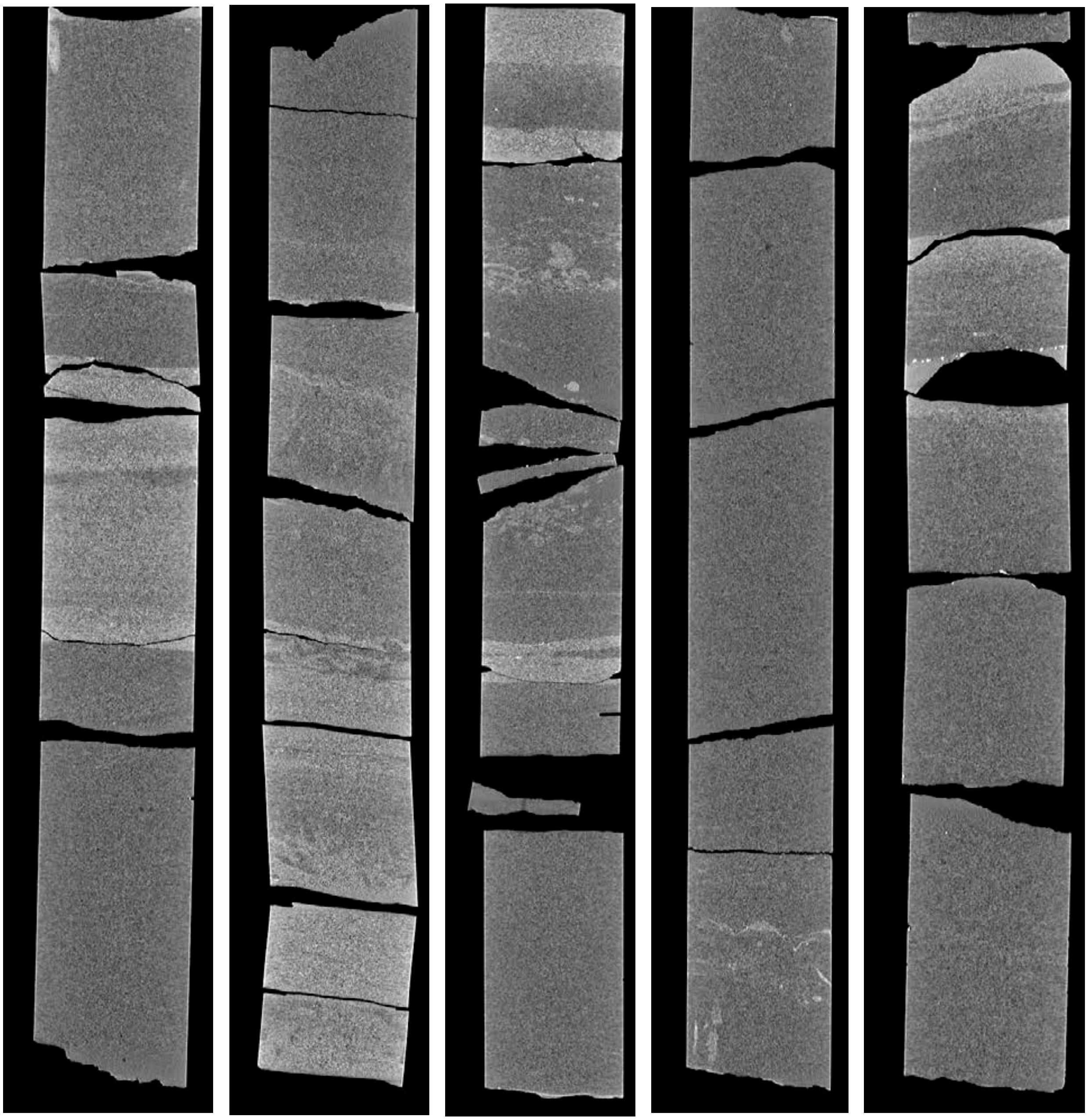

7,406–7,408 **7,408–7,410.5** **7,410.5–7,413** **7,413–7,415** **7,415–7,417**

Figure 67: 2D isolated planes through the vertical center of the medical CT scans of the Pres-119 core from 7,406 to 7,417 ft.

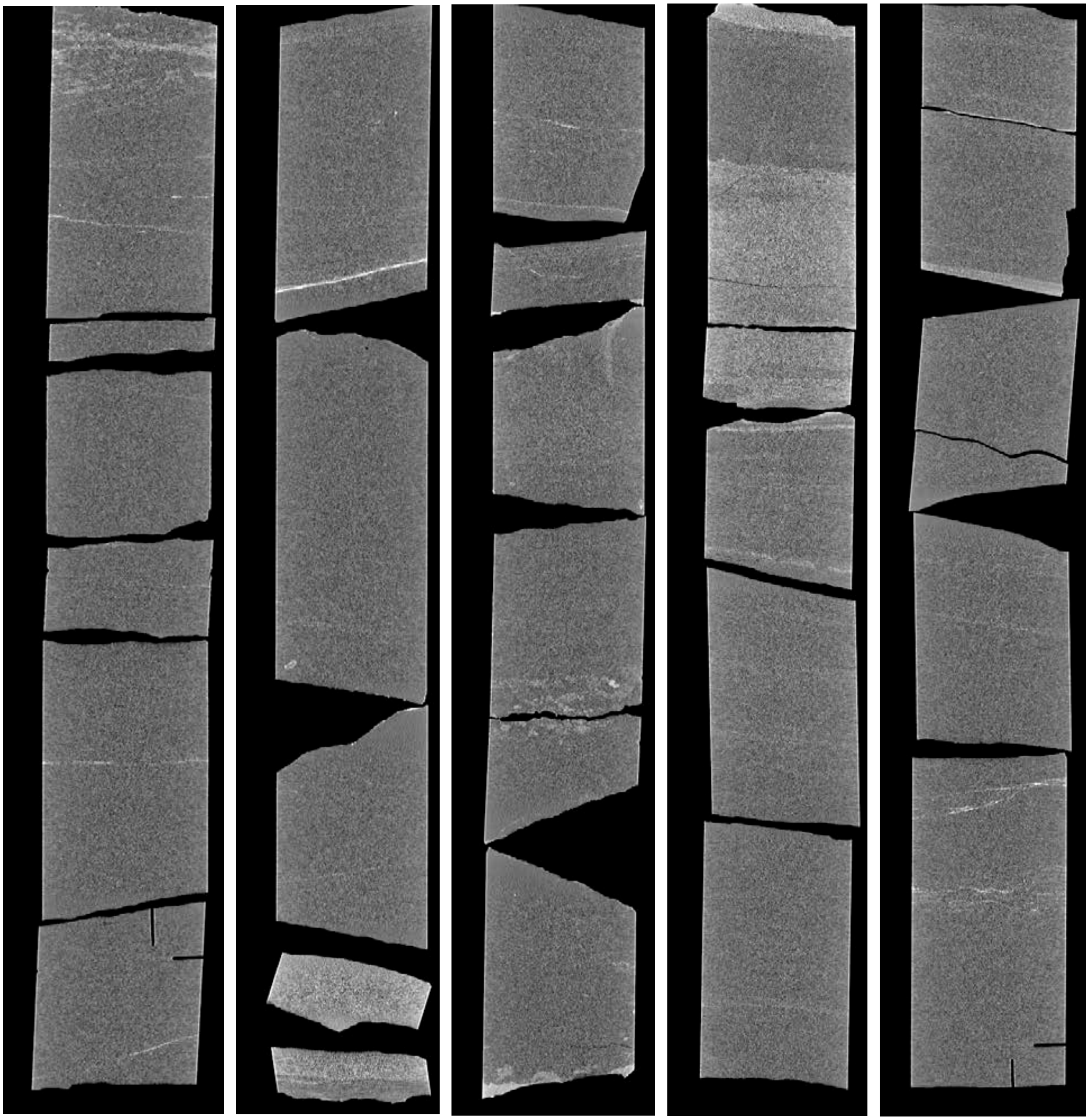

7,417–7,419 | 7,419.5–7,422 | 7,422–7,424 | 7,424–7,426 | 7,426–7,429

Figure 68: 2D isolated planes through the vertical center of the medical CT scans of the Pres-119 core from 7,417 to 7,429 ft.

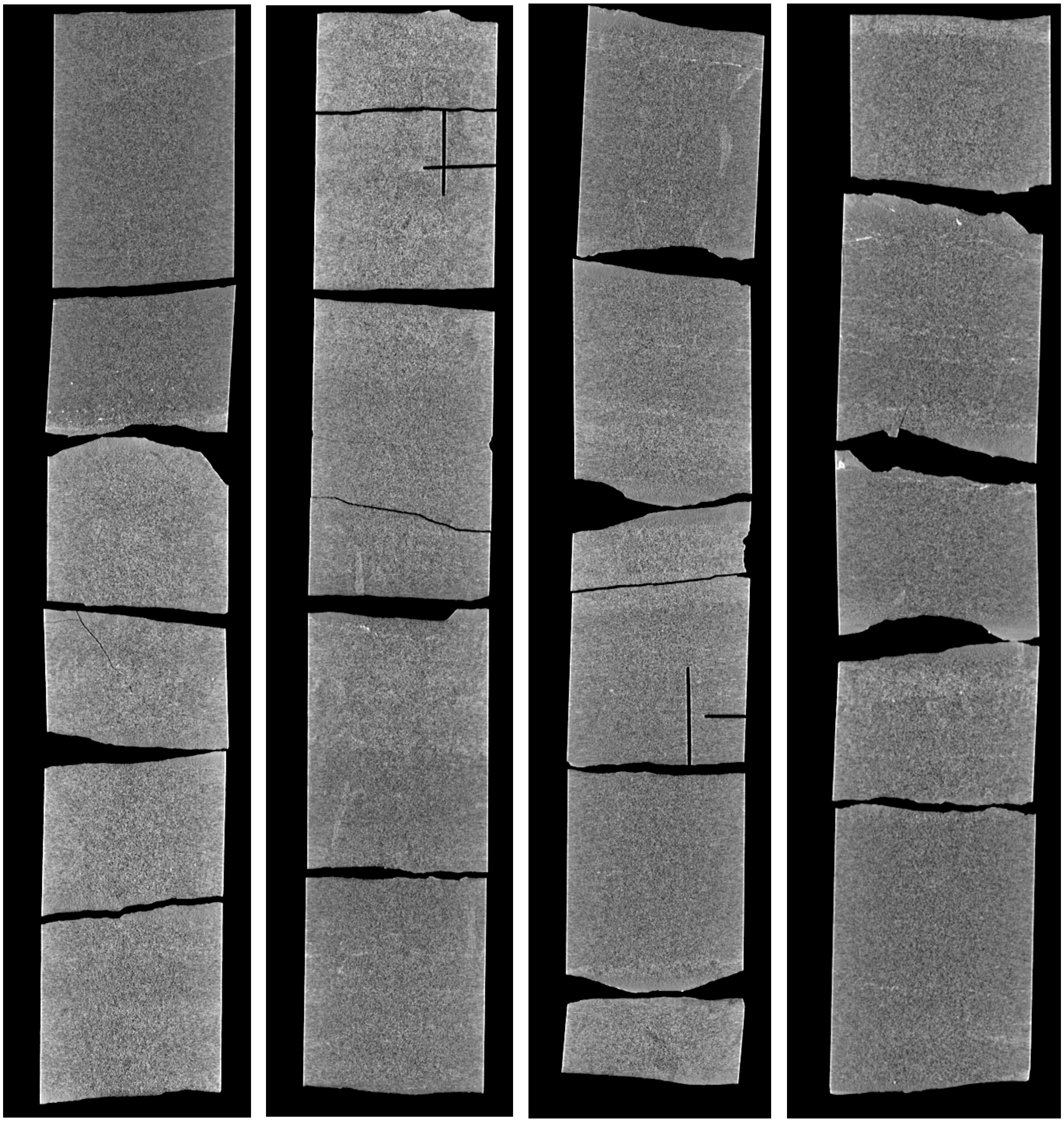

7,429–7,432 **7,432–7,434** **7,434–7,436** **7,436–7,438**

Figure 69: 2D isolated planes through the vertical center of the medical CT scans of the Pres-119 core from 7,429 to 7,438 ft.

4.2 ADDITIONAL CT DATA

Additional CT data can be accessed from NETL's EDX online system using the following link: https://edx.netl.doe.gov/dataset/preston-119-well. The original CT data is available as 16-bit tif stacks suitable for reading with ImageJ (Rasband, 2018) or other image analysis software. In addition, videos showing the variation along the length of the cross-section images shown in the previous section are available for download and viewing. A single image from these videos is shown in Figure 70, where the distribution of high density minerals in a cross section of the core around a depth of 7,372 ft is shown. Here, the red line through the XZ-plane image of the core shows the location of the XY-plane displayed above. The videos on https://edx.netl.doe.gov/dataset/preston-119-well show this XY variation along the entire length of the core.

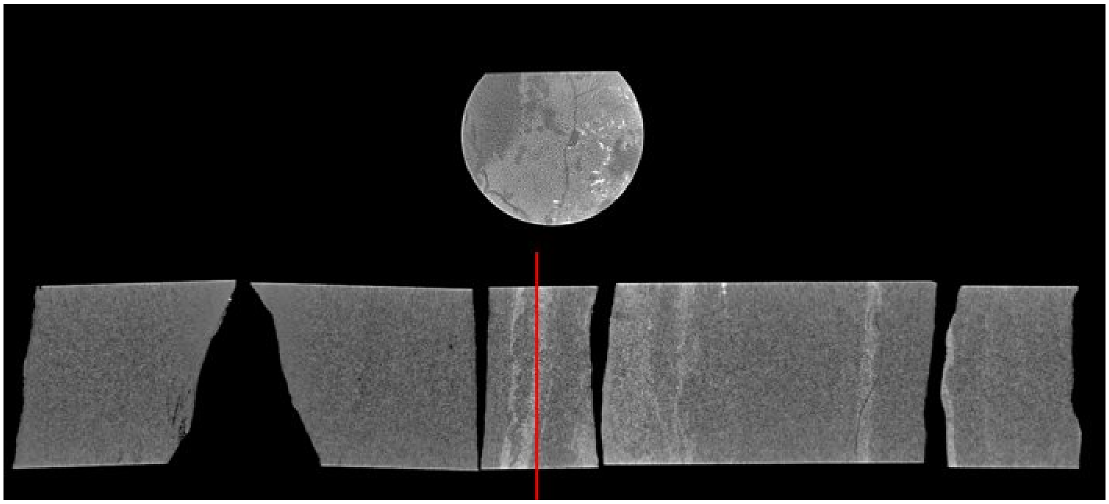

Figure 70: Single image from a video file available on EDX showing variation in the core around 7,372 ft. Image above shows the variation in composition within the matrix perpendicular to the core length.

4.3 DUAL ENERGY

Dual Energy CT scanning uses two sets of images, produced from different x-ray energies, to approximate the density (ρ_B) and the effective atomic number (Z_{eff}) (Siddiqui and Khamees, 2004; Johnson, 2012). The technique relies on the use of several standards of known ρ_B and Z_{eff} to be scanned at the same energies as the specimen. These scans are performed at lower energies (<100 KeV) and higher energies (>100 KeV) to induce two types of photon interactions with the object (Figure 71). The lower energy scans induce photoelectric absorption, which occurs when the energy of the photon is completely absorbed by the object mass and causes ejection of an outer orbital electron (Figure 71a). The high energy scans induce Compton scattering, which causes a secondary emission of a lower energy photon due to incomplete absorption of the photon energy in addition to an electron ejection (Figure 71b).

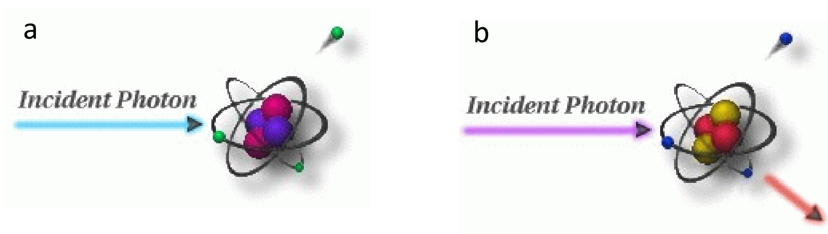

Figure 71: Photon interactions at varying energies. A) Photoelectric absorption, B) Compton scattering. Modified from NDT Resource Center (2018).

Medical grade CT scanners are typically calibrated to known standards, with the output being translated in CT numbers (CTN) or Hounsfield Units (HU). Convention for HU defines air as -1000 and water as 0. A linear transform of recorded HU values is preformed to convert them into CTN. This study used CTN as it is the native export format for the instrument, but it is possible to use HU. Dual energy CT requires at least 3 calibration points and it is prudent to utilize standards that approximate the object or material of interest. Pure samples of aluminum, graphite, and sodium chloride were used as the calibration standards as they most closely approximate the rocks and minerals of interest (Table 1). Most materials denser than water or with higher atomic masses have a non-linear response to differing CT energies (Table 2).

Table 1: Calibration standards

Material	ρ_B (g/cm^3)	Z_{eff}
Air	0.001	7.22
Water	1	7.52
Graphite	2.3	6
Sodium Chloride	2.16	15.33
Aluminum	2.7	13

Table 2: Response to differing CT energies

Material	HU		CTN	
	80 KeV	135 KeV	80 KeV	135 Kev
Air	-993	-994	31,775	31,774
Water	-3.56	-2.09	32,764	32,766
Graphite	381	437	33,149	33,205
Sodium Chloride	1,846	1,237	34,614	34,005
Aluminum	2,683	2,025	35,451	34,793

Dual energy CT utilizes these differences to calibrate to the X-ray spectra. Two equations with 3 unknowns each are utilized to find ρ_B and Z_{eff}:

$$\rho_B = mCTN_{low} + pCTN_{high} + q$$

$$Z_{eff} = \sqrt[3.6]{\frac{(rCTN_{low}+sCTN_{high}+t)}{(0.9342 * \rho_B + 0.1759)}}$$

Where [m, p, and q] and [r, s, and t] are unknown coefficients that can be solved by setting up a system of equations with four 3 x 3 determinants. The CTN is obtained from the CT scans for each of the homogenous calibration standards.

In this study the high and low energy image stacks were loaded into Python as arrays. A 3-D Gaussian blur filter with a sigma of 2 was used to reduce noise in the images. The scipy.solv module of Python was then employed to solve for the coefficients based on the calibration CTN values. The ρ_B and Z_{eff} were both solved for each pixel in the 3D volume and saved as two new separate image stacks.

ImageJ (Rasband, 2018) was used to reslice the image stacks to produce 2D representative cross-sections of the entire core-length. A 6-shade look up table was used to apply a gradational color scale to the image with the total range of values limited to densities from 2 to 4.5 g/cm^3; this eliminated much of the noise in the air portion of the scans and at the edges of the sample. The average density along the length of the cores was calculated by excluding all densities below 2 g/cm^3. This study assumed that the cores were free of water and liquids as they were air dried and that the cores do not contain an appreciable quantity of elements with densities lower than 2.0 g/cm^3.

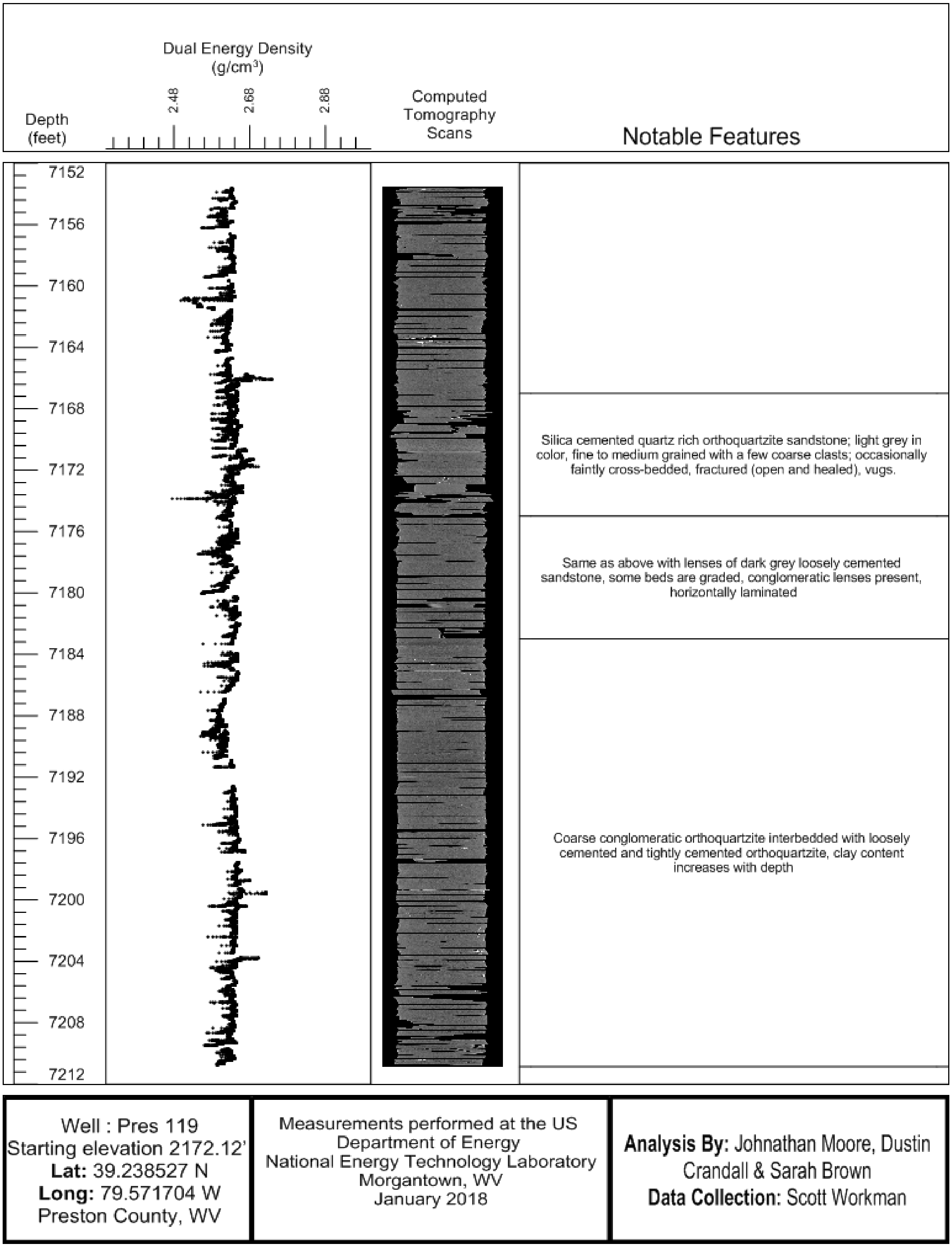

Figure 72: Dual-energy density, CT images, and core description for the Pres-119 core from 7,153 to 7,211 ft.

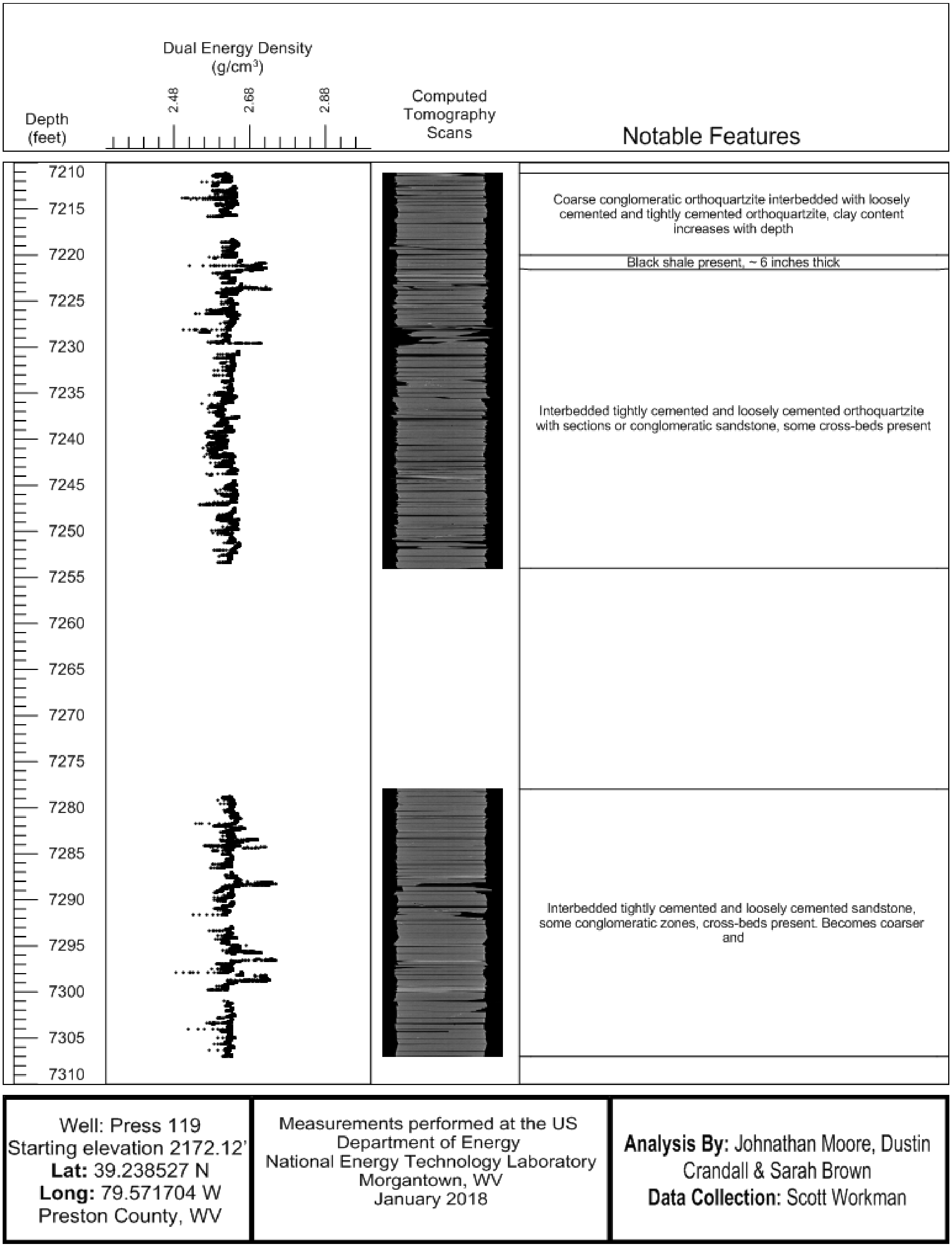

Figure 73: Dual-energy density, CT images, and core description for the Pres-119 core from 7,211 to 7,307 ft.

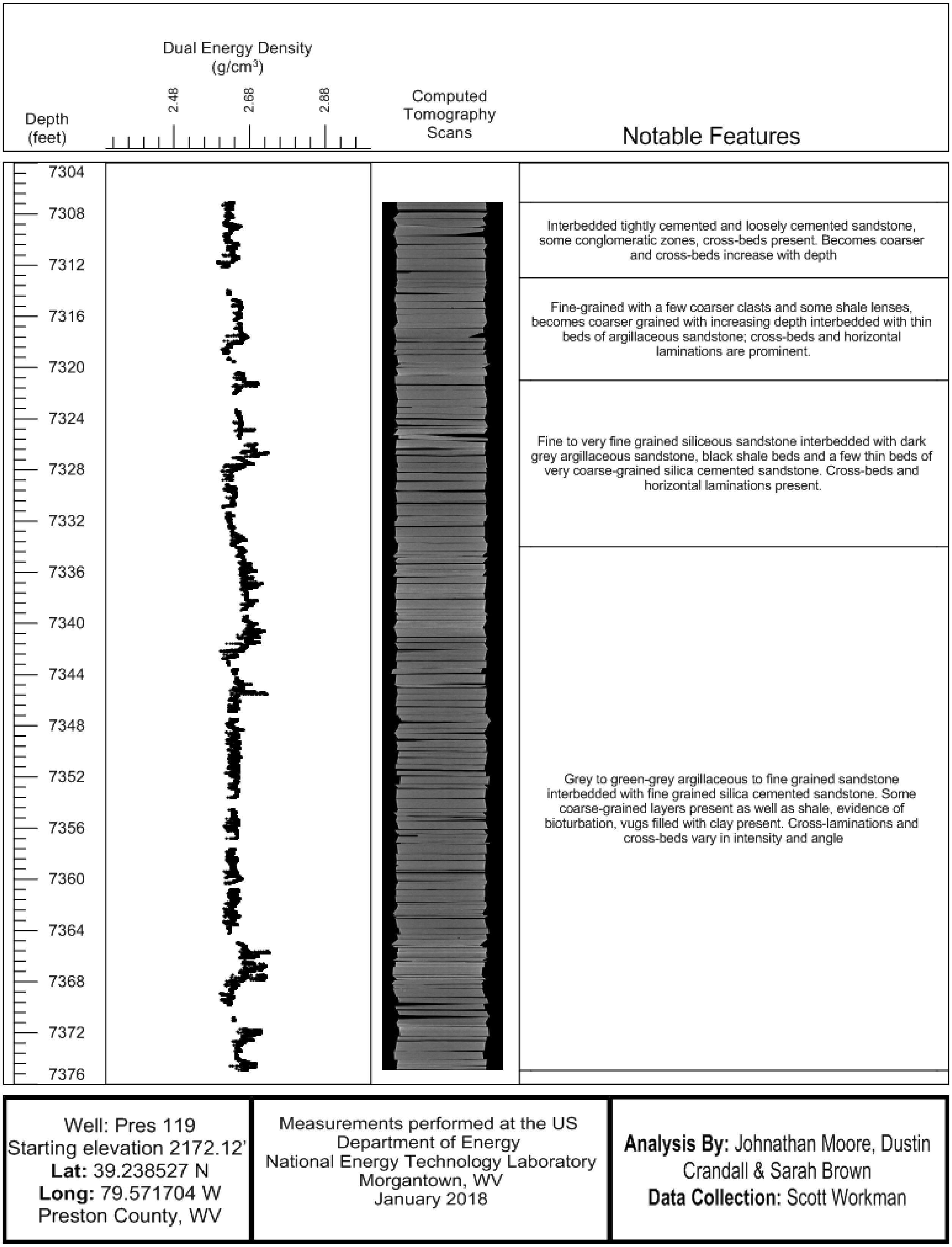

Figure 74: Dual-energy density, CT images, and core description for the Pres-119 core from 7,307 to 7,372 ft.

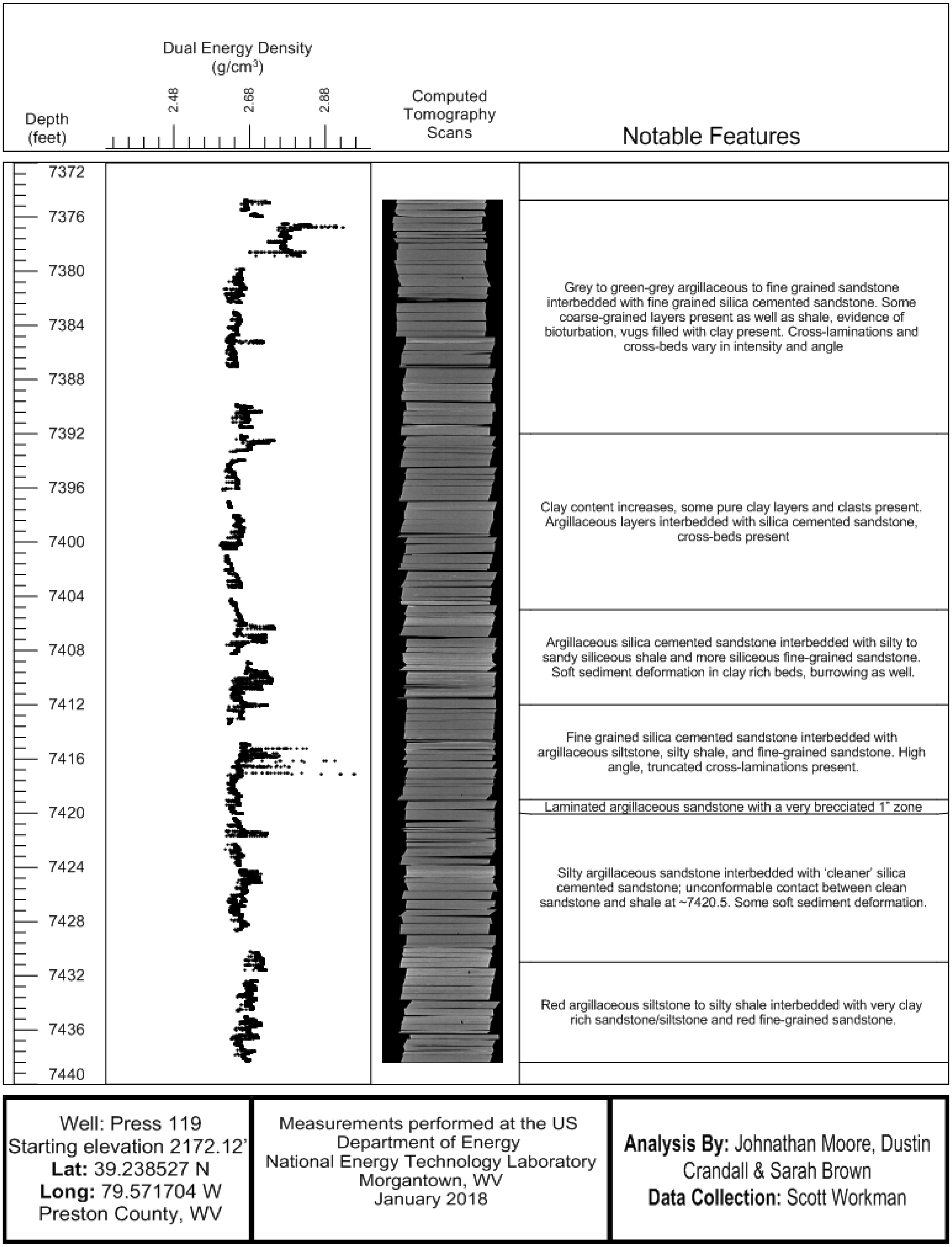

Figure 75: Dual-energy density, CT images, and core description for the Pres-119 core from 7,372 to 7,438 ft.

5. DISCUSSION

CT analysis provides a unique look into of the internal structure of the core and macroscopic changes in lithology. The multiple CT techniques used here:

- Are non-destructive
- Provide density values over the core length
- Can be used to identify zones of interest for detailed analysis, experimentation, and quantification
- Provide a detailed digital record of the core, before any destructive testing or further degradation, that is accessible and can be referenced for future studies

6. REFERENCES

Johnson, T. R. Dual-Energy CT: General Principles. *American Journal of Roentgenology* **2012,** *199*, S3-S8. DOI:10.2214/ajr.12.9116.

Rasband, W. S.; ImageJ. U.S. National Institutes of Health: Bethesda, MD, 1997–2016, http://imagej.nih.gov/ij/ (accessed 2018).

Siddiqui, S.; Khamees, A. *Dual-Energy CT-Scanning Applications in Rock Characterization (SPE 90520).* Society of Petroleum Engineers Annual Technical Conference and Exhibition, Houston, TX, 2004.

Sources of Attenuation. Nondestructive Testing Resource Center. www.nde-ed.org/EducationResources/CommunityCollege/Radiography/Physics/attenuation.htm. (accessed 2018)

West Virginia Geological & Economic Survey, Pipeline-Plus Scanned Records Search, API =4707700119. http://www.wvgs.wvnet.edu/pipe2/EfileViewer.aspx, (accessed online, Feb 2018); 4707700119docs.pdf; p 11.

This page intentionally left blank.

Sean Plasynski, Ph.D.
Director (Acting)
National Energy Technology Laboratory
U.S. Department of Energy

Jared Ciferno
Associate Director
Oil and Gas
Technology Development & Integration Center
National Energy Technology Laboratory
U.S. Department of Energy

Elena Melchert
Director
Division of Upstream Oil and Gas Research
U.S. Department of Energy

Bryan Morreale
Executive Director
Research and Innovation Center
National Energy Technology Laboratory
U.S. Department of Energy